Historical reconstruction of sediment accumulation rates as an indicator of global change impacts in a tropical crater lake

Ruiz-Fernández, A. C., Sanchez-Cabeza, J. A., Blaauw, M., Pérez-Bernal, L. H., Cardoso-Mohedano, J. G., Aquino-López, M. A., Keaveney, E., & Giralt, S. (2022). Historical reconstruction of sediment accumulation rates as an indicator of global change impacts in a tropical crater lake. *Journal of Paleolimnology*. Advance online publication. https://doi.org/10.1007/s10933-022-00254-9

Published in:
Journal of Paleolimnology

Document Version:
Peer reviewed version

Historical reconstruction of sediment accumulation rates as an indicator of global change impacts in a tropical crater lake

Ruiz-Fernández A.C.[1*], Hernández-Rivera D.M.[2], Sanchez-Cabeza J. A.[1], Blaauw M.[3], Pérez-Bernal L. H.[1], Cardoso-Mohedano J. G.[4], Aquino-López M. A.[5], Keaveney E.[3], Giralt S.[6]

[1]Universidad Nacional Autónoma de México. Instituto de Ciencias del Mar y Limnología. Unidad Académica Mazatlán. Calz. Joel Montes Camarena s/n, Col. Playa Sur, 82040 Mazatlán, Sin., México. E-mail: caro@ola.icmyl.unam.mx, jasanchez@cmarl.unam.mx

[2]Universidad Nacional Autónoma de México. Posgrado en Ciencias del Mar y Limnología. Calz. Joel Montes Camarena s/n, Col. Playa Sur, 82040 Mazatlán, Sin., México. E-mail: donamhr@gmail.com

[3] Queen´s University Belfast. Archaeology and Palaeoecology, School of Natural and Built Environment. 42 Fitzwilliam Street, Belfast BT9 6AX United Kingdom. E-mail: maarten.blaauw@qub.ac.uk

[4]Universidad Nacional Autónoma de México. Instituto de Ciencias del Mar y Limnología, Estación El Carmen, México. Carretera Carmen-Puerto Real Km. 9.5, 24157 Ciudad del Carmen, Camp. E-mail: gcardoso@cmarl.unam.mx

[5]Centro de Investigación en Matemáticas (CIMAT), Jalisco s/n, Valenciana, 36023 Guanajuato, Gto, Mexico. E-mail: aquino@cimat.mx

[6]Geosciences Barcelona (Geo3BCN-CSIC). Lluís Solé i Sabarís s/n, 08028 Barcelona, España. E-mail: sgiralt@geo3bcn.csic.es

*Corresponding author

Keywords: tropical crater lake, ^{210}Pb, ^{14}C, ^{137}Cs, plutonium isotopes, sedimentation rates

Abstract

Lakes are effective sentinels of global change owing to their sensitivity to land-use changes and climate variability in their catchment. Santa María del Oro Lake (SAMO, NW Mexico) is of interest both for global change studies and as a natural resource to sustain the economy of local communities. Four sediment cores were used to evaluate the long-term temporal variations of sediment accumulation, under the hypothesis that changes in sediment input are mostly driven by anthropic activities developed in the lake surroundings. Radiocarbon (^{14}C) dating of SAMO sediments was precluded by a large and variable reservoir effect, inducing an age offset of ~4,000 years. Well-constrained chronologies over the past century were obtained by ^{210}Pb dating, corroborated by the stratigraphic markers ^{137}Cs, $^{239+240}Pu$, and ^{14}C-fraction modern. Geochemical, magnetic susceptibility, and meteorological data were used to elucidate the main controls of sedimentation processes in the lake. Mass accumulation rates (MAR) were high (range 0.01 - 0.80 g cm^{-2} yr^{-1}) likely because of the natural vulnerability of catchment soils to hydric and aeolian erosion. The highest values, observed towards the lakeshore, were attributed to the influence of seasonal runoff from surrounding steep hills and the proximity of human settlements and agriculture fields. MAR increased with time, although the most recent values were comparable to the mean values during CE 1900-1950 (0.05±0.04 g cm^{-2} yr^{-1}). Accumulation maxima across the lake, occurring mostly since the 1980s, concurred with precipitation minima and were related to terrigenous pulses associated with soil erosion, likely favored by lower soil humidity and the occurrence of wildfires during dryer years. Controls on the development of human settlement and agriculture practices should be included in the long-term environmental management plans for the conservation of the lake resources.

Introduction

Continental erosion caused by land-use changes and global warming are two of the main consequences of global change (GC), and both have accelerated during the second half of the twentieth century (the Great Acceleration) (Steffen et al. 2005). The retrospective evaluation of GC trends requires long-term monitoring data, which are scarce in most parts of the world due to logistical and economic limitations. Thus, sedimentary records are often the only alternative to evaluate the impacts of GC on aquatic and terrestrial ecosystems (Sanchez-Cabeza and Druffel 2009). Such records require precise and reliable chronologies to properly interpret environmental changes over time.

^{210}Pb dating (Krishnaswamy et al. 1971) is the most used method to establish sediment chronologies within the past ~100 years, the period of interest for most GC studies, as it allows evaluating the environmental changes that occurred since the Great Acceleration in comparison with the period 1900–1950. The total ^{210}Pb activity ($^{210}Pb_{tot}$) in the sediments include a detrital fraction (supported ^{210}Pb, $^{210}Pb_{sup}$), assumed to exist in secular equilibrium with ^{226}Ra, and a fraction that is scavenged from the water column (excess ^{210}Pb, $^{210}Pb_{xs}$), which is the one used for ^{210}Pb dating (Krishnaswamy et al. 1971). Beyond the ^{210}Pb temporal frame, ^{14}C dating is the most relevant method to obtain ages up to ~50,000 yr, and the combination of both dating methods can be useful for a better understanding of the environment´s natural variability. ^{210}Pb dating is usually complemented with stratigraphic markers to corroborate the age models. Above-ground nuclear bomb testing performed between the 1950s and 1960s resulted in elevated atmospheric concentrations of ^{137}Cs, plutonium isotopes, and ^{14}C. Therefore, it is expected that a core dated with ^{210}Pb would show maximum activities of these artificially produced radionuclides around 1962-1964, the period of maximum radioactive fallout from the atmospheric nuclear tests (UNSCEAR 2000).

Lakes provide a wide range of ecosystem services, such as water supply, flood damage reduction, biodiversity conservation, recreation, and aesthetic experiences. However, such valuable ecosystems may undergo rapid environmental changes, caused either by natural or anthropogenic causes. Pollution by sediments is a threat to lakes worldwide (Smol 2008). Increased sedimentation rates in lakes have been associated with diverse environmental problems, including water quality deterioration (Moges et al. 2017); shoaling, swamping, loss of water storage capacity, increased water levels, and flooding (Du et al. 2011; Degife et al. 2021); impacts on benthic ecosystems, which can affect organisms higher in the food web (Gravina et al. 2020); alteration of spawning grounds and reduction of the stock abundance of economically important fish species (Ranjan et al. 2019; McGlue et al. 2020). Stopping or reversing these negative changes requires effective lake management, for which it is critical to identify the sedimentation patterns and their drivers (Xu et al. 2017).

In many lakes, increasing sedimentation rates over the last century result from accelerated catchment soil erosion by runoff or wind, associated with land-use change and land management (Neff et al. 2008). Where anthropic influence is limited, climate variability may cause enhanced soil erosion and increased productivity (Pastor et al. 2019). Lakes with topographically closed basins (such as crater lakes), where the hydrological balance is primarily a function of rainfall and evaporation, are markedly sensitive to climate (Barr et al. 2014).

Temporal variations of magnetic susceptibility (MS) and element ratios (e.g. Rb/Sr, Ti/Ca, Ti/Al) have been used as proxies to evaluate changes in sediment provenance (Ruiz-Fernández et al. 2005) or climate variability (Shen et al. 2013; Jin et al. 2006; Martinez-Ruiz et al. 2015). The underlying assumption is that the mineral or major and trace element content in the detrital components of sediments may vary due to i) sediment input from sources with different mineralogy, or ii) chemical weathering of minerals (e.g., hydrolysis and solution)

driven by moisture and temperature (Wei et al. 2006). Humid conditions may favor higher values of MS (owing to the formation of secondary ferrimagnetic minerals; Dearing et al. 1996), of Rb/Sr (due to the significant increase of Rb in residual weathered debris relative to its source rocks; Jin et al. 2006) and Ti/Ca (as in-lake carbonate precipitation from evaporative concentration is reduced; Davies et al. 2015), but lower Ti/Al, owing to lower aeolian input (Martinez-Ruiz et al. 2015).

Santa María del Oro Lake (SAMO) is a small tropical crater lake in northwestern Mexico, surrounded by rural settlements. It has been described as a pristine reference site for paleoecological and environmental research (Zárate del Valle et al. 2007). Radiocarbon-dated sediment records from SAMO have provided information on long-term climate variability through identification of (a) variations of anoxic/oxic conditions in sediments during hot and dry periods, especially during *circa* 600 - 1140 CE, and 1410 - 1830 BCE (Vazquez-Castro et al. 2008), (b) the occurrence of droughts during the last 700 years, attributed to solar activity variability and/or climatic factors such as El Niño Southern Oscillation (Sosa-Nájera et al. 2010), (c) the alternation of dry and wet periods within the past ca. 2600 years, associated with variations of the intensities of the North American monsoon (Rodríguez-Ramírez et al. 2015), and (d) the impacts of drought on vegetation diversity (between 300 and 4200 cal BP) (Lozano-García et al. 2021).

Owing to its unique scenic beauty, SAMO has gradually developed as a tourist destination for at least 40 years, more importantly since 1995. In this short period, the environment has been modified, particularly through the construction of tourism facilities, which promoted the higher affluence of visitors (Moreno Moreno et al. 2015). The lake has also been affected by direct wastewater discharges from human settlements for several decades and by the proliferation of tourist boats. It has been used for small-scale cage fish farming projects and receives surface runoff through the surrounding agricultural areas and the culture of blue

agave for tequila production since 1999 (González-Bernal 2008). All these activities have likely contributed to changes in the environmental conditions of the system, including siltation, but this has not yet been assessed.

Our objective was to evaluate the temporal variations in sediment input to SAMO, using a combination of ^{14}C and ^{210}Pb dating. This is the first study on the recent evolution of accumulation rates in the lake, and we hypothesized that these changes are mainly due to anthropic induced catchment erosion, caused by population growth and agricultural activities.

High-resolution ^{210}Pb-dated sediment cores, corroborated with ^{137}Cs and $^{239+240}Pu$ (as stratigraphic markers for the maximum fallout caused by atmospheric thermonuclear weapon tests) allowed the retrospective reconstruction of sediment input to the lake within the past ~100 years. ^{14}C dating, attempted to determine the sedimentation rates beyond ^{210}Pb temporal framework, was unsuccessful and the reasons are discussed. Climate variability was also evaluated as a secondary driver of sediment input changes, by comparing the temporal variation of mass accumulation rates and the precipitation and evaporation data available for the past ~50 years from a nearby meteorological station. Multivariate techniques (cluster and factor analysis) were used to understand the dominant sources of sediments, and to evaluate the usefulness of MS and the element ratios Rb/Sr, Ti/Ca, and Ti/Al obtained from the dated cores, as proxies to investigate the factors controlling sedimentation.

Study area

SAMO is located at 750 m above sea level, within the Santa María del Oro Municipality (Mexican State of Nayarit), at ~4 km NE from the Santa Maria del Oro City (23,477 inhabitants in 2017; Fig. 1A). The lake lies within an extinct volcanic crater, part of the Trans-Mexican Volcanic Belt, which probably dates to the Pleistocene (Vázquez-Castro et al. 2008). It has a 2 km diameter, 3.7 km^2 surface area, 65 m maximum depth (Serrano et al. 2002), and

is characterized by steep sides and an almost flat bottom (Fig. 1B). SAMO is fed by rainfall, surface runoff, and groundwater, whereas water outflows mainly through evaporation, seepage (Rodríguez-Ramírez et al. 2015), and local water consumption. The aquifer that feeds SAMO is confined in volcanic (rhyolite, ignimbrite, basalt, porphyry, diorite, dacite, and andesite) rocks, and its water is sodium-bicarbonate type (DOF 2016).

SAMO is a warm oligomictic lake (surface water temperature ranging from 22.9°C to 31.1°C), that remains stratified most of the year (thermocline between 20 and 37 m depth) but has a short and incomplete mixing phase during winter (Cardoso et al. 2019). It is a mesotrophic lake, with high concentrations of silica (mean value: 356 ± 42 μM L^{-1}) and soluble reactive phosphorus (mean value: 3.0 ± 3.5 μM L^{-1}), it is slightly alkaline (pH >8) and has moderately hard waters (Caballero et al. 2013).

The climate in the region is classified as semi-warm sub-humid with summer rains (INEGI 2009), with mean monthly air temperatures ranging from 12.9°C to 29.1°C, mean annual rainfall of 1,220.4 mm, and mean annual evaporation of 1,705.6 mm (SMN 2020). The region has been reportedly affected by strong to very strong droughts (Hernández Cerda and Valdez Madero 2004). The catchment is characterized by extrusive igneous rocks (rhyolite acidic-tuff (45%) and basalt (37%)) and the main soil types are luvisol (30%) and regosol (23%) (INEGI 2009). The main productive activity in Santa María del Oro Municipality is agriculture, and the SAMO catchment (Fig. 1C) is reportedly affected by accelerated erosion, associated with agriculture, deforestation, and forest fires (PO 2003). The expanding agriculture frontier has been recognized among the critical zones for forest fires in Nayarit State since slash-and-burn agriculture is still in practice. A specific concern is associated with sugar cane and agave cultivation because farmers invade mountain lands, and each harvest season the wastes are burned carelessly, the fire spreads to the forest, creating large-scale forest fires (SEDATU, 2013; DEPCB, 2015).

Materials and methods

Field work

Cores SAMO 14-1, 14-2, and 14-3 were collected in 2014 at deep locations (below the thermocline, between 48 and 55 m depth), and SAMO 18-4, in 2018, at a shallower location (30 m), in a zone known as Agua Caliente Bay (Fig. 1B). The cores were retrieved with a UWITEC™ gravity corer, which provides intact sediment surfaces, using a transparent PVC tube (86 mm inner diameter, 1.0 m long). No signs of sediment disturbance (e.g. bubbles, burrows) were observed. As the sediments consisted of liquified soft muds, which could be easily disturbed during transportation, the cores were extruded onsite and sectioned at 1 cm intervals. An additional core, collected at the SAMO 14-1 location for lithologic description (Fig. ESM1), showed that the sediments were mainly made up of clayey silts without visible sandy layers. The uppermost segment (~31 cm) was composed of millimetric laminated dark greenish sediments, interbedded with whitish millimetric laminae, possibly formed by endogenous carbonates. The rest of the core consisted of alternating dark and light layers (mm-to-cm thick) except in the 44 to 58 cm segment, where homogeneous light greenish sediments were found.

Sinking particulate material was collected during two periods of six months each (May to November 2017, and November 2017 to May 2018) by using a sediment trap (PVC tube, 1 m long, 0.1 m inner diameter, aspect ratio of 10) located at 30 m depth (below the thermocline). Ten surface soil samples (1 cm thickness) were also collected in the lake surroundings in May 2019 (Fig. 1A). The sediment core, sediment trap, and soil samples were freeze-dried. The dry weight, thickness, and area of each core section were used to estimate dry bulk density

(g cm^{-3}). All samples were ground to powder with a porcelain mortar and pestle (except aliquots used for grain size determination) and kept in polyethylene bags until analysis.

Laboratory analysis

$^{210}Pb_{tot}$ activities were determined by alpha spectrometry (Alpha Ensemble Ortec/Ametek) according to Ruiz-Fernández and Hillaire-Marcel (2009). Gamma-ray spectrometry measurements were used to determine the activities of ^{226}Ra (through its daughter radionuclide in secular equilibrium ^{214}Pb; 352 keV) and ^{137}Cs (662 keV) in some of the core samples, using an OrtecHPGe well-detector (Ruiz-Fernández et al. 2014; Diaz-Asencio et al. 2020). $^{210}Pb_{sup}$ activities were estimated from the mean value of ^{210}Pb from the data where the ^{210}Pb activities are almost constant (Binford, 1990) and were confirmed by the ^{226}Ra activities. ^{137}Cs and $^{239+240}Pu$ activities (determined by alpha-particle spectrometry; Ruiz-Fernández et al. 2014) were used to corroborate the ^{210}Pb chronologies.

With the purpose to obtain information on sediment accumulation rates beyond the ^{210}Pb dating temporal frame, ^{14}C analyses were performed in bulk sediment samples from thirteen sections of core SAMO 14-2, one soil and two sediment trap samples (Table ESM1 in the electronic supplementary material), by accelerator mass spectrometry at ^{14}CHRONO Centre, Queen's University Belfast. One of the sediment trap samples (May-Nov, 2017) was also analyzed by ramped pyroxidation, a method by which bulk material can be partitioned into individual fractions, based on their resistance to decay (Rosenheim 2013), allowing to distinguish the presence of different sources of carbon. Data are reported as ^{14}C fraction modern ($F^{14}C$) and conventional ^{14}C ages; uncertainties are one standard deviation of the mean value.

Grain size distribution was determined by laser diffraction (Malvern Mastersizer 2000E). Loss on ignition, determined by sediment calcination at 550°C (LOI_{550}) and 950°C (LOI_{950}), were used to estimate the content of organic carbon (C_{org}) and inorganic carbon (C_{inorg}), respectively (Dean 1974). For magnetic susceptibility (MS) analysis, sediment aliquots (~1.5 g) were placed in a polyethylene tube (33 mm length, 6 mm internal diameter) and measured with a Bartington MS2 magnetic susceptibility meter coupled to an MSG2 frequency sensor. The elemental composition was determined by X-ray fluorescence spectrometry (XRF, Spectrolab Xepos-3) and results are expressed on a dry-weight basis.

Analysis of reference materials provided results within the reported range of the certified values: IAEA-300 (Radionuclides in Baltic Sea sediment, International Atomic Energy Agency) for ^{210}Pb and ^{137}Cs activities, IAEA-158 (Trace elements and methylmercury in marine sediment, International Atomic Energy Agency), and PACS-2 (Marine sediment reference materials for trace metals and other constituents, National Research Council Canada) for element concentrations, QAS3002 (Quality audit standard, Malvern™) for grain size percentages, and the reference material G-039 for magnetic susceptibility. Replicate analysis of a single sample (n = 6) yielded variation coefficients <10% for ^{210}Pb activities, <3% for elemental composition, <5% for grain size distribution and <3% for magnetic susceptibility.

Meteorological data

Mean monthly values of temperature, precipitation, and evaporation data (period 1963-2014) were obtained from the meteorological station Cerro Blanco (code 18005; SMN 2020), located at ~5 km NW from SAMO (Fig. 1A; 21°22'36" N, 104°37'06" W, 965.0 m above sea level). Missing records accounted ~2% of the total expected data for precipitation (14

monthly observations within eight different years), 12% for evaporation (65 observations, within 13 different years, including the whole period 2009-2012), and 6% for temperature (36 values within 8 years, including almost the whole period 1963-1964).

Data treatment

Sediment dating

The ^{210}Pb-derived chronologies were calculated with the constant flux (CF) model (Robbins 1978; Sanchez-Cabeza and Ruiz-Fernández 2012). This is a very robust model, with applicability in a wide type of environments (Sanchez-Cabeza et al. 2014), which assumes that $^{210}Pb_{ex}$ activities are directly proportional to the $^{210}Pb_{ex}$ flux to the sediments, but inversely proportional to the sediment mass loading (Krishnaswamy et al. 1971; Sanchez-Cabeza and Ruiz-Fernández, 2012). As its main hypothesis is that the $^{210}Pb_{ex}$ flux to the sediments is constant, it allows inferring temporal variations of sediment accumulation rates (SAR) and mass accumulation rates (MAR). Dating uncertainties were estimated by Monte Carlo simulations, a robust strategy that limits the overestimation of uncertainties, in comparison with the commonly used method of quadratic propagation of uncertainties (Sanchez-Cabeza et al. 2014).

Statistical analyses

Differences among the cores in the analyzed variables were assessed through analysis of variance (ANOVA) and Tukey post-hoc test, performed at a 95% confidence level by using R (R Core Team, 2021); significant differences are reported as $p<0.05$.

Factor Analysis (FA) was performed to identify the main sources of sediments to SAMO and how these vary among cores. It included 14 variables (MS, silt, sand, C_{org}, C_{inorg}, Al, Ca, Fe, K, Rb, Sr, Th, Ti, and Zr) from core sections and soil sample data (Minitab 15®). The communalities of all variables were >0.60, and the significant variables were those with loadings >0.70 (Hair et al. 2010).

A cluster analysis (complete linkage) was used to evaluate the association of the meteorological data (mean monthly values of temperature, and accumulated precipitation and evaporation) with MAR, MS, and the element ratios Rb/Sr, Ti/Ca, and Ti/Al, to assess their potential use as climate proxies to distinguish between wet and dry periods. The missing values of the meteorological database were filled with the mean value for the corresponding month (obtained from the whole database), and the monthly values were integrated to match the periods comprised in the sediment core sections, according to the ^{210}Pb ages.

Results

^{210}Pb dating

The $^{210}Pb_{sup}$ values were comparable among the cores (38.3±4.3 to 47.5±8.0 Bq kg^{-1}). The $^{210}Pb_{xs}$ activities decreased with depth in all cores, although in some core sections $^{210}Pb_{xs}$ values departed from an exponential decay trend (Fig. 2A). $^{210}Pb_{xs}$ fluxes (derived from the inventories; Sanchez-Cabeza and Ruiz-Fernández 2012) were comparable between cores SAMO 14-3 (159.2±6.1 Bq m^{-2} yr^{-1}) and SAMO 18-4 (147.7±7.9 Bq m^{-2} yr^{-1}), and higher than in cores SAMO 14-1 (108.7±4.8 Bq m^{-2} yr^{-1}) and SAMO 14-2 (80.5±4.3 Bq m^{-2} yr^{-1}). All sediment records spanned more than 100 years (Table 1).

Global fallout radionuclides

^{137}Cs activities

^{137}Cs activities (<1.0 – 33.3 Bq kg^{-1}) were similar among cores. The depth profiles of ^{137}Cs showed maxima at different depths (Fig. 2B), which according to the ^{210}Pb age model, correspond to similar age periods (SAMO 14-1: 16-17 cm, 1962-1966; SAMO 14-2: 16-17 cm, 1957-1964; SAMO 14-3: 28-29 cm, 1961-1963; and SAMO 18-4: 29-30 cm, 1964-1968).

^{239,240}Pu activities

Plutonium isotopes were determined in cores SAMO 14-2 and SAMO 18-4. ^{239,240}Pu activity ranges were 6.5 – 3,193 mBq kg^{-1} in SAMO 14-2, and 165 - 262 mBq kg^{-1} in SAMO 18-4 (Fig. 2B). The ^{239,240}Pu activity maxima were in SAMO 14-2 at 16-17 cm (1957 – 1964) and in SAMO 18-4 at 29-30 cm (1964 – 1968).

^{14}C dating

The F^{14}C values were below 1.0 at all analyzed sections of core SAMO 14-2, the sediment trap, and the soil samples (Table ESM1). A peak value of F^{14}C in the core was observed at the 13-14 cm depth section, 3 cm shallower than the ^{137}Cs and ^{239,240}Pu maxima (Fig. 2B). ^{14}C uncalibrated ages in SAMO 14-2 ranged from 1630±26 yr (56-57 cm depth) to 4012±33 yr (20-21 cm depth). The ^{14}C age of the soil sample (377±24 yr) was considerably younger than the core and sediment trap samples. The different fractions of the trap sample analyzed by ramped pyroxidation yielded similar ages (between 4,125±38 yr and 4,782±44 yr).

Accumulation rates

The overall accumulation rate ranges (Table 1) were 0.04-2.86 cm yr^{-1} (SAR) and 0.01-0.80 g cm^{-2} yr^{-1} (MAR; Fig. 3). In SAMO18-4, collected in a shallower location closer to the lakeshore (Fig. 1B), the MAR values (0.04-0.8 g cm^{-2} yr^{-1}) were higher than in the rest of the cores (overall range 0.01-0.65 g cm^{-2} yr^{-1}).

Between 1900 and 1950 (pre-1950 period), the mean SAR values ranged from 0.11±0.05 cm yr^{-1} (SAMO 14-2) to 0.22±0.09 cm yr^{-1} (SAMO 14-1), and mean MAR values ranged from 0.02±0.01 g cm^{-2} yr^{-1} (SAMO 14-2) to 0.09±0.07 g cm^{-2} yr^{-1} (SAMO 18-4). Neither SAR nor MAR showed significant differences among the cores; thus, the mean pre-1950 values (0.17±0.09 cm yr^{-1} and 0.05±0.04 g cm^{-2} yr^{-1}) can be used as reference values for SAMO.

Since 1950 onwards (post-1950 period), SAR and MAR values in all cores fluctuated considerably, with asynchronous subsurface maxima after the 1980s (Fig. ESM2). Also, all cores showed MAR values decreasing towards the surface, with topmost MAR values within the reference value interval (except for SAMO 14-3). During the post-1950 period, MARs in core SAMO 18-4 (0.26±0.17 g cm^{-2} yr^{-1}) were higher than in the cores from the deepest sampling sites (ranging from 0.07±0.09 g cm^{-2} yr^{-1} in SAMO 14-2 to 0.12±0.08 g cm^{-2} yr^{-1} in SAMO 14-3).

Sediment characterization

SAMO cores were mainly composed of silt (60 - 91%), with variable percentages of clay (7% - 29%) and sand (0 - 32%). The contents of sand, silt, clay, C_{inorg}, Mg, Zr, Sr, and U were comparable among cores, whereas the highest mean values of MS, Al, Ti, K, Rb, Fe, and Th,

and the lowest mean values of C_{org}, Mn and Ca were usually observed in core SAMO 18-4 (Fig. ESM3).

The temporal element profiles (Fig. 3) were similar among the cores. Between the 1900s and early 1960s, the profiles generally showed decreasing upwards values of MS and Al, Ti, Rb, and Zr concentrations, and increasing Ca and Sr concentrations, but afterward the records are noisier, with recurrent subsurface minima and maxima. The MAR maxima (Fig. 3) coincided with those of MS and terrigenous elements (e.g. Al, Ti, Rb), but not the other way around.

Sediment sources

In the factor analysis, the first two factors explained ~84% of the dataset variance (Fig. 4A, Table ESM2). In Factor 1 (~69% of the explained variance) the significant variables with positive loadings were elements related to terrigenous inputs (Th, K, Rb, Fe, Ti, Al, Zr) and MS, and with negative loadings, C_{inorg} and elements associated with carbonate precipitation (Ca, and Sr; Salminen et al. 2005). Factor 2 (~15% of the variance) included the silt percentages with positive loading, and of sand with negative loading. The distribution of the core sections was almost indistinguishable (Fig. 4B), while all soil samples grouped on the positive side of F1 (characterized by the association of the terrigenous elements), where most of the SAMO 18-4 samples are also found.

Influence of climate variability on sedimentation

Unlike temperature, the time series of annual accumulated precipitation and evaporation showed significant ($p<0.05$) decreasing trends (Fig. ESM4). Within the period with available

meteorological data, MAR maxima in all cores corresponded to precipitation minima and evaporation maxima (except in core SAMO 14-3). Also, most MAR maxima coincided with maxima of MS, Rb/Sr and Ti/Ca, and minima of Ti/Al (Fig. 5). Cluster analyses showed two main groups (Fig. 6) in all cores: the first one (brown) usually included MAR, MS, Rb/Sr, and Ti/Ca, and the second one (blue) included Ti/Al, precipitation, and evaporation, except for SAMO 18-4, in which MS was included in the second group. Mean temperature was in both groups (in the first one in cores 14-2 and 18-4; in the second one in cores 14-1 and 14-3). In brief, only Ti/Al ratios were consistently related to rainfall and evaporation in all cores.

Discussion

^{210}Pb dating

All cores showed some sections in which $^{210}Pb_{xs}$ activities did not follow an exponentially decreasing trend according to the radioactive decay law. This is not surprising since $^{210}Pb_{xs}$ activities are the balance between the $^{210}Pb_{ex}$ flux and MAR (Krishnaswamy et al. 1971), for which $^{210}Pb_{xs}$ activities can be diluted or enhanced by changes in sediment input. Thus, the non-monotonic $^{210}Pb_{xs}$ activity depth profiles were interpreted as a result of changes in sediment accumulation rates. The ^{210}Pb fluxes to the SAMO cores (80±4 - 159±6 Bq m^{-2} yr^{-1}) were comparable to the average $^{210}Pb_{ex}$ fallout estimated for North America (140 –185 Bq m^{-2} yr^{-1}, latitude 10 – 30 N; Preiss et al. 1996). This finding indicates that atmospheric deposition is the predominant pathway of $^{210}Pb_{ex}$ supply to the lake.

Reliability of the ^{210}Pb-derived age models

The ^{137}Cs and $^{239+240}Pu$ activity profiles were in good agreement and provided a proper corroboration of the ^{210}Pb chronologies in all cores (at least for the post-nuclear test period). In addition, the CF-derived ^{210}Pb chronologies were corroborated by using the Bayesian model Plum, and the comparison of both age models for SAMO 14-2 is presented in Aquino-López et al. (2020).

Compared to $^{239-240}Pu$, the broader peak of ^{137}Cs in SAMO 18-4 (Fig. 2B) is most likely caused by the delayed ^{137}Cs input through the accumulation of eroded soils from the catchment (Appleby et al. 2019) or post-depositional mobility of ^{137}Cs (Wang et al. 2017). $F^{14}C$ is defined as 1.0 for the preindustrial atmosphere (Schuur et al. 2016) and its value in a sample is used to distinguish between old (pre-1950, $F^{14}C < 1$) and modern (post-1950, $F^{14}C > 1$) (McCorkle et al. 2016). $F^{14}C$ values are <1.0 in all SAMO 14-2 sections, implying the presence of old carbon, even in sections deposited after the 1950s (Fig. 2C), and the increasing values between 13 and 17 cm most likely result from the ^{14}C atmospheric release during atmospheric nuclear weapons testing. The $F^{14}C$ subsurface maximum (13-14 cm, 1976.5±2.6) was above the ^{137}Cs and $^{239+240}Pu$ maxima, implying a time lag of ~11 years according to ^{210}Pb dating. This is because $^{239+240}Pu$ and ^{137}Cs are directly deposited to the water surface through atmospheric fallout and adsorbed onto sinking suspended matter; whereas the incorporation of ^{14}C into the sediments implies the air-water exchange of CO_2 (Glynn et al. 2013), its incorporation into the dissolved inorganic carbon pool and its assimilation as biomass of plants and photo- and chemo-autotrophic microbes (Gougoulias et al. 2014), that finally becomes part of the sinking matter that conforms the sediments.

^{14}C ages

As $F^{14}C$ indicated the presence of old carbon in the samples, before attempting to establish a ^{14}C chronology for SAMO 14-2, we evaluated the reservoir effect (RE) in the lake through comparison of the well corroborated ^{210}Pb-derived ages and conventional ^{14}C ages (Saulnier-Talbot et al. 2009; Blaauw et al. 2011) obtained for the same core sections (16-17 cm, ^{210}Pb age = 57±4 yr, ^{14}C age = 3874±34 BP; and 20-21 cm, ^{210}Pb age = 91±8 yr, ^{14}C age = 4012±33 BP). The age offset (~3,817 and ~3,921 yr, respectively) was comparable with the ^{14}C age of the sediment trap samples (~4,000 years, Table ESM1). The similar ages for the different fractions of the sediment trap sample from May-Nov, 2017 (low, medium, and high-temperature combustion, Table ESM1) indicated that all fractions have the same source. This indicates the occurrence of ^{14}C-depleted carbon in the lake, either caused by in-wash of eroded soil (containing reworked old organic material or detrital carbonates) or by a large lake reservoir effect. The youngest ^{14}C age (377±24 years) of the soil sample (compared with those from the sediment core and the trap samples, Table ESM1) did not stand for the input of such old carbon through eroded soils.

No previous study at SAMO reported problems related to ^{14}C dating. This may be due to the use of matrices other than bulk sediments (peat and wood; Vázquez-Castro et al. 2008, Rodríguez-Ramírez et al. 2015) and, when bulk sediments were used, age inconsistencies were not discussed (Sosa-Nájera et al. 2010; Lozano-García et al. 2021). None of those studies reported ^{210}Pb dating which, in this case, confirmed that the surface sediments in the SAMO cores are modern, thus, the ^{14}C values reflect a strong reservoir effect.

The reservoir effect can be temporally and spatially variable within the same lake, owing to differences in CO_2 air-water exchange rates, or in old carbon supply from the catchment (Zhou et al. 2020). The very variable ^{14}C ages of the SAMO sediments denoted a varying reservoir effect with time, making unfeasible to calibrate the ^{14}C ages and provide a longer-

term age-depth model. These results emphasize the convenience of combining well corroborated ^{210}Pb dating and ^{14}C to confirm the reliability of ^{14}C dates.

Accumulation rate ranges and temporal variability

The SAR ranges in SAMO were wider than those reported for other crater lakes in Mexico and other areas in the world, irrespective of altitude, annual precipitation, or type of environment (protected areas, rural or urban) surrounding the lakes (Table 2). High SAR values in SAMO could be related to the large soil erodibility of the predominant luvisols in the catchment, which is affected by high precipitation events, aeolian soil erosion, and soil degradation promoted by agricultural activities, especially in those areas where pasture lands are combined with rain-fed agriculture (Zamudio and Méndez 2011).

As SAR might be affected by compaction, MAR is a more reliable parameter to evaluate the impact of global change. Results showed that the sedimentation process in SAMO is spatially heterogeneous, with higher MAR towards the lakeshore (SAMO 18-4, Table 1), and variable over time, with higher MAR fluctuations during the post-1950 period (more evident since the 1980s; Fig. ESM2) but lower values in the more recent segment of all cores.

Influence of human activities on sedimentation

The factor analysis indicated that terrigenous input and carbonate precipitation are the dominant sediment sources at SAMO. Their influence is quite homogenous across the lake, and element composition variation is independent of the grain size distribution. The association of MS with terrigenous elements (Table ESM2, Fig. 4A) indicated that the strong changes of MS along the cores are related to changes in terrigenous supply to the lake, and

that MS could serve as a proxy for detrital influx variations. Soil erosion induced by land-use changes (e.g. land clearance for agriculture, cattle grazing, and development of human settlements) is an important factor for sediment accumulation in SAMO, especially towards the western side of the lake, which is surrounded by seasonal agriculture farmlands (Fig. 1C). This would also explain why SAMO 18-4 had (a) the lowest $^{210}Pb_{xs}$ activities, owing to dilution by higher sediment loads (Table 1); (b) the highest concentrations of terrigenous element concentrations (Fig. 3), and (c) the highest MAR values (Table 1).

The MAR fluctuations in the sediment records were not explained by the population growth (Fig. ESM5) or the temporal variations of the cultivated area (Fig. ESM6) in Santa María del Oro Municipality (where the agriculture data series are too short). However, it is noteworthy that corn, sugar cane, and agave cultivated areas have declined towards present (Fig. ESM6), particularly during the last decade, when MAR values also decreased. Likely, the reduction of the cultivated areas (and consequently, of the common activities that promote soil erosion, such as plowing and burning) has contributed to some extent, to reduce the erosion in the catchment and control the sedimentation pulses in SAMO.

Influence of climate variability on sedimentation

Rainfall may be the primary cause of erosion in many environmental settings, as water facilitates the weathering process that precedes erosion in most environmental settings, and it is also one of the main agents for sediment transport (Mishra et al. 2019). Considering the underlying assumptions behind the use of the element ratios and the decreasing trends in annual accumulated precipitation and evaporation (Fig. ESM4), the decreasing values of MS, Rb/Sr, and Ti/Ca before the 1980s (Fig. 5) would indicate lower terrigenous supply and higher endogenic carbonate precipitation, favored by higher lake water evaporation rates (Jin et al.

2006; Davies et al. 2015), and increasing Ti/Al values would account for a higher aeolian input (Martínez-Ruiz et al. 2015), in both cases promoted by the development of drier climate conditions in the area. Thus, MS and element ratios can reproduce the general pattern of rain variability before the 1980s, and the interrupted increasing MAR trends in all cores between 1960s and 1980s (Fig. 5). However, all MAR maxima occurring after the 1980s corresponded to annual accumulated precipitation minima (Fig. 5) and were usually characterized by maxima of MS, Rb/Sr, and Ti/Ca, and minima of Ti/Al, which would be indicative of humid conditions. This contradiction is caused by the relatively high concentrations of Al, Ti, and Rb in the core sections where the MAR maxima were recorded (Fig. 3), which also indicated that these sporadic sedimentation pulses have a terrigenous origin.

These results may be conditioned by some limitations. The meteorological data come from a station 5 km apart and 200 m above the SAMO altitude, so they may not accurately reflect the specific conditions at the study site; and these series are relatively short and have several gaps (mainly evaporation data). Moreover, the cores were cut into 1 cm thick sections and, given the millimeter-laminated nature of these sediments, it is possible that sediments with different origins may have been mixed. In addition, within the period for which meteorological data are available (1964-2014), the geochemical records of the sediment cores are noisier (Fig. 3).

We speculate that the terrigenous pulses could be related to the accelerated erosion of the SAMO catchment (PO 2003), caused by deforestation, agriculture, and forest fires. These fires are attributed to extreme temperatures, droughts, and uncontrolled (domestic and agriculture) waste burning (INIFAP 2012; SEDATU 2013). The coincident MAR and MS maxima could be the result of topsoil magnetic enhancement produced by wildfires, owing to the pyrogenic-induced transformation on mineral constituents of the soils or in vegetation ashes (Till et al. 2021). Specific records on the frequency and extent of the wildfires in the

study area are not available to test this hypothesis. Nonetheless, soil erodibility increases during dry periods due to lower soil moisture (Toy et al. 2002), and sediment yields may significantly increase after wildfires (DiBiase and Lamb 2019) owing to the loss of protective ground cover holding the soil in place, which reduces the threshold of intensity and amount of rainfall needed for erosion in normal conditions. Post-fire erodibility is highest because of water repellency and exposure of denuded soils to rainfall. Increased sediment loading can produce episodes of exceptionally high rates of sediment transport, which tend to be transient and irregular; however, with vegetation recovery, rates of hillslope erosion typically return to pre-burn levels within a few years to one decade (Ryan et al. 2011). It is expected that climate change will increase the extent of wildfires worldwide, increasing catchment erosion and sedimentation in aquatic ecosystems, which would reduce the water storage and may impact the water quality owing to the input of contaminants adsorbed to the sediments (Sankey et al. 2017).

Conclusions

The temporal variations of sediment accumulation rates within the past ~100 years were reconstructed through the study of ^{210}Pb-dated sediment cores, collected from Santa María del Oro Lake, a developing tourism spot in northwestern Mexico. Results showed that lake sedimentation is spatially and temporally heterogeneous with overall mass accumulation rates (MAR) ranging from 0.01 to 0.80 g cm^{-2} yr^{-1}, and sediment accumulation rates (SAR) from 0.04 to 2.86 cm yr^{-1}. Highest MAR and SAR values were observed near the lakeshore (at Agua Caliente Bay), most likely caused by its shallowness, the closeness to surrounding human settlements and agriculture fields, as well as the influence of seasonal runoff entering the lake from surrounding hills. The highest variations in MAR and SAR values in all cores

were observed within the second half of the last century, although only in Agua Caliente Bay the post-1950s values of MAR (0.26 ± 0.17 g cm^{-2} yr^{-1}) were significantly higher than during the first half of the century (0.08±0.07 g cm^{-2} yr^{-1}). MAR variations were mainly attributed to a combination of land-use change and climate variability. Sedimentation pulses observed in all cores, mostly since the 1980s, have occurred during years of minimum precipitation. This could be the result of increasing soil erodibility due to lower soil moisture and the occurrence of wildfires in the catchment. Despite MARs having decreased in the last decade, results highlighted the lake´s susceptibility to siltation problems; sedimentation pulses may happen again and unregulated human activities can only worsen this problem. Considering the close relation between drier conditions, wildfires, and soil erosion, it is foreseen that climate change would promote higher sedimentation in downstream rivers and reservoirs, negatively impacting water supply and quality. Thus, controls on human settlement developments, agriculture practices, and mitigation measures against catchment erosion should be implemented in the surroundings of SAMO to preserve the conditions of this valuable water resource.

Acknowledgments

This work was supported by the grants UNAM DGAPA-PAPIIT/104718 and Newton Mobility Grant NMG\R2\170126. Support by the Posgrado en Ciencias del Mar y Limnología, UNAM and a postgraduate studies fellowship from CONACyT (CVU 969662) is acknowledged by DMHR. Thanks are due to Cuellar-Martínez T.C., López-Mendoza P. G., Ramírez-Macías E. S., Sanchez-Rivas J.L., and García-Arvizu J. M. for technical support in radiometric analysis; and to Germán Ramírez, Carlos Suárez and León Felipe Álvarez for data curation and artwork assistance.

References

Alcocer J, Ruiz-Fernández AC, Oseguera LA, Caballero M, Sanchez-Cabeza JA, Pérez-Bernal LH, Hernández-Rivera DM (2020) Sediment carbon storage increases during the Anthropocene in tropical, oligotrophic, high-mountain lakes. Anthropocene 32, 100272

Alvisi F, Frignani M (1996) ^{210}Pb-derived sediment accumulation rates for the central Adriatic Sea and crater lakes Albano and Nemi (central Italy) In: Palaeoenvironmental analysis of Italian Crater Lake and Adriatic Sediments P Guilizzoni and F Oldfield (eds) Memorie dell'Istituto Italiano di Idrobiologia. Int J Limnol 55: 303-320

Appleby PG, Semertzidou P, Piliposian GT, Chiverrell RC, Schillereff DN, Warburton J (2019) The transport and mass balance of fallout radionuclides in Brotherswater, Cumbria (UK). J Paleolimnol 62, 389 – 407

Aquino-López MA, Ruiz-Fernández AC, Blaauw M, Sanchez-Cabeza JA (2020). Comparing classical and Bayesian ^{210}Pb dating models in human-impacted aquatic environments. Quat Geochronol 60, 101106

Barr C, Tibby J, Gell P, Tyler J, Zawadzki A, Jacobsen GE (2014) Climate variability in south-eastern Australia over the last 1500 years inferred from the high-resolution diatom records of two crater lakes. Quat Sci Rev 95, 115-131

Blaauw M, van Geel B, Kristen I, Plessen B, Lyaruu A, Engstrom DR, van der Plicht J, Verschuren D (2011) High-resolution ^{14}C dating of a 25,000-year lake-sediment record from equatorial East Africa. Quat Sci Rev 30, 3043-3059

Caballero M, Rodríguez A, Vilaclara G, Ortega B, Roy P, Lozano S (2013) Hydrochemistry, ostracods and diatoms in a deep, tropical, crater lake in Western Mexico. J Limnol 72: 512-523

Cardoso-Mohedano JG, Sanchez-Cabeza JA, Ruiz-Fernández AC, Pérez-Bernal LH, Lima-Rego J, Giralt S (2019) Fast deep water warming of a subtropical crater lake. Sci Total Environ 691: 1353-1361

Davies SJ, Lamb HF, Roberts SJ (2015). Micro-XRF Core Scanning in Palaeolimnology: Recent Developments. In: Croudace, I W, Rothwell, RG (2015) Micro-XRF Studies of Sediment Cores: Applications of a non-destructive tool for the environmental sciences. Springer, Dordrecht

Dean WE (1974) Determination of carbonate and organic matter in calcareous sediments and sedimentary rocks by loss on ignition: comparison with other methods. J Sediment Petrol 44: 242–248

Dearing JA, Hay KL, Baban SM, Huddleston AS, Wellington EM, Loveland P (1996) Magnetic susceptibility of soil: an evaluation of conflicting theories using a national data set. Geophys J Int 127: 728-734

Degife A, Worku H, Gizaw S (2021) Environmental implications of soil erosion and sediment yield in Lake Hawassa watershed, south-central Ethiopia. Environ Syst Res 10, 28, 2-24

Du Y, Xue HP, Wu SJ, Ling F, Xiao F, Wei XH (2011). Lake area changes in the middle Yangtze region of China over the 20th century. J Environ Manage 92, 4, 1248-1255

DEPCB (2015). Plan estatal de contingencias para incendios forestales 2015. Dirección Estatal de Protección Civil y Bomberos. http://www.proteccioncivil.gob.mx/work/models/ProteccionCivil/swbcalendario_ElementoSeccion/675/PROGRAMA_ESTATAL_DE_CONTINGENCIAS_PARA_INCENDIOS_FORESTALES_2015.PDF

Díaz-Asencio M, Sanchez-Cabeza JA, Ruiz-Fernández AC, Corcho-Alvarado JA, Pérez-Bernal LH (2020). Calibration and use of well-type germanium detectors for low-level gamma-ray spectrometry of sediments using a semi-empirical method. J Environ Radioact 225: 106385

DiBiase RA, Lamb MP (2019) Dry sediment loading of headwater channels fuels post-wildfire debris flows in bedrock landscapes. Geology 48: 189–193

DOF (2016) Acuerdo por el que se da a conocer el resultado de los estudios técnicos de las aguas nacionales subterráneas del Acuífero Valle de Santa María del Oro, clave 1812, en el Estado de Nayarit, Región Hidrológico-Administrativa Lerma-Santiago-Pacífico 6. Diario Oficial de la Federación. https://www.dof.gob.mx/ Accessed: 2020-06-19

Glynn D, Druffel E, Griffin S, Dunbar RB, Osbourne M, Sanchez-Cabeza JA (2013) Early bomb radiocarbon detected in Palau Archipelago corals. Radiocarbon 55: 1659 – 1664

González-Bernal V M (2008) Problemática socioeconómica de los productores independientes de agave azul del municipio de Santa Maria del Oro, Nayarit, 1996-2006 Dissertation Universidad Autónoma de Nayarit Tepic, 115 pp (in Spanish)

Gougoulias C, Clark J M, Shaw LJ (2014) The role of soil microbes in the global carbon cycle: tracking the below- ground microbial processing of plant- derived carbon for manipulating carbon dynamics in agricultural systems. J Sci Food Agric 94: 2362-2371

Gravina A, Soreghan M, Bogan MT, Busch J, McGlue M, McIntyre P, Kimirei I, Cohen A (2020). Relationship of sediment influx to ostracode populations on the variably deforested Luiche and Mahale platform coasts of Lake Tanganyika, Tanzania. J Great Lakes Res 46, 5, 1207-1220

Hair J, Black W, Babin B, Anderson R (2010). Multivariate data analysis. 7th ed. Prentice Hall New Jersey

Hernández Cerda ME, Valdez Madero G (2004) Sequía meteorológica In: Cambio climático: una visión desde México J Martínez and A Fernández Bremauntz (eds) Instituto Nacional de Ecología, Mexico City, Mexico, pp 315-325

INEGI (2009) Prontuario de información geográfica municipal de los Estados Unidos Mexicanos Clave 18014 Instituto Nacional de Estadística, Geografía e Informática https://www.inegi.org.mx/contenidos/app/mexicocifras/datos_geograficos/18/18014.pdf Accessed: 2020-06-30

INIFAP (2012) Programa de Acción ante el Cambio Climático de Nayarit Resumen Ejecutivo. Instituto Nacional de Investigaciones Forestales, Agrícolas y Pecuarias Tepic, Mexico. https://www.gob.mx/cms/uploads/attachment/file/164935/2012_nay_pacc.pdf

Jin Z, Cao J, Wu J, Wang S (2006) A Rb/Sr record of catchment weathering response to Holocene climate change in Inner Mongolia. Earth Surf Processes Landforms 31: 285-291

Krishnaswamy S, Lal D, Martin JM, Meybeck M (1971). Geochronology of lake sediments. Earth Planet Sci Lett 11: 407-414

Lefkowitz JN, Varekamp J C, Reynolds RW, Thomas E (2017) A tale of two lakes: the Newberry Volcano twin crater lakes, Oregon, USA. In: Geochemistry and Geophysics of Active Volcanic Lakes Ohba, T, Capaccioni, B Caudron, C (eds). Spec Publ 437: 253–288

Lozano-García S, Figueroa-Rangel B, Sosa-Nájera S, Caballero M, Noren AJ, Metcalfe SE, Tellez-Valdés O, Ortega-Guerrero B (2021) Climatic and anthropogenic influences on vegetation changes during the last 5000 years in a seasonal dry tropical forest at the northern limits of the Neotropics. The Holocene 31(5) 802–813

Martinez-Ruiz F, Kastner M, Gallego-Torres D, Rodrigo-Gámiz M, Nieto-Moreno V, Ortega-Huertas M (2015) Paleoclimate and paleoceanography over the past 20,000 yr in the Mediterranean Sea Basins as indicated by sediment elemental proxies. Quat Sci Rev 107: 25-46

McCorkle EP, Berhe AA, Hunsaker CT, Johnsone DW, McFarlane KJ, Fogel ML, Hart SC (2016) Tracing the source of soil organic matter eroded from temperate forest catchments using carbon and nitrogen isotopes. Chem Geol 445, 172–184

McGlue MM, Yeager KM, Soreghan MJ, Behm M, Kimirei IA, Cohen AS, Apse C, Limbu P, Smiley RA, Doering D, Lucas JS, Mbonde A, McInytre PB (2021). Spatial variability in nearshore sediment pollution in Lake Tanganyika (East Africa) and implications for fisheries conservation. Anthropocene 33, 100281

Mishra AK, Placzek C, Jones R (2019) Coupled influence of precipitation and vegetation on millennial-scale erosion rates derived from ^{10}Be. PLoS ONE 14: e0211325

Moges MA, Schmitter P, Tilahun SA, Ayana EK, Ketema AA, Nigussie TE, Steenhuis TS (2017). Water Quality Assessment by Measuring and Using Landsat 7 ETM+ Images for the Current and Previous Trend Perspective: Lake Tana Ethiopia. Journal of Water Resource and Protection 9,12, 1564-1585

Moreno-Moreno LR, Orozco Espinosa P, Barrón Arreola KS (2015) Turismo y medio ambiente Una aplicación del método de costo de viaje en la Laguna de Santa María del Oro, Nayarit In: Temas selectos de turismo y sustentabilidad, KS Barrón Arreola, MA Fonseca Morales (Eds) Universidad Autónoma de Nayarit, Tepic, pp 157-182 (in Spanish)

Neff JC, Ballantyne AP, Farmer GL, Mahowald NM, Conroy JL, Landry CC, Overpeck JT, Painter TH, Lawrence CR, Reynolds RL (2008) Increasing eolian dust deposition in the western United States linked to human activity. Nat Geosci 1: 189-195

Ngos III S, Sirocko F, Lehné R, Giresse P, Servant M (2008) The evolution of the Holocene palaeoenvironment of the Adawama of Cameroon: evidence from sediments from two crater lakes near Ngaoundéré In: Dynamics of forest ecosystems in central Africa during the Holocene: past-present-future. Palaeoecology of Africa J Runge (ed) CRC Press, Boca Raton, USA, pp 103-120

Pastor AV, Nunes JP, Ciampalini R, Koopmans M, Baartman J, Huard F, Calheiros T, Le-Bissonnais Y, Keizer JJ, Raclot D (2019) Projecting future impacts of global change including fires on soil erosion to anticipate better land management in the forests of NW Portugal. Water 11, 2617, 2-19

PO (2003) Acuerdo por el que se expide el programa de ordenamiento ecológico de la cuenca de Santa María del Oro, Nayarit Periódico Oficial, 12 February 2003, CLXXII, 19, Tepic, Mexico (in Spanish), 93 pp

Preiss N, Mélieres MA, Pourchet M (1996) A compilation of data on lead-210 concentration in surface air and fluxes at the air-surface and water-sediment interfaces J Geophys Res 101: 28847–28862

R Core Team (2021). R: A language and environment for statistical computing. R Foundation for Statistical Computing, Vienna, Austria. Available online at https://www.R-project.org/

Ranjan R (2019). A forestry-based PES mechanism for enhancing the sustainability of Chilika Lake through reduced siltation loading. Forest Policy Econ 106, 101944

Robbins JA (1978) Geochemical and geophysical applications of radioactive lead In: Nriagu, JO (Ed), Biogeochemistry of Lead in the Environment Elsevier Scientific, Amsterdam, pp 285-393

Rodríguez-Ramírez A, Caballero M, Roy P, Ortega B, Vázquez-Castro G, Lozano-García S (2015) Climatic variability and human impact during the last 2000 years in western Mesoamerica: evidences of late Classic and Little Ice Age drought events. Clim Past 11: 1239-1248

Rosenheim BE, Santoro JA, Gunter M, Domack EW (2013) Improving Antarctic sediment ^{14}C dating using ramped pyrolysis: an example from the Hugo Island Trough. Radiocarbon 55: 115-126

Ruiz-Fernández AC, Hillaire-Marcel C, Páez-Osuna F, Ghaleb B, Caballero M (2007) ^{210}Pb chronology and trace metal geochemistry at Los Tuxtlas, Mexico, as evidenced by a sedimentary record from the Lago Verde Crater Lake. Quat Research 67: 181-192

Ruiz-Fernández AC, Hillaire-Marcel C (2009) ^{210}Pb-derived ages for the reconstruction of terrestrial contaminant history into the Mexican Pacific coast: Potential and limitations. Mar Pollut Bull 59: 134-145

Ruiz-Fernández AC, Maanan M, Sanchez-Cabeza,JA, Pérez Bernal LH, López Mendoza P, Limoges A (2014) Cronología de la sedimentación reciente y caracterización geoquímica de

los sedimentos de la laguna de Alvarado, Veracruz (suroeste del golfo de México). Cienc Mar 40: 291-303

Ruiz-Fernández AC, Páez-Osuna F, Urrutia-Fucugauchi J, Preda M (2005) ^{210}Pb geochronology of sediment accumulation rates in Mexico City Metropolitan Zone as recorded at Espejo de los Lirios lake sediments. Catena 61: 31-48

Ryan SE, Dwire KA, Dixon MK (2011) Impacts of wildfire on runoff and sediment loads at Little Granite Creek, western Wyoming. Geomorphology 129: 113–130

Salminen R, Bautista M J, Bidovec M, Demetriades A, De Vivo B, De Vos W, Duris M, Gilucis A, Gregorauskiene V, Halamic J, Heitzmann P, Lima A, Jordan G, Klaver G, Klein P, Lis J, Locutura J, Marsina K, Mazreku A, O'Connor PJ, Olsson SA, Ottesen RT, Petersell V, Plant JA, Reeder S, Salpeteur I, Sandström H, Siewers U, Steenfelt A, Tarvainen T (2005) Geochemical Atlas of Europe Part 1: Background Information, Methodology and Maps. Geological Survey of Finland, Espoo

Sanchez-Cabeza JA, Druffel ER (2009) Environmental records of anthropogenic impacts on coastal ecosystems: an introduction. Mar Pollut Bull 59: 87-90

Sanchez-Cabeza JA, Ruiz-Fernández AC (2012) ^{210}Pb sediment radiochronology: an integrated formulation and classification of dating models. Geochim Cosmochim Acta 82: 183-200

Sanchez-Cabeza JA, Ruiz-Fernández AC, Ontiveros-Cuadras JF, Pérez-Bernal LH, Olid C (2014) Monte Carlo uncertainty calculation of ^{210}Pb chronologies and accumulation rates of sediments and peat bogs. Quat Geochronol 23: 80-93

Sankey JB, Kreitler J, Hawbaker TJ, McVay JL, Miller ME, Mueller ER, Vaillant NM, Lowe SE, Sankey TT (2017) Climate, wildfire, and erosion ensemble foretells more sediment in western USA watersheds. Geophysical Research Letters 44: 8884-8892

Saulnier-Talbot E, Pienitz R, Stafford TW Jr (2009) Establishing Holocene sediment core chronologies for northern Ungava lakes, Canada, using humic acids (AMS ^{14}C) and ^{210}Pb. Quat Geochronol 4, 278–287

Schuur EAG, Druffel ERM, Trumbore SE (2016) Radiocarbon and Climate Change Mechanisms, Applications and Laboratory Techniques. Springer, Switzerland

SEDATU (2013) Atlas de riesgos del municipio de Santa María del Oro, Nayarit. Secretaría de Desarrollo Agrario, Territorial y Urbano Santa María del Oro, Mexico

Serrano D, Filonov A, Tereshchenko I (2002) Dynamic response to valley breeze circulation in Santa Maria del Oro, a volcanic lake in Mexico. Geophys Res Lett 29:27-31

Sert I (2018) Applying of modified constant rate of supply model to lake sediments in ^{210}Pb dating and assessment of some heavy metals. J Nat Appl Sci 22: 598-607

Shen J, Wu X, Zhang Z, Gong W, He T, Xu X, Dong H (2013) Ti content in Huguangyan maar lake sediment as a proxy for monsoon- induced vegetation density in the Holocene. Geophys Res Lett 40: 5757-5763

SMN (2020) Normales Climatológicas por Estado/Nayarit Servicio Meteorológico Nacional, Comisión Nacional del Agua https://smnconaguagobmx/es/informacion-climatologica-por-estado?estado=nay Accessed: 2020-05-28

Smol JP (2008) Pollution of Lakes and Rivers A Paleoenvironmental Perspective. Blackwell Publishing, Oxford

Soeprobowati TR, Suedy SWA, Hadiyanto, Lubis AA, Gell P (2018) Diatom assemblage in the 24 cm upper sediment associated with human activities in Lake Warna Dieng Plateau Indonesia. Environ Technol Inno 10: 314–323

Sosa-Nájera, S, Lozano-García, S, Roy, P D, Caballero, M (2010) Registro de sequías históricas en el occidente de México con base en el análisis elemental de sedimentos lacustres: El caso del lago de Santa María del Oro. Bol Soc Geol Mex 62: 437-451

Steffen W, Sanderson A, Tyson PD, Jäger J, Matson PA, Moore B III, Oldfield F, Richardson K, Schellnhuber HJ, Turner II BL, Wasson RJ (2005) Global Change and the Earth System - A Planet Under Pressure Springer, New York

Till JL, Moskowitz B, Poulton S W (2021) Magnetic properties of plant ashes and their influence on magnetic signatures of fire in soils. Front Earth Sci 8, 1-16

Toy TJ, Foster, GR, Renard KG (2002) Soil Erosion: Processes, Prediction, Measurement, and Control. John Wiley & Sons, New York

UNSCEAR (2000) Sources and effects of ionizing radiation United Nations Scientific Committee on the Effects of Atomic Radiation UNSCEAR 2000 Report to the General Assembly, with Scientific Annexes. Volume I: sources United Nations, New York

Vázquez-Castro G, Ortega-Guerrero B, Rodríguez A, Caballero M Lozano-García S (2008) Mineralogía magnética como indicador de sequía en los sedimentos lacustres de los últimos ca 2,600 años de Santa María del Oro, occidente de México. Revista Mexicana de Ciencias Geológicas 25: 21-38

Wang J, Baskaran M, Niedermiller J (2017) Mobility of ^{137}Cs in freshwater lakes: A mass balance and diffusion study of Lake St Clair, Southeast Michigan, USA. Geochim Cosmochim Acta 218: 323-342

Wei G, Li XH, Liu Y, Shao L, Liang X (2006) Geochemical record of chemical weathering and monsoon climate change since the early Miocene in the South China Sea. Paleoceanogr Paleoclimatol 21: 1-11

Yim SA, Chae JS, Byun JI, Ko SH (2018) Characteristics of artificial radionuclides in sedimentary soil cores from a volcanic crater lake. J Environ Radioact 192:532–542

Xu M, Dong X, Yang X, Chen X, Zhang Q, Liu Q, Wang R, Yao M, Davidson TA, Jeppesen E (2017). Recent Sedimentation Rates of Shallow Lakes in the Middle and Lower Reaches of the Yangtze River: Patterns, Controlling Factors and Implications for Lake Management. Water 9, 617, 2-18.

Zamudio V, Méndez E (2011) The vulnerability of agricultural soils to erosion in the central-south region of the State of Nayarit, Mexico. Ambiente y Desarrollo XV 28: 11-40

Zárate-Del Valle PF, Gomez-Hermosillo CM; Venegas-Garcia DJ (2007) Crater-lake Santa Maria del Oro as a Pristine Reference for Persistent Organic Pollutants (POP's) and Heavy Metals Content in Environmental Investigations in Western Mexico (Project CONACYT-SEMARNAT 2002-C01-0463, in Progress). American Geophysical Union, Fall Meeting 2007. Eos Trans AGU 88:(52), Fall Meet Suppl, Abstract B33C-1427

Zhou K, Xu H, Lan J, Yan D, Sheng E, Yu K, Song Y, Zhang J, Fu P, Xu S (2020) Variable Late Holocene 14C Reservoir Ages in Lake Bosten, Northwestern China. Frontiers in Earth Science 7, 328, 1-11

FIGURE CAPTIONS

Fig. 1. Sampling information. A= Santa María del Oro Lake (SAMO) and Santa María del Oro City, NW Mexico; yellow dots indicate CB (Cerro Blanco meteorological station) and the soil sample location. B = the inset shows Mexico, Nayarit (grey) and the lake location (black circle); bathymetry and sampling locations of sediment trap and cores in SAMO (SAMO 14-1: 21.369° N, 104.565° W, 55 m depth; SAMO 14-2: 21.370° N, 104.572° W, 48.2 m; SAMO 14-3: 21.372° N, 104.572° W, 52 m; and shallow core: SAMO 18-4: 21.371° N, 104.577° W, 30 m (Agua Caliente Bay)). C = land use and vegetation in the catchment of SAMO.

Fig. 2. Dating Information for sediment cores from Santa Maria del Oro Lake, NW Mexico. A= activity depth profiles of $^{210}Pb_{tot}$ and ^{226}Ra; B= ^{210}Pb-derived age models and activities of ^{137}Cs and $^{239+240}Pu$ (orange and gray bars, respectively; logarithmic values); C= on the left, depth profiles of $F^{14}C$ values (empty circles) and ^{137}Cs activities (orange circles); on the right, conventional ^{14}C ages in sediment core SAMO 14-2.

Fig. 3. Temporal profiles of sediment variables in cores from Santa María del Oro Lake, NW Mexico. Units are: mass accumulation rate (MAR, g cm^{-2} yr^{-1}; logarithmic values); magnetic susceptibility (x 10^{-5} SI); clay, silt, sand, C_{org}, C_{inorg}, Al, Ti, Fe, K and Ca (%); Rb, Zr, Th, and Sr (µg g^{-1}).

Fig. 4. Factor analysis results for sediments from Santa María del Oro Lake, NW Mexico. A= loadings of variables for factors 1 and 2; B = score of observations (sediment core and soil samples).

Fig. 5. Temporal profiles of mass accumulation rates (MAR, g cm^{-2} yr^{-1}), meteorological data (Cerro Blanco Station), magnetic susceptibility (MS) and element ratios for sediment cores from Santa María del Oro Lake, Mexico. Filled dots indicate the maxima of MAR (orange) and corresponding minima or maxima (blue) of other variables.

Fig. 6. Cluster analysis for meteorological data (mean annual temperature, and accumulated precipitation and evaporation from Cerro Blanco Station (1963 - 2014) and variables (mass accumulation rate, MAR; magnetic susceptibility, MS; and the ratios Rb/Sr, Ti/Ca, and Ti/Al) from sediment cores collected at Santa María del Oro Lake, NW Mexico.

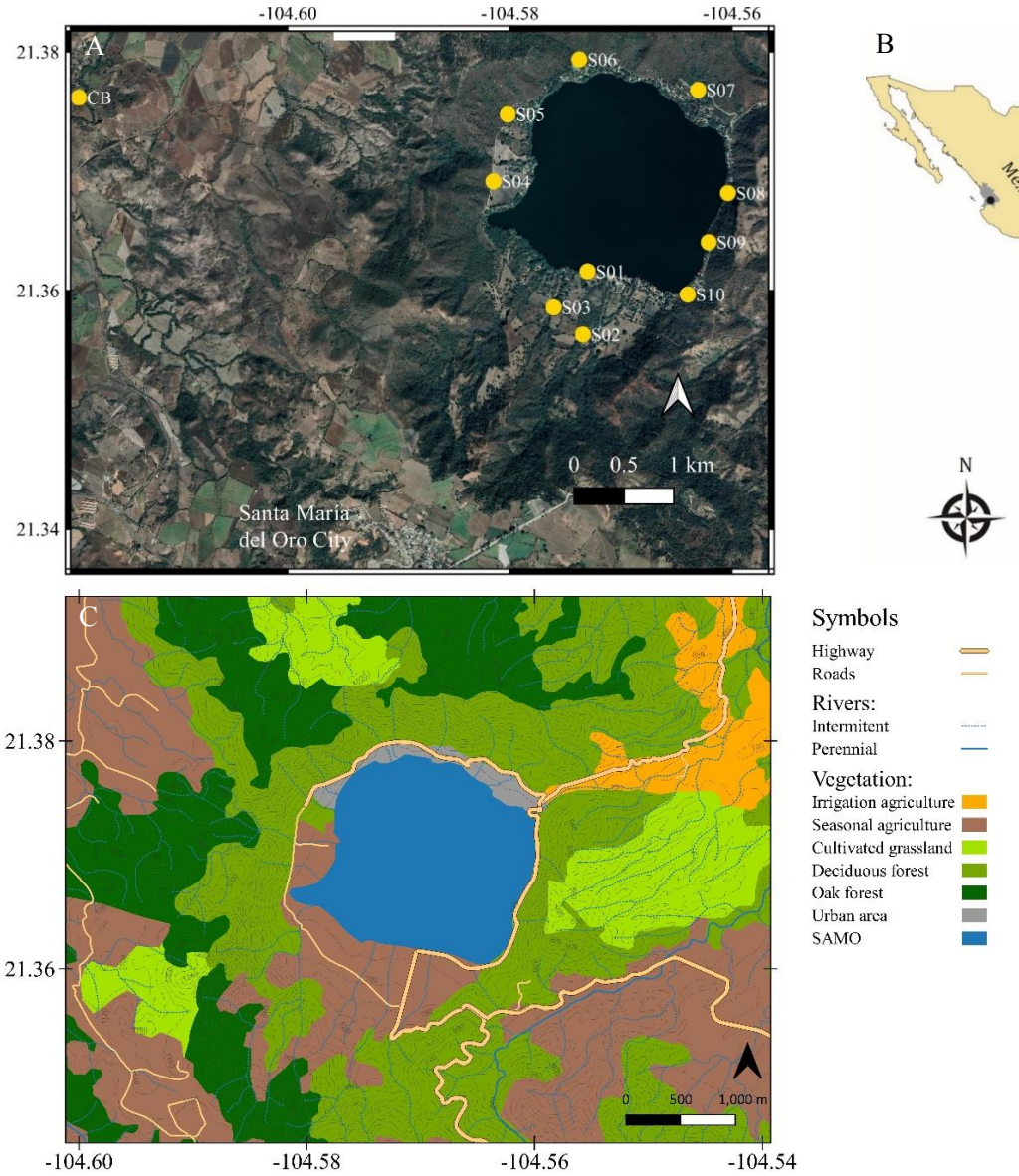

Fig 1.

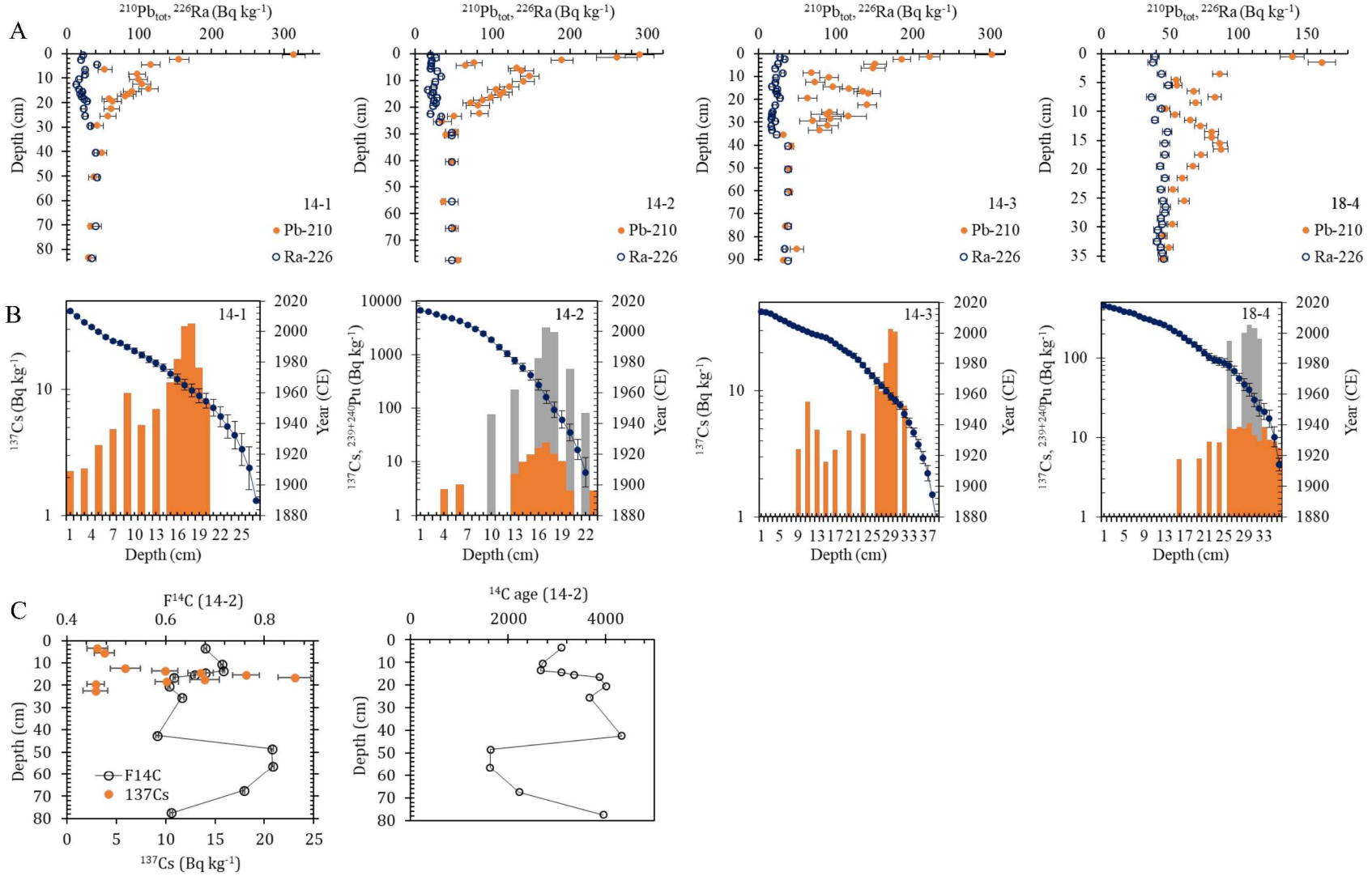
A
B
C
$^{210}Pb_{tot}$, ^{226}Ra (Bq kg^{-1})
Depth (cm)
14-1
14-2
14-3
18-4
Pb-210
Ra-226
^{137}Cs (Bq kg^{-1})
^{137}Cs, $^{239+240}Pu$ (Bq kg^{-1})
Year (CE)
Depth (cm)
F^{14}C (14-2)
^{14}C age (14-2)
F14C
137Cs
^{137}Cs (Bq kg^{-1})

Fig. 2.

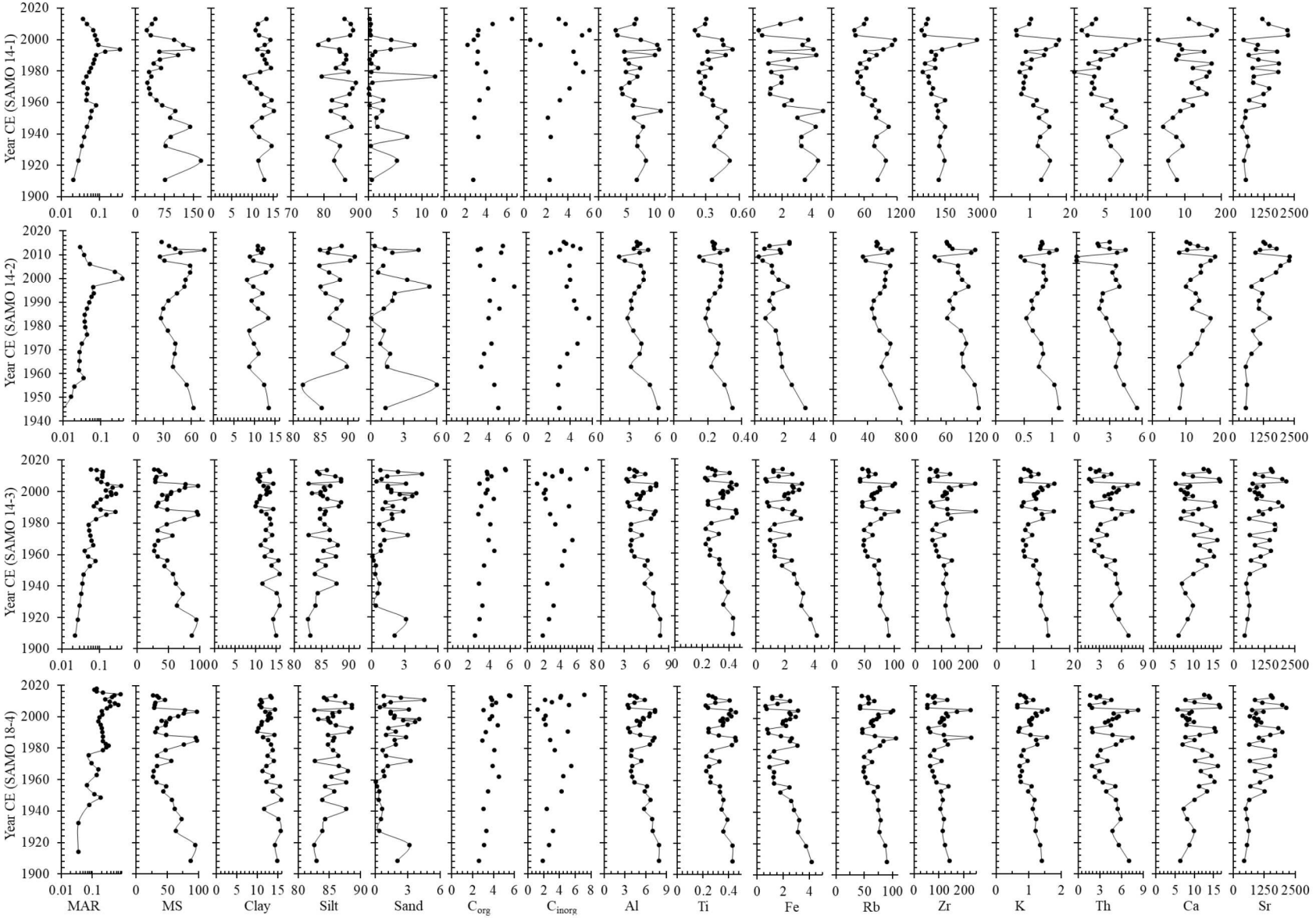
Year CE (SAMO 14-1)
Year CE (SAMO 14-2)
Year CE (SAMO 14-3)
Year CE (SAMO 18-4)
MAR
MS
Clay
Silt
Sand
C_{org}
C_{inorg}
Al
Ti
Fe
Rb
Zr
K
Th
Ca
Sr

Fig. 3.

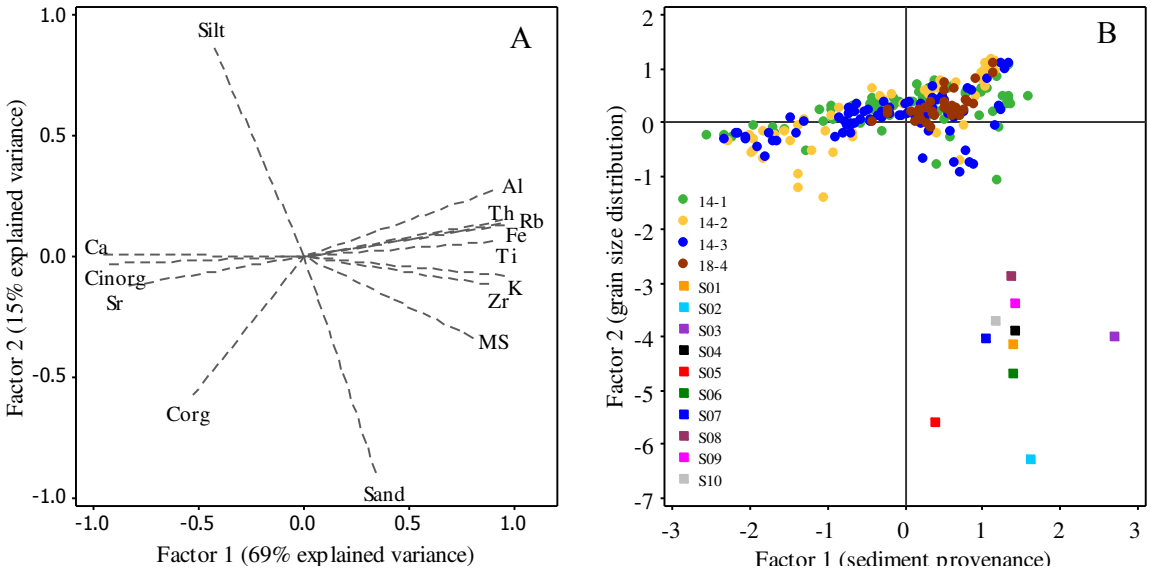
A
Silt
Al
Th
Rb
Fe
Ti
K
Zr
MS
Ca
Cinorg
Sr
Corg
Sand
Factor 2 (15% explained variance)
Factor 1 (69% explained variance)
1.0
0.5
0.0
-0.5
-1.0
B
14-1
14-2
14-3
18-4
S01
S02
S03
S04
S05
S06
S07
S08
S09
S10
Factor 2 (grain size distribution)
Factor 1 (sediment provenance)
2
1
0
-1
-2
-3
-4
-5
-6
-7
3

Fig. 4

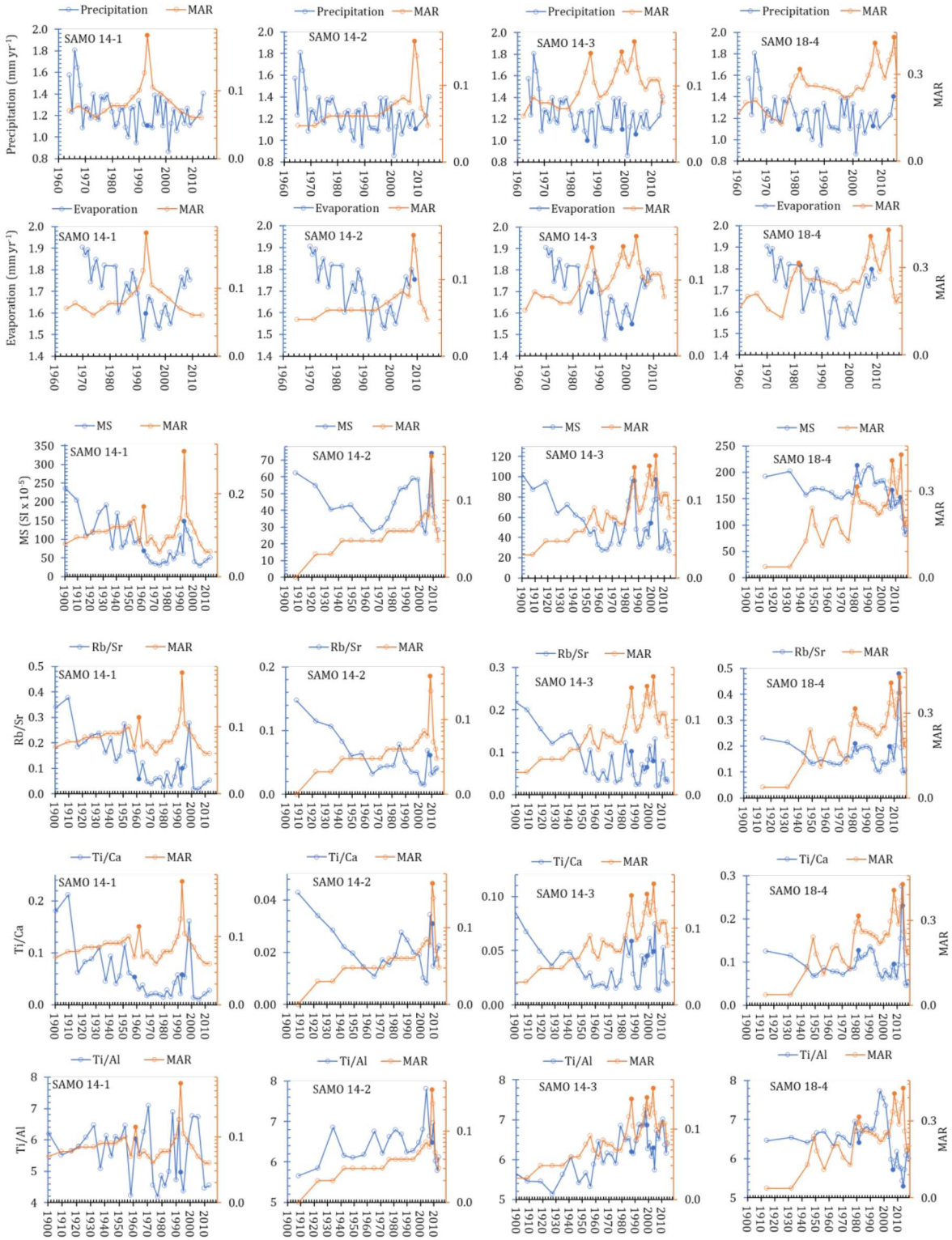
Precipitation
MAR
SAMO 14-1
SAMO 14-2
SAMO 14-3
SAMO 18-4
Precipitation (mm yr-1)
Evaporation
Evaporation (mm yr-1)
MS
MS (SI x 10-5)
Rb/Sr
Ti/Ca
Ti/Al

Fig. 5.

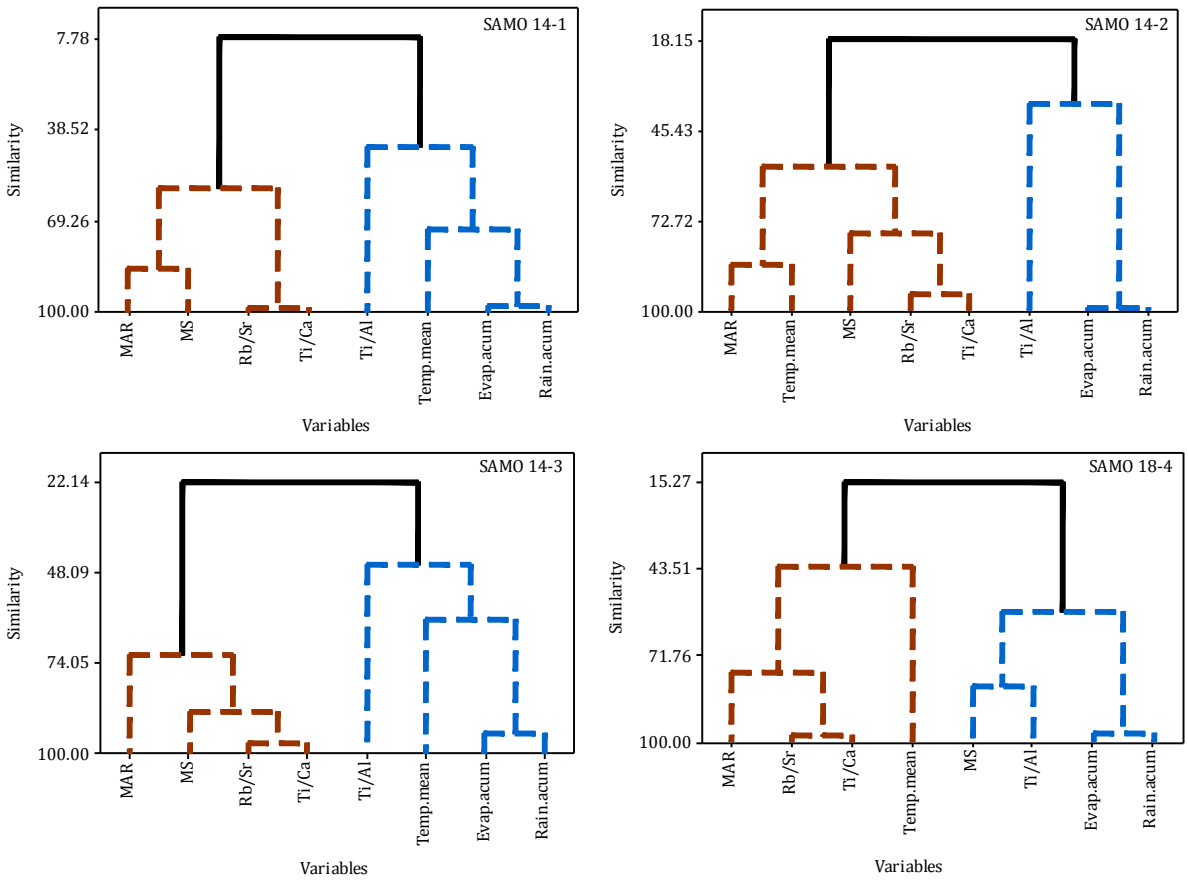
SAMO 14-1
Similarity
7.78
38.52
69.26
100.00
MAR
MS
Rb/Sr
Ti/Ca
Ti/Al
Temp.mean
Evap.acum
Rain.acum
Variables
SAMO 14-2
Similarity
18.15
45.43
72.72
100.00
MAR
Temp.mean
MS
Rb/Sr
Ti/Ca
Ti/Al
Evap.acum
Rain.acum
Variables
SAMO 14-3
Similarity
22.14
48.09
74.05
100.00
MAR
MS
Rb/Sr
Ti/Ca
Ti/Al
Temp.mean
Evap.acum
Rain.acum
Variables
SAMO 18-4
Similarity
15.27
43.51
71.76
100.00
MAR
Rb/Sr
Ti/Ca
Temp.mean
MS
Ti/Al
Evap.acum
Rain.acum
Variables

Fig. 6.

Table 1. ^{210}Pb and ^{137}Cs activity ranges, and ^{210}Pb-derived data in sediment cores from Santa María del Oro Lake, NW Mexico.

Core	$^{210}Pb_{sup}$ (Bq kg^{-1})	$^{210}Pb_{xs}$ (Bq kg^{-1})	^{137}Cs (Bq kg^{-1})	$^{210}Pb_{xs}$ inventory (Bq m^{-2})	$^{210}Pb_{xs}$ flux (Bq m^{-2} yr^{-1})	SAR (cm yr^{-1})	MAR (g cm^{-2} yr^{-1})	Age span (yr)/ depth (cm)
SAMO 14-1	44.2±3.0[a]	3.9-258.3[a,b]	2.0-33.3[a]	3487 ± 153[a]	109 ± 5[a]	0.04-1.59[a]	0.02-0.65[a]	118±9/32
SAMO 14-2	47.5±8.0[a]	17.9-284.1[a]	1.3-23.1[a]	2580 ± 138[b]	80 ± 4[b]	0.06-1.46[a,b]	0.01-0.38[a]	115±12/22
SAMO 14-3	38.3±4.3[a]	9.9-264.8[a]	1.0-30.8[a]	5015 ± 195[c]	159±6[c]	0.06-2.86[a,b]	0.01-0.38[a]	128±9/38
SAMO 18-4	38.3±4.3[a]	9.0-122.5[b]	1.7-12.4[a]	4738 ± 253[c]	147 ± 8[c]	0.05-1.96[b]	0.04-0.80[b]	114±2/36

$^{210}Pb_{sup}$ = supported ^{210}Pb; $^{210}Pb_{xs}$ = excess ^{210}Pb; MAR=mass accumulation rate; SAR=sediment accumulation rate. Different letters indicate groups with significant differences among cores ($p<0.05$).

Table 2. Accumulation rates in crater lakes in the world.

Crater lake	SAR (cm yr^{-1})	MAR (g cm^{-2} yr^{-1})	Altitude (m a.s.l.)	Rainfall (mm yr^{-1})	Environment type	Reference
Santa María del Oro, Mexico	0.04-2.86	0.01-0.80	750	1146	Rural	This study
Verde Lake, San Martín Volcano, Mexico	0.02-0.37	0.003-0.095	149	2500	Pristine	Ruiz-Fernández et al. (2007)
El Sol Lake, Nevado de Toluca Volcano, Mexico	0.02-0.42	0.01-0.14	4200	1227	Protected area	Alcocer et al. (2020)
La Luna Lake, Nevado de Toluca Volcano, Mexico	0.05-0.32	0.03-0.15	4200	1227	Protected area	Alcocer et al. (2020)
Lake Albano, Alban Hills, Italy	0.18-0.26	0.02-0.05	293	1244	Natural park	Alvisi and Frignani (1996)
Lake Nemi, Alban Hills, Itally	0.15-0.16	0.03-0.05	320	1244	Contaminated	Alvisi and Frignani (1996)
Mbalang Lake, Adamawa plateau, Cameroon	0.09	NA	1110	1500	Pristine	Ngos III et al. (2008)
Tisong Lake, Adamawa plateau, Cameroon	0.15	NA	1154	1500	Pristine	Ngos III et al. (2008)
Lake Surprise, volcanic plains of Western Victoria, Australia	<0.1	NA	93	798	National park	Barr et al. (2014)
Lake Elingamite, volcanic plains of Western Victoria, Australia	0.09	NA	121	781	National park	Barr et al. (2014)
East and Paulina Lakes, Newberry Volcano, USA	0.15–0.20	0.03-0.04	1930-1945	510-890	Protected area	Lefkowitz et al. (2017)
Lake Karagöl, Yamanlar Mountain, Turkey	0.02-0.06	0.02-0.59	1630-2588	738	Natural park	Sert (2018)
Baengnokdam Lake, Halla Mountain, Korea	0.20 - 0.86	NA	1950	>4500	National park	Yim et al. (2018)
Lake Warna, Dieng Plateau, Central Java, Indonesia	0.02 - 0.31	0.008-0.310	1965-2300	NA	Natural park, rural and urban development	Soeprobowati et al. (2018)

NA = not available

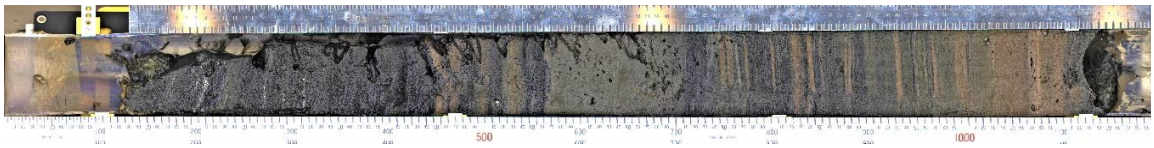

Fig. ESM1. High resolution image of sediments at SAMO 14-1 location, in Santa María del Oro Lake, NW Mexico.

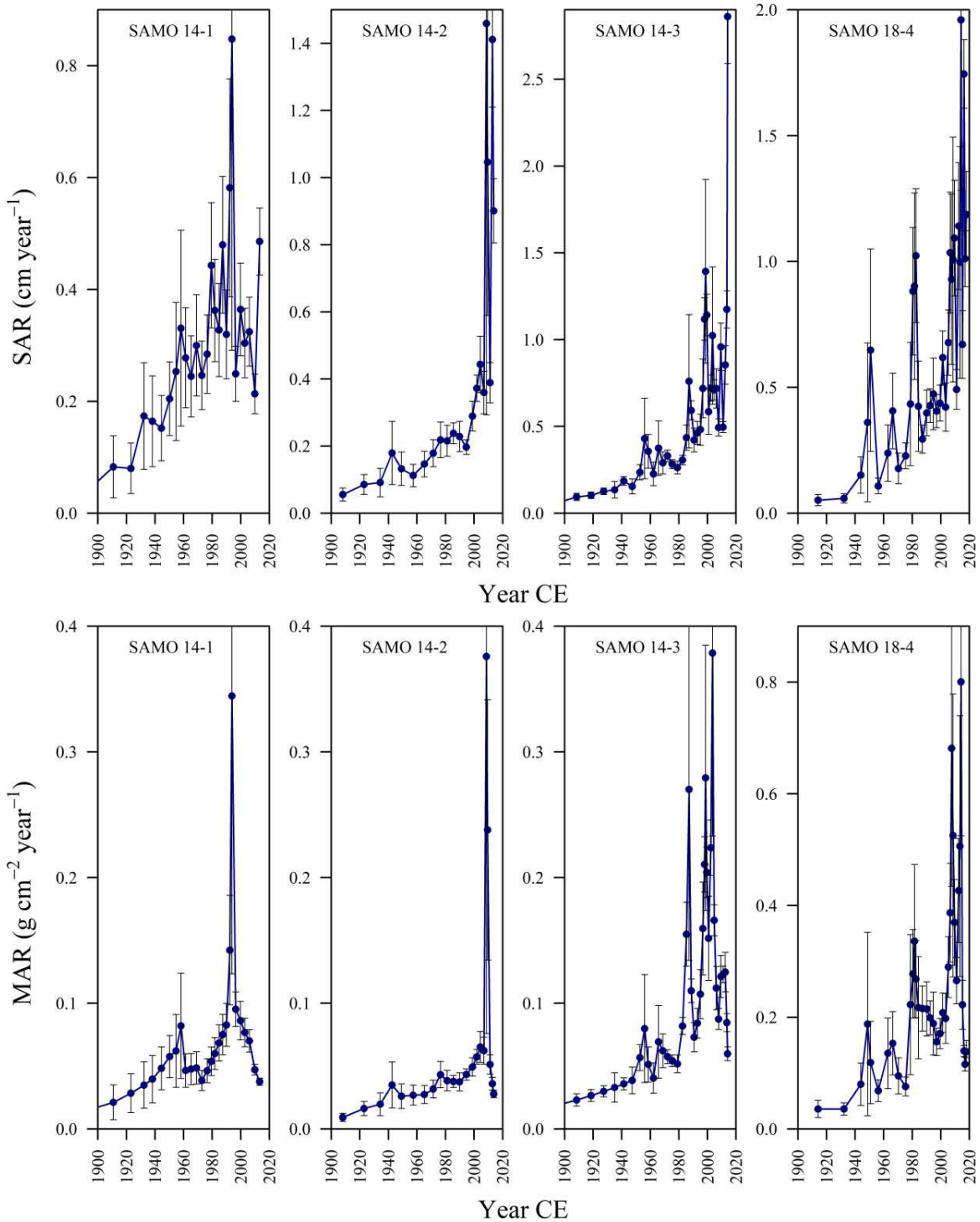

Fig. ESM2. Accumulation rate (SAR, upper panel; MAR, lower panel) temporal profiles for sediment cores from Santa Maria del Oro Lake, NW Mexico.

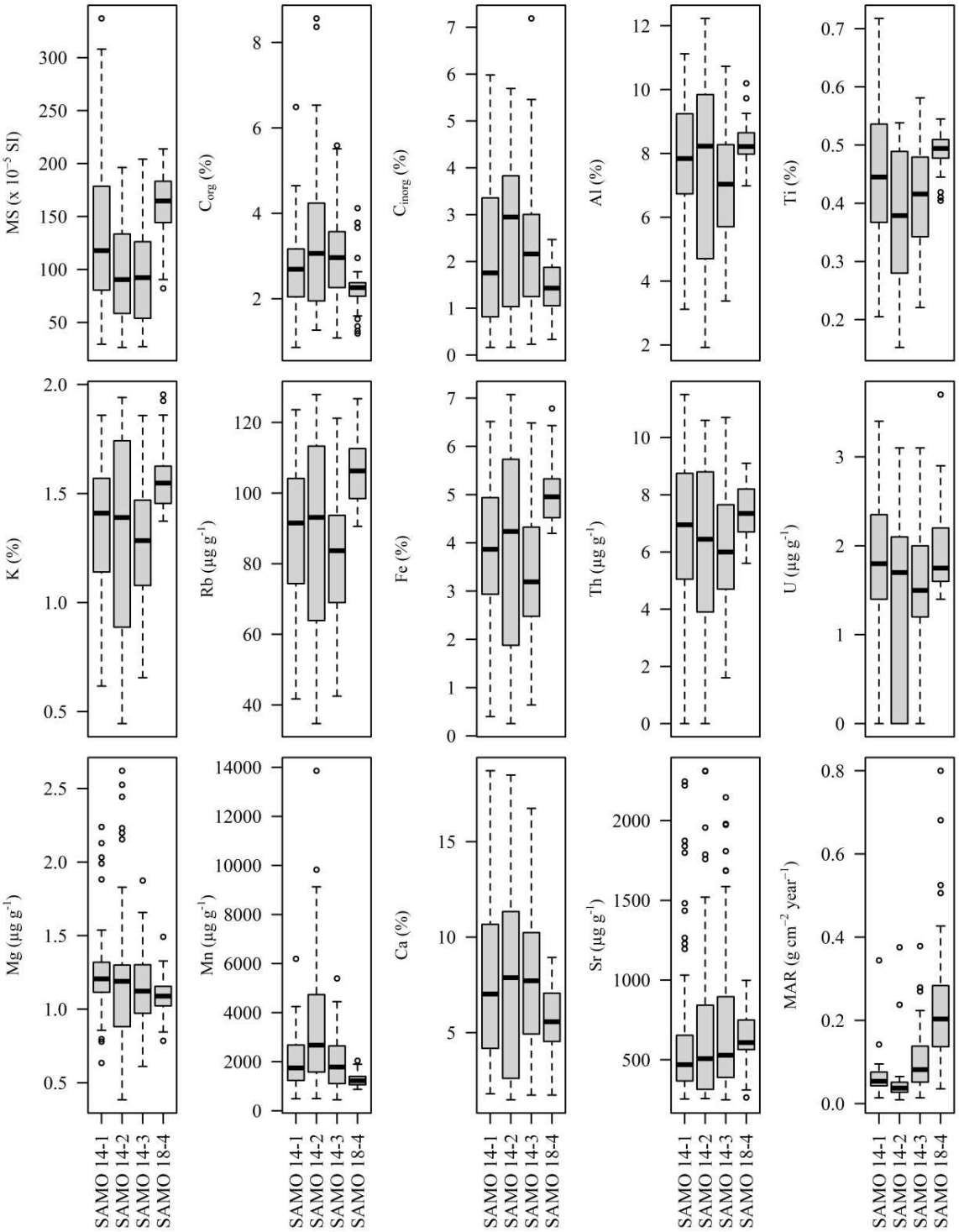

Fig. ESM3. Box plots of sediment characterization variables in cores from Santa María del Oro Lake, NW Mexico.

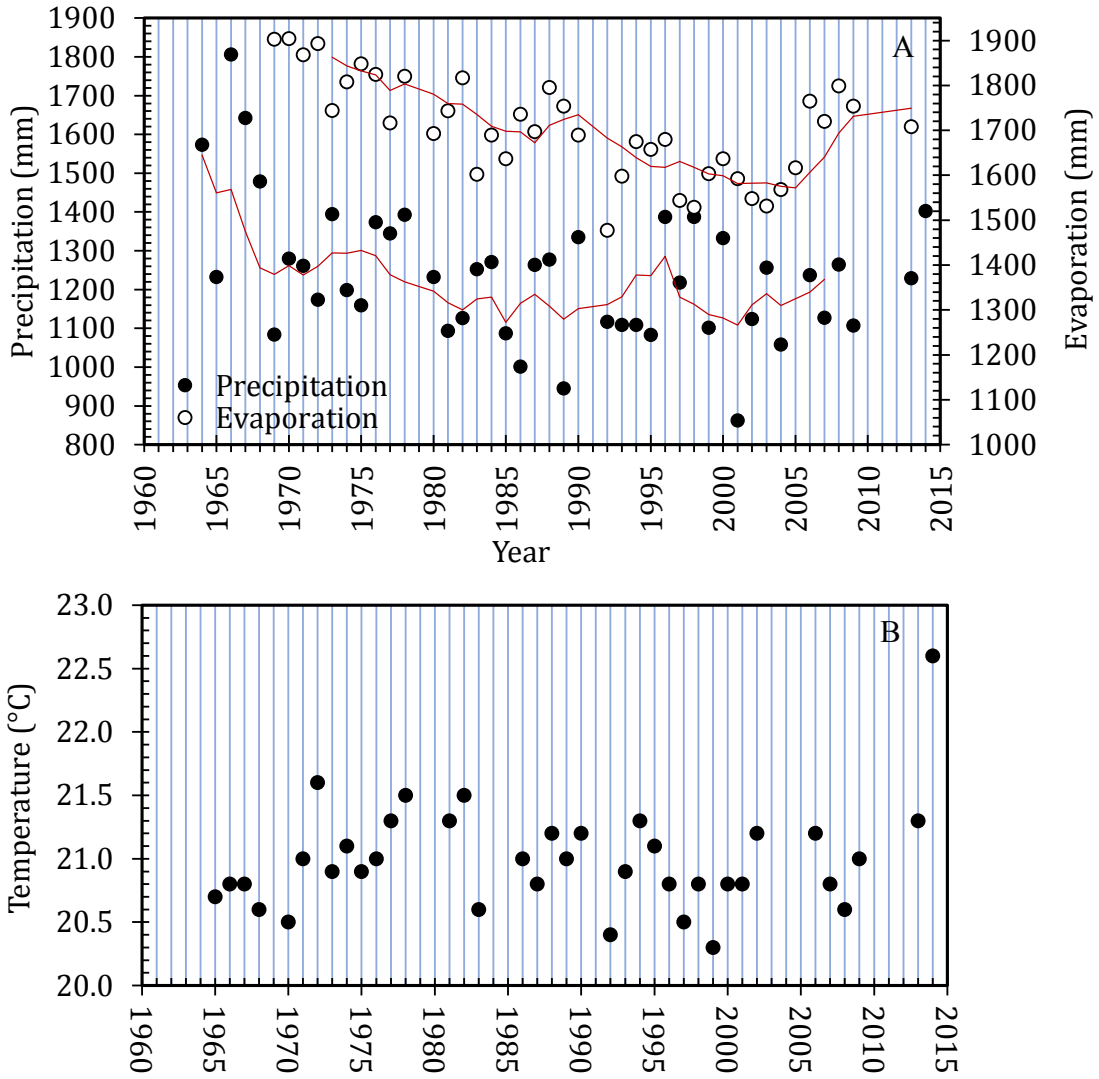

Fig. ESM4. Temporal variation of meteorological variables from Cerro Blanco Station (SMN, 2020), Nayarit. Only years with complete data are shown (12 monthly observations per year; see explanation in the text). A = annual accumulated precipitation and evaporation; B = mean annual temperature. Decreasing trends are significant ($p<0.05$): $r=-0.39$ for precipitation, and $r=-0.56$ for evaporation; the red line is a 5-year moving average.

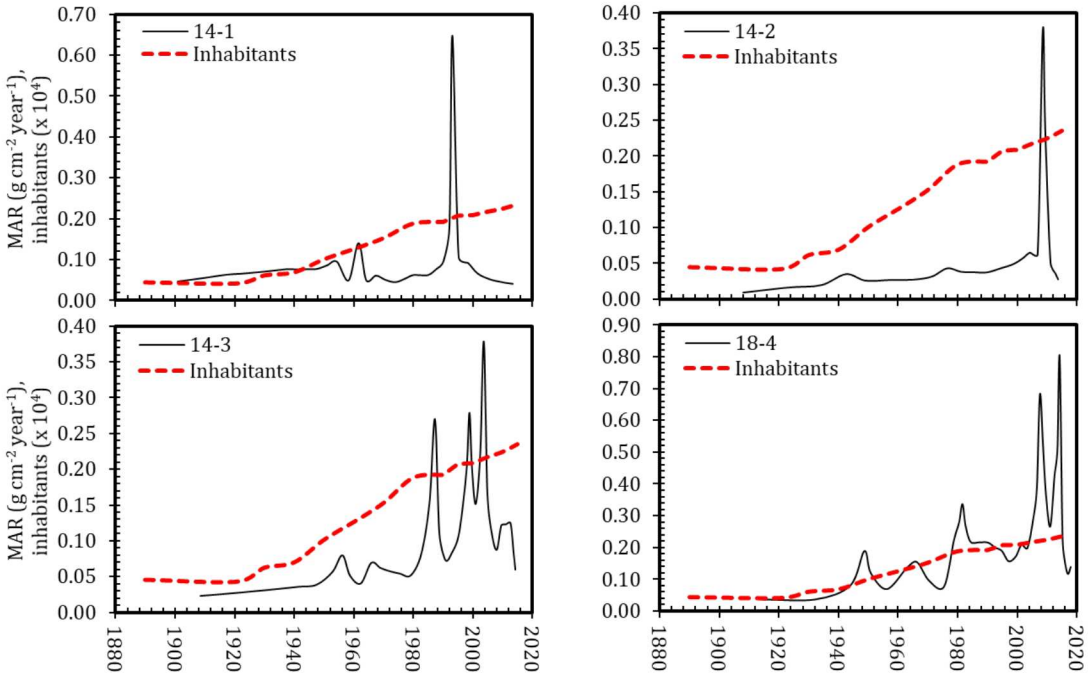

Fig. ESM5. Temporal variations of mass accumulation rates (MAR, g cm^{-2} $year^{-1}$, black lines) in sediment cores (14-1, 14-2, 14-3 and 18-4) from Santa María del Oro Lake, and population growth (dashed red lines) in the municipality of Santa María del Oro, NW Mexico (population data obtained from INEGI 2020a; SEPLAN 2020; SNIM 2020)

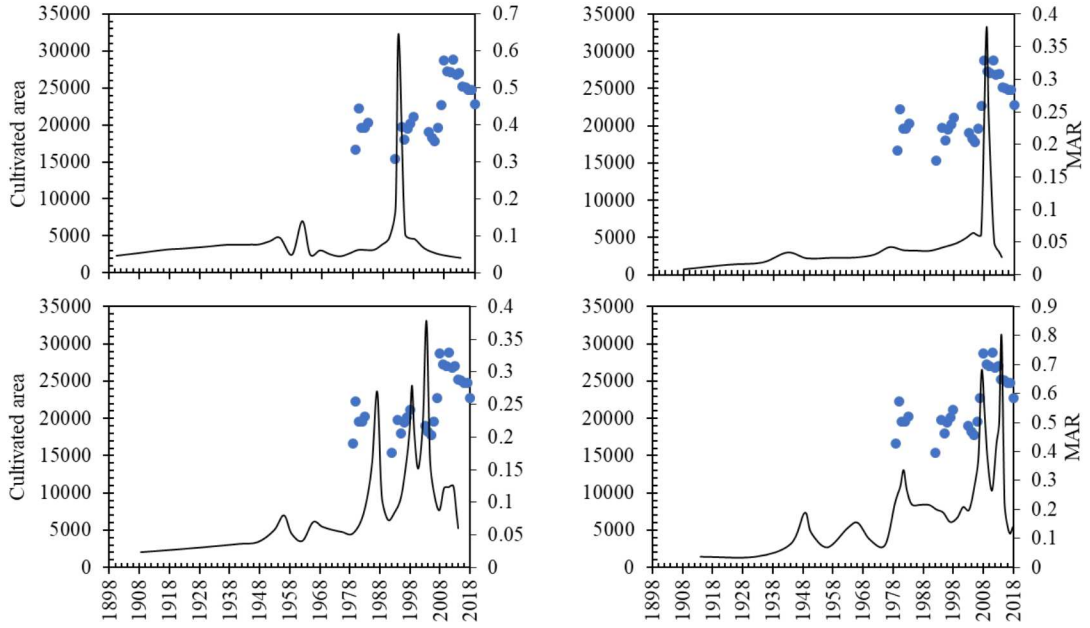

Fig. ESM6. Temporal variations of mass accumulation rates (MAR, g cm^{-2} $year^{-1}$; black lines) of sediment cores (14-1, 14-2, 14-3 and 18-4) from Santa María del Oro Lake, and of cultivated area (blue dots) in the municipality of Santa María del Oro, NW Mexico (cultivated are data obtained from INEGI 2020b; SIAP 2020)

Table ESM1. ^{14}C data for core SAMO 14-2 from Santa María del Oro Lake, NW Mexico. Uncertainties (±) are 1 σ.

Lab ID	Sample ID	^{14}C age[a]	±	$F^{14}C$[b]	±
UBA-35886	SAMO14-2_03-04 cm	3096	29	0.6802	0.0025
UBA-35887	SAMO14-2_10-11 cm	2709	28	0.7137	0.0025
UBA-40837	SAMO14-2_13-14 cm	2668	26	0.7174	0.0023
UBA-40838	SAMO14-2_14-15 cm	3099	24	0.6799	0.0020
UBA-40839	SAMO14-2_15-16 cm	3353	25	0.6587	0.0020
UBA-35888	SAMO14-2_16-17 cm	3874	34	0.6174	0.0026
UBA-35889	SAMO14-2_20-21 cm	4012	33	0.6068	0.0025
UBA-35890	SAMO14-2_25-26 cm	3673	45	0.6330	0.0035
UBA-41422	SAMO14-2_42-43 cm	4335	36	0.5830	0.0026
UBA-41423	SAMO14-2_48-49 cm	1640	26	0.8154	0.0026
UBA-41424	SAMO14-2_56-57 cm	1630	26	0.8164	0.0026
UBA-41425	SAMO14-2_67-68 cm	2225	27	0.7581	0.0026
UBA-41426	SAMO14-2_77-78 cm	3952	32	0.6114	0.0025
UBA-40835	Trap (May-Nov, 2017)	4268	26	0.5879	0.0019
UBA-40836	Trap (Nov 2017-May 2018)	4006	36	0.6073	0.0027
UBA-40834	Surface soil (May 2019)	377	24	0.9541	0.0029
Ramped pyroxidation analysis for a trap sample					
UBA-42285	Trap (May-Nov, 2017) 212-235 (224±12)[c]	4704	43	0.5568	0.0030
UBA-42281	Trap (May-Nov, 2017) 260-272 (266±6)[c]	4661	41	0.5598	0.0028
UBA-42282	Trap (May-Nov, 2017) 344-358 (351±7)[c]	4782	44	0.5514	0.0030
UBA-42284	Trap (May-Nov, 2017) 564-570 (567±3)[c]	4125	38	0.5984	0.0028

[a] Conventional (uncalibrated) ^{14}C ages. [b] Fraction modern. [c] Sample ID and temperature intervals (in °C): low temperature - high temperature (mean temperature ± 1 σ).

Table ESM2. Factor analysis (factor loadings from Varimax rotation) for sediment cores from Santa Maria del Oro Lake, Mexico.

Variable	Factor 1	Factor 2	Communality
Th	0.96	0.13	0.93
Ca	-0.95	0.01	0.91
K	0.95	-0.08	0.90
Rb	0.95	0.15	0.92
Fe	0.93	0.14	0.88
C_{inorg}	-0.92	-0.03	0.85
Ti	0.90	0.06	0.81
Al	0.90	0.27	0.88
Zr	0.88	-0.12	0.79
Sr	-0.83	-0.12	0.70
MS	0.80	-0.34	0.76
Sand	0.34	-0.90	0.92
Silt	-0.43	0.87	0.94
C_{org}	-0.53	-0.58	0.62

The explained variance of F1 is 68.6% and of F2 is 15.5%, for a total of 84.2%. Significant loadings are >0.7

References

INEGI 2020a. Censos y conteos de población y vivienda. Nayarit (Colección: Tabulados). Instituto Nacional de Estadística y Geografía. https://www.inegi.org.mx/

INEGI 2020b. Anuario estadístico de Nayarit (Colección: Publicaciones). Instituto Nacional de Estadística y Geografía. https://www.inegi.org.mx/

SEPLAN 2020. Planes de Desarrollo Municipal de Santa Maria Del Oro, Nayarit. Secretaría de Desarrollo Sustentable. Planes municipales de desarrollo. https://sds.nayarit.gob.mx

SIAP 2020. Anuario Estadístico de la Producción Agrícola. Servicio de Información Agroalimentaria y Pesquera. https://nube.siap.gob.mx/cierreagricola/

SNIM 2020. Población 1990-2020. Sistema Nacional de Información Municipal. http://www.snim.rami.gob.mx/

Historical reconstruction of sediment accumulation rates as an indicator of global change impacts in a tropical crater lake

Ruiz-Fernández A.C.[1*], Hernández-Rivera D.M.[2], Sanchez-Cabeza J. A.[1], Blaauw M.[3], Pérez-Bernal L. H.[1], Cardoso-Mohedano J. G.[4], Aquino-López M. A.[5], Keaveney E.[3], Giralt S.[6]

[1]Universidad Nacional Autónoma de México. Instituto de Ciencias del Mar y Limnología. Unidad Académica Mazatlán. Calz. Joel Montes Camarena s/n, Col. Playa Sur, 82040 Mazatlán, Sin., México. E-mail: caro@ola.icmyl.unam.mx, jasanchez@cmarl.unam.mx

[2]Universidad Nacional Autónoma de México. Posgrado en Ciencias del Mar y Limnología. Calz. Joel Montes Camarena s/n, Col. Playa Sur, 82040 Mazatlán, Sin., México. E-mail: donamhr@gmail.com

[3] Queen´s University Belfast. Archaeology and Palaeoecology, School of Natural and Built Environment. 42 Fitzwilliam Street, Belfast BT9 6AX United Kingdom. E-mail: maarten.blaauw@qub.ac.uk

[4]Universidad Nacional Autónoma de México. Instituto de Ciencias del Mar y Limnología, Estación El Carmen, México. Carretera Carmen-Puerto Real Km. 9.5, 24157 Ciudad del Carmen, Camp. E-mail: gcardoso@cmarl.unam.mx

[5]Centro de Investigación en Matemáticas (CIMAT), Jalisco s/n, Valenciana, 36023 Guanajuato, Gto, Mexico. E-mail: aquino@cimat.mx

[6]Geosciences Barcelona (Geo3BCN-CSIC). Lluís Solé i Sabarís s/n, 08028 Barcelona, España. E-mail: sgiralt@geo3bcn.csic.es

*Corresponding author

Keywords: tropical crater lake, ^{210}Pb, ^{14}C, ^{137}Cs, plutonium isotopes, sedimentation rates

Abstract

Lakes are effective sentinels of global change owing to their sensitivity to land-use changes and climate variability in their catchment. Santa María del Oro Lake (SAMO, NW Mexico) is of interest both for global change studies and as a natural resource to sustain the economy of local communities. Four sediment cores were used to evaluate the long-term temporal variations of sediment accumulation, under the hypothesis that changes in sediment input are mostly driven by anthropic activities developed in the lake surroundings. Radiocarbon (^{14}C) dating of SAMO sediments was precluded by a large and variable reservoir effect, inducing an age offset of ~4,000 years. Well-constrained chronologies over the past century were obtained by ^{210}Pb dating, corroborated by the stratigraphic markers ^{137}Cs, $^{239+240}Pu$, and ^{14}C-fraction modern. Geochemical, magnetic susceptibility, and meteorological data were used to elucidate the main controls of sedimentation processes in the lake. Mass accumulation rates (MAR) were high (range 0.01 - 0.80 g cm^{-2} yr^{-1}) likely because of the natural vulnerability of catchment soils to hydric and aeolian erosion. The highest values, observed towards the lakeshore, were attributed to the influence of seasonal runoff from surrounding steep hills and the proximity of human settlements and agriculture fields. MAR increased with time, although the most recent values were comparable to the mean values during CE 1900-1950 (0.05±0.04 g cm^{-2} yr^{-1}). Accumulation maxima across the lake, occurring mostly since the 1980s, concurred with precipitation minima and were related to terrigenous pulses associated with soil erosion, likely favored by lower soil humidity and the occurrence of wildfires during dryer years. Controls on the development of human settlement and agriculture practices should be included in the long-term environmental management plans for the conservation of the lake resources.

Introduction

Continental erosion caused by land-use changes and global warming are two of the main consequences of global change (GC), and both have accelerated during the second half of the twentieth century (the Great Acceleration) (Steffen et al. 2005). The retrospective evaluation of GC trends requires long-term monitoring data, which are scarce in most parts of the world due to logistical and economic limitations. Thus, sedimentary records are often the only alternative to evaluate the impacts of GC on aquatic and terrestrial ecosystems (Sanchez-Cabeza and Druffel 2009). Such records require precise and reliable chronologies to properly interpret environmental changes over time.

^{210}Pb dating (Krishnaswamy et al. 1971) is the most used method to establish sediment chronologies within the past ~100 years, the period of interest for most GC studies, as it allows evaluating the environmental changes that occurred since the Great Acceleration in comparison with the period 1900–1950. The total ^{210}Pb activity ($^{210}Pb_{tot}$) in the sediments include a detrital fraction (supported ^{210}Pb, $^{210}Pb_{sup}$), assumed to exist in secular equilibrium with ^{226}Ra, and a fraction that is scavenged from the water column (excess ^{210}Pb, $^{210}Pb_{xs}$), which is the one used for ^{210}Pb dating (Krishnaswamy et al. 1971). Beyond the ^{210}Pb temporal frame, ^{14}C dating is the most relevant method to obtain ages up to ~50,000 yr, and the combination of both dating methods can be useful for a better understanding of the environment´s natural variability. ^{210}Pb dating is usually complemented with stratigraphic markers to corroborate the age models. Above-ground nuclear bomb testing performed between the 1950s and 1960s resulted in elevated atmospheric concentrations of ^{137}Cs, plutonium isotopes, and ^{14}C. Therefore, it is expected that a core dated with ^{210}Pb would show maximum activities of these artificially produced radionuclides around 1962-1964, the period of maximum radioactive fallout from the atmospheric nuclear tests (UNSCEAR 2000).

Lakes provide a wide range of ecosystem services, such as water supply, flood damage reduction, biodiversity conservation, recreation, and aesthetic experiences. However, such valuable ecosystems may undergo rapid environmental changes, caused either by natural or anthropogenic causes. Pollution by sediments is a threat to lakes worldwide (Smol 2008). Increased sedimentation rates in lakes have been associated with diverse environmental problems, including water quality deterioration (Moges et al. 2017); shoaling, swamping, loss of water storage capacity, increased water levels, and flooding (Du et al. 2011; Degife et al. 2021); impacts on benthic ecosystems, which can affect organisms higher in the food web (Gravina et al. 2020); alteration of spawning grounds and reduction of the stock abundance of economically important fish species (Ranjan et al. 2019; McGlue et al. 2020). Stopping or reversing these negative changes requires effective lake management, for which it is critical to identify the sedimentation patterns and their drivers (Xu et al. 2017).

In many lakes, increasing sedimentation rates over the last century result from accelerated catchment soil erosion by runoff or wind, associated with land-use change and land management (Neff et al. 2008). Where anthropic influence is limited, climate variability may cause enhanced soil erosion and increased productivity (Pastor et al. 2019). Lakes with topographically closed basins (such as crater lakes), where the hydrological balance is primarily a function of rainfall and evaporation, are markedly sensitive to climate (Barr et al. 2014).

Temporal variations of magnetic susceptibility (MS) and element ratios (e.g. Rb/Sr, Ti/Ca, Ti/Al) have been used as proxies to evaluate changes in sediment provenance (Ruiz-Fernández et al. 2005) or climate variability (Shen et al. 2013; Jin et al. 2006; Martinez-Ruiz et al. 2015). The underlying assumption is that the mineral or major and trace element content in the detrital components of sediments may vary due to i) sediment input from sources with different mineralogy, or ii) chemical weathering of minerals (e.g., hydrolysis and solution)

driven by moisture and temperature (Wei et al. 2006). Humid conditions may favor higher values of MS (owing to the formation of secondary ferrimagnetic minerals; Dearing et al. 1996), of Rb/Sr (due to the significant increase of Rb in residual weathered debris relative to its source rocks; Jin et al. 2006) and Ti/Ca (as in-lake carbonate precipitation from evaporative concentration is reduced; Davies et al. 2015), but lower Ti/Al, owing to lower aeolian input (Martinez-Ruiz et al. 2015).

Santa María del Oro Lake (SAMO) is a small tropical crater lake in northwestern Mexico, surrounded by rural settlements. It has been described as a pristine reference site for paleoecological and environmental research (Zárate del Valle et al. 2007). Radiocarbon-dated sediment records from SAMO have provided information on long-term climate variability through identification of (a) variations of anoxic/oxic conditions in sediments during hot and dry periods, especially during *circa* 600 - 1140 CE, and 1410 - 1830 BCE (Vazquez-Castro et al. 2008), (b) the occurrence of droughts during the last 700 years, attributed to solar activity variability and/or climatic factors such as El Niño Southern Oscillation (Sosa-Nájera et al. 2010), (c) the alternation of dry and wet periods within the past ca. 2600 years, associated with variations of the intensities of the North American monsoon (Rodríguez-Ramírez et al. 2015), and (d) the impacts of drought on vegetation diversity (between 300 and 4200 cal BP) (Lozano-García et al. 2021).

Owing to its unique scenic beauty, SAMO has gradually developed as a tourist destination for at least 40 years, more importantly since 1995. In this short period, the environment has been modified, particularly through the construction of tourism facilities, which promoted the higher affluence of visitors (Moreno Moreno et al. 2015). The lake has also been affected by direct wastewater discharges from human settlements for several decades and by the proliferation of tourist boats. It has been used for small-scale cage fish farming projects and receives surface runoff through the surrounding agricultural areas and the culture of blue

agave for tequila production since 1999 (González-Bernal 2008). All these activities have likely contributed to changes in the environmental conditions of the system, including siltation, but this has not yet been assessed.

Our objective was to evaluate the temporal variations in sediment input to SAMO, using a combination of ^{14}C and ^{210}Pb dating. This is the first study on the recent evolution of accumulation rates in the lake, and we hypothesized that these changes are mainly due to anthropic induced catchment erosion, caused by population growth and agricultural activities.

High-resolution ^{210}Pb-dated sediment cores, corroborated with ^{137}Cs and $^{239+240}Pu$ (as stratigraphic markers for the maximum fallout caused by atmospheric thermonuclear weapon tests) allowed the retrospective reconstruction of sediment input to the lake within the past ~100 years. ^{14}C dating, attempted to determine the sedimentation rates beyond ^{210}Pb temporal framework, was unsuccessful and the reasons are discussed. Climate variability was also evaluated as a secondary driver of sediment input changes, by comparing the temporal variation of mass accumulation rates and the precipitation and evaporation data available for the past ~50 years from a nearby meteorological station. Multivariate techniques (cluster and factor analysis) were used to understand the dominant sources of sediments, and to evaluate the usefulness of MS and the element ratios Rb/Sr, Ti/Ca, and Ti/Al obtained from the dated cores, as proxies to investigate the factors controlling sedimentation.

Study area

SAMO is located at 750 m above sea level, within the Santa María del Oro Municipality (Mexican State of Nayarit), at ~4 km NE from the Santa Maria del Oro City (23,477 inhabitants in 2017; Fig. 1A). The lake lies within an extinct volcanic crater, part of the Trans-Mexican Volcanic Belt, which probably dates to the Pleistocene (Vázquez-Castro et al. 2008). It has a 2 km diameter, 3.7 km^2 surface area, 65 m maximum depth (Serrano et al. 2002), and

is characterized by steep sides and an almost flat bottom (Fig. 1B). SAMO is fed by rainfall, surface runoff, and groundwater, whereas water outflows mainly through evaporation, seepage (Rodríguez-Ramírez et al. 2015), and local water consumption. The aquifer that feeds SAMO is confined in volcanic (rhyolite, ignimbrite, basalt, porphyry, diorite, dacite, and andesite) rocks, and its water is sodium-bicarbonate type (DOF 2016).

SAMO is a warm oligomictic lake (surface water temperature ranging from 22.9°C to 31.1°C), that remains stratified most of the year (thermocline between 20 and 37 m depth) but has a short and incomplete mixing phase during winter (Cardoso et al. 2019). It is a mesotrophic lake, with high concentrations of silica (mean value: 356 ± 42 µM L^{-1}) and soluble reactive phosphorus (mean value: 3.0 ± 3.5 µM L^{-1}), it is slightly alkaline (pH >8) and has moderately hard waters (Caballero et al. 2013).

The climate in the region is classified as semi-warm sub-humid with summer rains (INEGI 2009), with mean monthly air temperatures ranging from 12.9°C to 29.1°C, mean annual rainfall of 1,220.4 mm, and mean annual evaporation of 1,705.6 mm (SMN 2020). The region has been reportedly affected by strong to very strong droughts (Hernández Cerda and Valdez Madero 2004). The catchment is characterized by extrusive igneous rocks (rhyolite acidic-tuff (45%) and basalt (37%)) and the main soil types are luvisol (30%) and regosol (23%) (INEGI 2009). The main productive activity in Santa María del Oro Municipality is agriculture, and the SAMO catchment (Fig. 1C) is reportedly affected by accelerated erosion, associated with agriculture, deforestation, and forest fires (PO 2003). The expanding agriculture frontier has been recognized among the critical zones for forest fires in Nayarit State since slash-and-burn agriculture is still in practice. A specific concern is associated with sugar cane and agave cultivation because farmers invade mountain lands, and each harvest season the wastes are burned carelessly, the fire spreads to the forest, creating large-scale forest fires (SEDATU, 2013; DEPCB, 2015).

Materials and methods

Field work

Cores SAMO 14-1, 14-2, and 14-3 were collected in 2014 at deep locations (below the thermocline, between 48 and 55 m depth), and SAMO 18-4, in 2018, at a shallower location (30 m), in a zone known as Agua Caliente Bay (Fig. 1B). The cores were retrieved with a UWITEC™ gravity corer, which provides intact sediment surfaces, using a transparent PVC tube (86 mm inner diameter, 1.0 m long). No signs of sediment disturbance (e.g. bubbles, burrows) were observed. As the sediments consisted of liquified soft muds, which could be easily disturbed during transportation, the cores were extruded onsite and sectioned at 1 cm intervals. An additional core, collected at the SAMO 14-1 location for lithologic description (Fig. ESM1), showed that the sediments were mainly made up of clayey silts without visible sandy layers. The uppermost segment (~31 cm) was composed of millimetric laminated dark greenish sediments, interbedded with whitish millimetric laminae, possibly formed by endogenous carbonates. The rest of the core consisted of alternating dark and light layers (mm-to-cm thick) except in the 44 to 58 cm segment, where homogeneous light greenish sediments were found.

Sinking particulate material was collected during two periods of six months each (May to November 2017, and November 2017 to May 2018) by using a sediment trap (PVC tube, 1 m long, 0.1 m inner diameter, aspect ratio of 10) located at 30 m depth (below the thermocline). Ten surface soil samples (1 cm thickness) were also collected in the lake surroundings in May 2019 (Fig. 1A). The sediment core, sediment trap, and soil samples were freeze-dried. The dry weight, thickness, and area of each core section were used to estimate dry bulk density

(g cm^{-3}). All samples were ground to powder with a porcelain mortar and pestle (except aliquots used for grain size determination) and kept in polyethylene bags until analysis.

Laboratory analysis

$^{210}Pb_{tot}$ activities were determined by alpha spectrometry (Alpha Ensemble Ortec/Ametek) according to Ruiz-Fernández and Hillaire-Marcel (2009). Gamma-ray spectrometry measurements were used to determine the activities of ^{226}Ra (through its daughter radionuclide in secular equilibrium ^{214}Pb; 352 keV) and ^{137}Cs (662 keV) in some of the core samples, using an OrtecHPGe well-detector (Ruiz-Fernández et al. 2014; Diaz-Asencio et al. 2020). $^{210}Pb_{sup}$ activities were estimated from the mean value of ^{210}Pb from the data where the ^{210}Pb activities are almost constant (Binford, 1990) and were confirmed by the ^{226}Ra activities. ^{137}Cs and $^{239+240}Pu$ activities (determined by alpha-particle spectrometry; Ruiz-Fernández et al. 2014) were used to corroborate the ^{210}Pb chronologies.

With the purpose to obtain information on sediment accumulation rates beyond the ^{210}Pb dating temporal frame, ^{14}C analyses were performed in bulk sediment samples from thirteen sections of core SAMO 14-2, one soil and two sediment trap samples (Table ESM1 in the electronic supplementary material), by accelerator mass spectrometry at ^{14}CHRONO Centre, Queen's University Belfast. One of the sediment trap samples (May-Nov, 2017) was also analyzed by ramped pyroxidation, a method by which bulk material can be partitioned into individual fractions, based on their resistance to decay (Rosenheim 2013), allowing to distinguish the presence of different sources of carbon. Data are reported as ^{14}C fraction modern ($F^{14}C$) and conventional ^{14}C ages; uncertainties are one standard deviation of the mean value.

Grain size distribution was determined by laser diffraction (Malvern Mastersizer 2000E). Loss on ignition, determined by sediment calcination at 550°C (LOI_{550}) and 950°C (LOI_{950}), were used to estimate the content of organic carbon (C_{org}) and inorganic carbon (C_{inorg}), respectively (Dean 1974). For magnetic susceptibility (MS) analysis, sediment aliquots (~1.5 g) were placed in a polyethylene tube (33 mm length, 6 mm internal diameter) and measured with a Bartington MS2 magnetic susceptibility meter coupled to an MSG2 frequency sensor. The elemental composition was determined by X-ray fluorescence spectrometry (XRF, Spectrolab Xepos-3) and results are expressed on a dry-weight basis.

Analysis of reference materials provided results within the reported range of the certified values: IAEA-300 (Radionuclides in Baltic Sea sediment, International Atomic Energy Agency) for ^{210}Pb and ^{137}Cs activities, IAEA-158 (Trace elements and methylmercury in marine sediment, International Atomic Energy Agency), and PACS-2 (Marine sediment reference materials for trace metals and other constituents, National Research Council Canada) for element concentrations, QAS3002 (Quality audit standard, Malvern™) for grain size percentages, and the reference material G-039 for magnetic susceptibility. Replicate analysis of a single sample (n = 6) yielded variation coefficients <10% for ^{210}Pb activities, <3% for elemental composition, <5% for grain size distribution and <3% for magnetic susceptibility.

Meteorological data

Mean monthly values of temperature, precipitation, and evaporation data (period 1963-2014) were obtained from the meteorological station Cerro Blanco (code 18005; SMN 2020), located at ~5 km NW from SAMO (Fig. 1A; 21°22'36" N, 104°37'06" W, 965.0 m above sea level). Missing records accounted ~2% of the total expected data for precipitation (14

monthly observations within eight different years), 12% for evaporation (65 observations, within 13 different years, including the whole period 2009-2012), and 6% for temperature (36 values within 8 years, including almost the whole period 1963-1964).

Data treatment

Sediment dating

The ^{210}Pb-derived chronologies were calculated with the constant flux (CF) model (Robbins 1978; Sanchez-Cabeza and Ruiz-Fernández 2012). This is a very robust model, with applicability in a wide type of environments (Sanchez-Cabeza et al. 2014), which assumes that $^{210}Pb_{ex}$ activities are directly proportional to the $^{210}Pb_{ex}$ flux to the sediments, but inversely proportional to the sediment mass loading (Krishnaswamy et al. 1971; Sanchez-Cabeza and Ruiz-Fernández, 2012). As its main hypothesis is that the $^{210}Pb_{ex}$ flux to the sediments is constant, it allows inferring temporal variations of sediment accumulation rates (SAR) and mass accumulation rates (MAR). Dating uncertainties were estimated by Monte Carlo simulations, a robust strategy that limits the overestimation of uncertainties, in comparison with the commonly used method of quadratic propagation of uncertainties (Sanchez-Cabeza et al. 2014).

Statistical analyses

Differences among the cores in the analyzed variables were assessed through analysis of variance (ANOVA) and Tukey post-hoc test, performed at a 95% confidence level by using R (R Core Team, 2021); significant differences are reported as $p<0.05$.

Factor Analysis (FA) was performed to identify the main sources of sediments to SAMO and how these vary among cores. It included 14 variables (MS, silt, sand, C_{org}, C_{inorg}, Al, Ca, Fe, K, Rb, Sr, Th, Ti, and Zr) from core sections and soil sample data (Minitab 15®). The communalities of all variables were >0.60, and the significant variables were those with loadings >0.70 (Hair et al. 2010).

A cluster analysis (complete linkage) was used to evaluate the association of the meteorological data (mean monthly values of temperature, and accumulated precipitation and evaporation) with MAR, MS, and the element ratios Rb/Sr, Ti/Ca, and Ti/Al, to assess their potential use as climate proxies to distinguish between wet and dry periods. The missing values of the meteorological database were filled with the mean value for the corresponding month (obtained from the whole database), and the monthly values were integrated to match the periods comprised in the sediment core sections, according to the ^{210}Pb ages.

Results

^{210}Pb dating

The $^{210}Pb_{sup}$ values were comparable among the cores (38.3±4.3 to 47.5±8.0 Bq kg^{-1}). The $^{210}Pb_{xs}$ activities decreased with depth in all cores, although in some core sections $^{210}Pb_{xs}$ values departed from an exponential decay trend (Fig. 2A). $^{210}Pb_{xs}$ fluxes (derived from the inventories; Sanchez-Cabeza and Ruiz-Fernández 2012) were comparable between cores SAMO 14-3 (159.2±6.1 Bq m^{-2} yr^{-1}) and SAMO 18-4 (147.7±7.9 Bq m^{-2} yr^{-1}), and higher than in cores SAMO 14-1 (108.7±4.8 Bq m^{-2} yr^{-1}) and SAMO 14-2 (80.5±4.3 Bq m^{-2} yr^{-1}). All sediment records spanned more than 100 years (Table 1).

Global fallout radionuclides

^{137}Cs activities

^{137}Cs activities (<1.0 – 33.3 Bq kg^{-1}) were similar among cores. The depth profiles of ^{137}Cs showed maxima at different depths (Fig. 2B), which according to the ^{210}Pb age model, correspond to similar age periods (SAMO 14-1: 16-17 cm, 1962-1966; SAMO 14-2: 16-17 cm, 1957-1964; SAMO 14-3: 28-29 cm, 1961-1963; and SAMO 18-4: 29-30 cm, 1964-1968).

^{239,240}Pu activities

Plutonium isotopes were determined in cores SAMO 14-2 and SAMO 18-4. ^{239,240}Pu activity ranges were 6.5 – 3,193 mBq kg^{-1} in SAMO 14-2, and 165 - 262 mBq kg^{-1} in SAMO 18-4 (Fig. 2B). The ^{239,240}Pu activity maxima were in SAMO 14-2 at 16-17 cm (1957 – 1964) and in SAMO 18-4 at 29-30 cm (1964 – 1968).

^{14}C dating

The F^{14}C values were below 1.0 at all analyzed sections of core SAMO 14-2, the sediment trap, and the soil samples (Table ESM1). A peak value of F^{14}C in the core was observed at the 13-14 cm depth section, 3 cm shallower than the ^{137}Cs and ^{239,240}Pu maxima (Fig. 2B). ^{14}C uncalibrated ages in SAMO 14-2 ranged from 1630±26 yr (56-57 cm depth) to 4012±33 yr (20-21 cm depth). The ^{14}C age of the soil sample (377±24 yr) was considerably younger than the core and sediment trap samples. The different fractions of the trap sample analyzed by ramped pyroxidation yielded similar ages (between 4,125±38 yr and 4,782±44 yr).

Accumulation rates

The overall accumulation rate ranges (Table 1) were 0.04-2.86 cm yr^{-1} (SAR) and 0.01-0.80 g cm^{-2} yr^{-1} (MAR; Fig. 3). In SAMO18-4, collected in a shallower location closer to the lakeshore (Fig. 1B), the MAR values (0.04-0.8 g cm^{-2} yr^{-1}) were higher than in the rest of the cores (overall range 0.01-0.65 g cm^{-2} yr^{-1}).

Between 1900 and 1950 (pre-1950 period), the mean SAR values ranged from 0.11±0.05 cm yr^{-1} (SAMO 14-2) to 0.22±0.09 cm yr^{-1} (SAMO 14-1), and mean MAR values ranged from 0.02±0.01 g cm^{-2} yr^{-1} (SAMO 14-2) to 0.09±0.07 g cm^{-2} yr^{-1} (SAMO 18-4). Neither SAR nor MAR showed significant differences among the cores; thus, the mean pre-1950 values (0.17±0.09 cm yr^{-1} and 0.05±0.04 g cm^{-2} yr^{-1}) can be used as reference values for SAMO.

Since 1950 onwards (post-1950 period), SAR and MAR values in all cores fluctuated considerably, with asynchronous subsurface maxima after the 1980s (Fig. ESM2). Also, all cores showed MAR values decreasing towards the surface, with topmost MAR values within the reference value interval (except for SAMO 14-3). During the post-1950 period, MARs in core SAMO 18-4 (0.26±0.17 g cm^{-2} yr^{-1}) were higher than in the cores from the deepest sampling sites (ranging from 0.07±0.09 g cm^{-2} yr^{-1} in SAMO 14-2 to 0.12±0.08 g cm^{-2} yr^{-1} in SAMO 14-3).

Sediment characterization

SAMO cores were mainly composed of silt (60 - 91%), with variable percentages of clay (7% - 29%) and sand (0 - 32%). The contents of sand, silt, clay, C_{inorg}, Mg, Zr, Sr, and U were comparable among cores, whereas the highest mean values of MS, Al, Ti, K, Rb, Fe, and Th,

and the lowest mean values of C_{org}, Mn and Ca were usually observed in core SAMO 18-4 (Fig. ESM3).

The temporal element profiles (Fig. 3) were similar among the cores. Between the 1900s and early 1960s, the profiles generally showed decreasing upwards values of MS and Al, Ti, Rb, and Zr concentrations, and increasing Ca and Sr concentrations, but afterward the records are noisier, with recurrent subsurface minima and maxima. The MAR maxima (Fig. 3) coincided with those of MS and terrigenous elements (e.g. Al, Ti, Rb), but not the other way around.

Sediment sources

In the factor analysis, the first two factors explained ~84% of the dataset variance (Fig. 4A, Table ESM2). In Factor 1 (~69% of the explained variance) the significant variables with positive loadings were elements related to terrigenous inputs (Th, K, Rb, Fe, Ti, Al, Zr) and MS, and with negative loadings, C_{inorg} and elements associated with carbonate precipitation (Ca, and Sr; Salminen et al. 2005). Factor 2 (~15% of the variance) included the silt percentages with positive loading, and of sand with negative loading. The distribution of the core sections was almost indistinguishable (Fig. 4B), while all soil samples grouped on the positive side of F1 (characterized by the association of the terrigenous elements), where most of the SAMO 18-4 samples are also found.

Influence of climate variability on sedimentation

Unlike temperature, the time series of annual accumulated precipitation and evaporation showed significant ($p<0.05$) decreasing trends (Fig. ESM4). Within the period with available

meteorological data, MAR maxima in all cores corresponded to precipitation minima and evaporation maxima (except in core SAMO 14-3). Also, most MAR maxima coincided with maxima of MS, Rb/Sr and Ti/Ca, and minima of Ti/Al (Fig. 5). Cluster analyses showed two main groups (Fig. 6) in all cores: the first one (brown) usually included MAR, MS, Rb/Sr, and Ti/Ca, and the second one (blue) included Ti/Al, precipitation, and evaporation, except for SAMO 18-4, in which MS was included in the second group. Mean temperature was in both groups (in the first one in cores 14-2 and 18-4; in the second one in cores 14-1 and 14-3). In brief, only Ti/Al ratios were consistently related to rainfall and evaporation in all cores.

Discussion

^{210}Pb dating

All cores showed some sections in which $^{210}Pb_{xs}$ activities did not follow an exponentially decreasing trend according to the radioactive decay law. This is not surprising since $^{210}Pb_{xs}$ activities are the balance between the $^{210}Pb_{ex}$ flux and MAR (Krishnaswamy et al. 1971), for which $^{210}Pb_{xs}$ activities can be diluted or enhanced by changes in sediment input. Thus, the non-monotonic $^{210}Pb_{xs}$ activity depth profiles were interpreted as a result of changes in sediment accumulation rates. The ^{210}Pb fluxes to the SAMO cores (80±4 - 159±6 Bq m^{-2} yr^{-1}) were comparable to the average $^{210}Pb_{ex}$ fallout estimated for North America (140 –185 Bq m^{-2} yr^{-1}, latitude 10 – 30 N; Preiss et al. 1996). This finding indicates that atmospheric deposition is the predominant pathway of $^{210}Pb_{ex}$ supply to the lake.

Reliability of the ^{210}Pb-derived age models

The ^{137}Cs and $^{239+240}Pu$ activity profiles were in good agreement and provided a proper corroboration of the ^{210}Pb chronologies in all cores (at least for the post-nuclear test period). In addition, the CF-derived ^{210}Pb chronologies were corroborated by using the Bayesian model Plum, and the comparison of both age models for SAMO 14-2 is presented in Aquino-López et al. (2020).

Compared to $^{239-240}Pu$, the broader peak of ^{137}Cs in SAMO 18-4 (Fig. 2B) is most likely caused by the delayed ^{137}Cs input through the accumulation of eroded soils from the catchment (Appleby et al. 2019) or post-depositional mobility of ^{137}Cs (Wang et al. 2017). $F^{14}C$ is defined as 1.0 for the preindustrial atmosphere (Schuur et al. 2016) and its value in a sample is used to distinguish between old (pre-1950, $F^{14}C < 1$) and modern (post-1950, $F^{14}C > 1$) (McCorkle et al. 2016). $F^{14}C$ values are <1.0 in all SAMO 14-2 sections, implying the presence of old carbon, even in sections deposited after the 1950s (Fig. 2C), and the increasing values between 13 and 17 cm most likely result from the ^{14}C atmospheric release during atmospheric nuclear weapons testing. The $F^{14}C$ subsurface maximum (13-14 cm, 1976.5±2.6) was above the ^{137}Cs and $^{239+240}Pu$ maxima, implying a time lag of ~11 years according to ^{210}Pb dating. This is because $^{239+240}Pu$ and ^{137}Cs are directly deposited to the water surface through atmospheric fallout and adsorbed onto sinking suspended matter; whereas the incorporation of ^{14}C into the sediments implies the air-water exchange of CO_2 (Glynn et al. 2013), its incorporation into the dissolved inorganic carbon pool and its assimilation as biomass of plants and photo- and chemo-autotrophic microbes (Gougoulias et al. 2014), that finally becomes part of the sinking matter that conforms the sediments.

^{14}C ages

As $F^{14}C$ indicated the presence of old carbon in the samples, before attempting to establish a ^{14}C chronology for SAMO 14-2, we evaluated the reservoir effect (RE) in the lake through comparison of the well corroborated ^{210}Pb-derived ages and conventional ^{14}C ages (Saulnier-Talbot et al. 2009; Blaauw et al. 2011) obtained for the same core sections (16-17 cm, ^{210}Pb age = 57±4 yr, ^{14}C age = 3874±34 BP; and 20-21 cm, ^{210}Pb age = 91±8 yr, ^{14}C age = 4012±33 BP). The age offset (~3,817 and ~3,921 yr, respectively) was comparable with the ^{14}C age of the sediment trap samples (~4,000 years, Table ESM1). The similar ages for the different fractions of the sediment trap sample from May-Nov, 2017 (low, medium, and high-temperature combustion, Table ESM1) indicated that all fractions have the same source. This indicates the occurrence of ^{14}C-depleted carbon in the lake, either caused by in-wash of eroded soil (containing reworked old organic material or detrital carbonates) or by a large lake reservoir effect. The youngest ^{14}C age (377±24 years) of the soil sample (compared with those from the sediment core and the trap samples, Table ESM1) did not stand for the input of such old carbon through eroded soils.

No previous study at SAMO reported problems related to ^{14}C dating. This may be due to the use of matrices other than bulk sediments (peat and wood; Vázquez-Castro et al. 2008, Rodríguez-Ramírez et al. 2015) and, when bulk sediments were used, age inconsistencies were not discussed (Sosa-Nájera et al. 2010; Lozano-García et al. 2021). None of those studies reported ^{210}Pb dating which, in this case, confirmed that the surface sediments in the SAMO cores are modern, thus, the ^{14}C values reflect a strong reservoir effect.

The reservoir effect can be temporally and spatially variable within the same lake, owing to differences in CO_2 air-water exchange rates, or in old carbon supply from the catchment (Zhou et al. 2020). The very variable ^{14}C ages of the SAMO sediments denoted a varying reservoir effect with time, making unfeasible to calibrate the ^{14}C ages and provide a longer-

term age-depth model. These results emphasize the convenience of combining well corroborated ^{210}Pb dating and ^{14}C to confirm the reliability of ^{14}C dates.

Accumulation rate ranges and temporal variability

The SAR ranges in SAMO were wider than those reported for other crater lakes in Mexico and other areas in the world, irrespective of altitude, annual precipitation, or type of environment (protected areas, rural or urban) surrounding the lakes (Table 2). High SAR values in SAMO could be related to the large soil erodibility of the predominant luvisols in the catchment, which is affected by high precipitation events, aeolian soil erosion, and soil degradation promoted by agricultural activities, especially in those areas where pasture lands are combined with rain-fed agriculture (Zamudio and Méndez 2011).

As SAR might be affected by compaction, MAR is a more reliable parameter to evaluate the impact of global change. Results showed that the sedimentation process in SAMO is spatially heterogeneous, with higher MAR towards the lakeshore (SAMO 18-4, Table 1), and variable over time, with higher MAR fluctuations during the post-1950 period (more evident since the 1980s; Fig. ESM2) but lower values in the more recent segment of all cores.

Influence of human activities on sedimentation

The factor analysis indicated that terrigenous input and carbonate precipitation are the dominant sediment sources at SAMO. Their influence is quite homogenous across the lake, and element composition variation is independent of the grain size distribution. The association of MS with terrigenous elements (Table ESM2, Fig. 4A) indicated that the strong changes of MS along the cores are related to changes in terrigenous supply to the lake, and

that MS could serve as a proxy for detrital influx variations. Soil erosion induced by land-use changes (e.g. land clearance for agriculture, cattle grazing, and development of human settlements) is an important factor for sediment accumulation in SAMO, especially towards the western side of the lake, which is surrounded by seasonal agriculture farmlands (Fig. 1C). This would also explain why SAMO 18-4 had (a) the lowest $^{210}Pb_{xs}$ activities, owing to dilution by higher sediment loads (Table 1); (b) the highest concentrations of terrigenous element concentrations (Fig. 3), and (c) the highest MAR values (Table 1).

The MAR fluctuations in the sediment records were not explained by the population growth (Fig. ESM5) or the temporal variations of the cultivated area (Fig. ESM6) in Santa María del Oro Municipality (where the agriculture data series are too short). However, it is noteworthy that corn, sugar cane, and agave cultivated areas have declined towards present (Fig. ESM6), particularly during the last decade, when MAR values also decreased. Likely, the reduction of the cultivated areas (and consequently, of the common activities that promote soil erosion, such as plowing and burning) has contributed to some extent, to reduce the erosion in the catchment and control the sedimentation pulses in SAMO.

Influence of climate variability on sedimentation

Rainfall may be the primary cause of erosion in many environmental settings, as water facilitates the weathering process that precedes erosion in most environmental settings, and it is also one of the main agents for sediment transport (Mishra et al. 2019). Considering the underlying assumptions behind the use of the element ratios and the decreasing trends in annual accumulated precipitation and evaporation (Fig. ESM4), the decreasing values of MS, Rb/Sr, and Ti/Ca before the 1980s (Fig. 5) would indicate lower terrigenous supply and higher endogenic carbonate precipitation, favored by higher lake water evaporation rates (Jin et al.

2006; Davies et al. 2015), and increasing Ti/Al values would account for a higher aeolian input (Martínez-Ruiz et al. 2015), in both cases promoted by the development of drier climate conditions in the area. Thus, MS and element ratios can reproduce the general pattern of rain variability before the 1980s, and the interrupted increasing MAR trends in all cores between 1960s and 1980s (Fig. 5). However, all MAR maxima occurring after the 1980s corresponded to annual accumulated precipitation minima (Fig. 5) and were usually characterized by maxima of MS, Rb/Sr, and Ti/Ca, and minima of Ti/Al, which would be indicative of humid conditions. This contradiction is caused by the relatively high concentrations of Al, Ti, and Rb in the core sections where the MAR maxima were recorded (Fig. 3), which also indicated that these sporadic sedimentation pulses have a terrigenous origin.

These results may be conditioned by some limitations. The meteorological data come from a station 5 km apart and 200 m above the SAMO altitude, so they may not accurately reflect the specific conditions at the study site; and these series are relatively short and have several gaps (mainly evaporation data). Moreover, the cores were cut into 1 cm thick sections and, given the millimeter-laminated nature of these sediments, it is possible that sediments with different origins may have been mixed. In addition, within the period for which meteorological data are available (1964-2014), the geochemical records of the sediment cores are noisier (Fig. 3).

We speculate that the terrigenous pulses could be related to the accelerated erosion of the SAMO catchment (PO 2003), caused by deforestation, agriculture, and forest fires. These fires are attributed to extreme temperatures, droughts, and uncontrolled (domestic and agriculture) waste burning (INIFAP 2012; SEDATU 2013). The coincident MAR and MS maxima could be the result of topsoil magnetic enhancement produced by wildfires, owing to the pyrogenic-induced transformation on mineral constituents of the soils or in vegetation ashes (Till et al. 2021). Specific records on the frequency and extent of the wildfires in the

study area are not available to test this hypothesis. Nonetheless, soil erodibility increases during dry periods due to lower soil moisture (Toy et al. 2002), and sediment yields may significantly increase after wildfires (DiBiase and Lamb 2019) owing to the loss of protective ground cover holding the soil in place, which reduces the threshold of intensity and amount of rainfall needed for erosion in normal conditions. Post-fire erodibility is highest because of water repellency and exposure of denuded soils to rainfall. Increased sediment loading can produce episodes of exceptionally high rates of sediment transport, which tend to be transient and irregular; however, with vegetation recovery, rates of hillslope erosion typically return to pre-burn levels within a few years to one decade (Ryan et al. 2011). It is expected that climate change will increase the extent of wildfires worldwide, increasing catchment erosion and sedimentation in aquatic ecosystems, which would reduce the water storage and may impact the water quality owing to the input of contaminants adsorbed to the sediments (Sankey et al. 2017).

Conclusions

The temporal variations of sediment accumulation rates within the past ~100 years were reconstructed through the study of ^{210}Pb-dated sediment cores, collected from Santa María del Oro Lake, a developing tourism spot in northwestern Mexico. Results showed that lake sedimentation is spatially and temporally heterogeneous with overall mass accumulation rates (MAR) ranging from 0.01 to 0.80 g cm^{-2} yr^{-1}, and sediment accumulation rates (SAR) from 0.04 to 2.86 cm yr^{-1}. Highest MAR and SAR values were observed near the lakeshore (at Agua Caliente Bay), most likely caused by its shallowness, the closeness to surrounding human settlements and agriculture fields, as well as the influence of seasonal runoff entering the lake from surrounding hills. The highest variations in MAR and SAR values in all cores

were observed within the second half of the last century, although only in Agua Caliente Bay the post-1950s values of MAR (0.26 ± 0.17 g cm^{-2} yr^{-1}) were significantly higher than during the first half of the century (0.08±0.07 g cm^{-2} yr^{-1}). MAR variations were mainly attributed to a combination of land-use change and climate variability. Sedimentation pulses observed in all cores, mostly since the 1980s, have occurred during years of minimum precipitation. This could be the result of increasing soil erodibility due to lower soil moisture and the occurrence of wildfires in the catchment. Despite MARs having decreased in the last decade, results highlighted the lake´s susceptibility to siltation problems; sedimentation pulses may happen again and unregulated human activities can only worsen this problem. Considering the close relation between drier conditions, wildfires, and soil erosion, it is foreseen that climate change would promote higher sedimentation in downstream rivers and reservoirs, negatively impacting water supply and quality. Thus, controls on human settlement developments, agriculture practices, and mitigation measures against catchment erosion should be implemented in the surroundings of SAMO to preserve the conditions of this valuable water resource.

Acknowledgments

This work was supported by the grants UNAM DGAPA-PAPIIT/104718 and Newton Mobility Grant NMG\R2\170126. Support by the Posgrado en Ciencias del Mar y Limnología, UNAM and a postgraduate studies fellowship from CONACyT (CVU 969662) is acknowledged by DMHR. Thanks are due to Cuellar-Martínez T.C., López-Mendoza P. G., Ramírez-Macías E. S., Sanchez-Rivas J.L., and García-Arvizu J. M. for technical support in radiometric analysis; and to Germán Ramírez, Carlos Suárez and León Felipe Álvarez for data curation and artwork assistance.

References

Alcocer J, Ruiz-Fernández AC, Oseguera LA, Caballero M, Sanchez-Cabeza JA, Pérez-Bernal LH, Hernández-Rivera DM (2020) Sediment carbon storage increases during the Anthropocene in tropical, oligotrophic, high-mountain lakes. Anthropocene 32, 100272

Alvisi F, Frignani M (1996) ^{210}Pb-derived sediment accumulation rates for the central Adriatic Sea and crater lakes Albano and Nemi (central Italy) In: Palaeoenvironmental analysis of Italian Crater Lake and Adriatic Sediments P Guilizzoni and F Oldfield (eds) Memorie dell'Istituto Italiano di Idrobiologia. Int J Limnol 55: 303-320

Appleby PG, Semertzidou P, Piliposian GT, Chiverrell RC, Schillereff DN, Warburton J (2019) The transport and mass balance of fallout radionuclides in Brotherswater, Cumbria (UK). J Paleolimnol 62, 389 – 407

Aquino-López MA, Ruiz-Fernández AC, Blaauw M, Sanchez-Cabeza JA (2020). Comparing classical and Bayesian ^{210}Pb dating models in human-impacted aquatic environments. Quat Geochronol 60, 101106

Barr C, Tibby J, Gell P, Tyler J, Zawadzki A, Jacobsen GE (2014) Climate variability in south-eastern Australia over the last 1500 years inferred from the high-resolution diatom records of two crater lakes. Quat Sci Rev 95, 115-131

Blaauw M, van Geel B, Kristen I, Plessen B, Lyaruu A, Engstrom DR, van der Plicht J, Verschuren D (2011) High-resolution ^{14}C dating of a 25,000-year lake-sediment record from equatorial East Africa. Quat Sci Rev 30, 3043-3059

Caballero M, Rodríguez A, Vilaclara G, Ortega B, Roy P, Lozano S (2013) Hydrochemistry, ostracods and diatoms in a deep, tropical, crater lake in Western Mexico. J Limnol 72: 512-523

Cardoso-Mohedano JG, Sanchez-Cabeza JA, Ruiz-Fernández AC, Pérez-Bernal LH, Lima-Rego J, Giralt S (2019) Fast deep water warming of a subtropical crater lake. Sci Total Environ 691: 1353-1361

Davies SJ, Lamb HF, Roberts SJ (2015). Micro-XRF Core Scanning in Palaeolimnology: Recent Developments. In: Croudace, I W, Rothwell, RG (2015) Micro-XRF Studies of Sediment Cores: Applications of a non-destructive tool for the environmental sciences. Springer, Dordrecht

Dean WE (1974) Determination of carbonate and organic matter in calcareous sediments and sedimentary rocks by loss on ignition: comparison with other methods. J Sediment Petrol 44: 242–248

Dearing JA, Hay KL, Baban SM, Huddleston AS, Wellington EM, Loveland P (1996) Magnetic susceptibility of soil: an evaluation of conflicting theories using a national data set. Geophys J Int 127: 728-734

Degife A, Worku H, Gizaw S (2021) Environmental implications of soil erosion and sediment yield in Lake Hawassa watershed, south-central Ethiopia. Environ Syst Res 10, 28, 2-24

Du Y, Xue HP, Wu SJ, Ling F, Xiao F, Wei XH (2011). Lake area changes in the middle Yangtze region of China over the 20th century. J Environ Manage 92, 4, 1248-1255

DEPCB (2015). Plan estatal de contingencias para incendios forestales 2015. Dirección Estatal de Protección Civil y Bomberos. http://www.proteccioncivil.gob.mx/work/models/ProteccionCivil/swbcalendario_ElementoSeccion/675/PROGRAMA_ESTATAL_DE_CONTINGENCIAS_PARA_INCENDIOS_FORESTALES_2015.PDF

Díaz-Asencio M, Sanchez-Cabeza JA, Ruiz-Fernández AC, Corcho-Alvarado JA, Pérez-Bernal LH (2020). Calibration and use of well-type germanium detectors for low-level gamma-ray spectrometry of sediments using a semi-empirical method. J Environ Radioact 225: 106385

DiBiase RA, Lamb MP (2019) Dry sediment loading of headwater channels fuels post-wildfire debris flows in bedrock landscapes. Geology 48: 189–193

DOF (2016) Acuerdo por el que se da a conocer el resultado de los estudios técnicos de las aguas nacionales subterráneas del Acuífero Valle de Santa María del Oro, clave 1812, en el Estado de Nayarit, Región Hidrológico-Administrativa Lerma-Santiago-Pacífico 6. Diario Oficial de la Federación. https://www.dof.gob.mx/ Accessed: 2020-06-19

Glynn D, Druffel E, Griffin S, Dunbar RB, Osbourne M, Sanchez-Cabeza JA (2013) Early bomb radiocarbon detected in Palau Archipelago corals. Radiocarbon 55: 1659 – 1664

González-Bernal V M (2008) Problemática socioeconómica de los productores independientes de agave azul del municipio de Santa Maria del Oro, Nayarit, 1996-2006 Dissertation Universidad Autónoma de Nayarit Tepic, 115 pp (in Spanish)

Gougoulias C, Clark J M, Shaw LJ (2014) The role of soil microbes in the global carbon cycle: tracking the below- ground microbial processing of plant- derived carbon for manipulating carbon dynamics in agricultural systems. J Sci Food Agric 94: 2362-2371

Gravina A, Soreghan M, Bogan MT, Busch J, McGlue M, McIntyre P, Kimirei I, Cohen A (2020). Relationship of sediment influx to ostracode populations on the variably deforested Luiche and Mahale platform coasts of Lake Tanganyika, Tanzania. J Great Lakes Res 46, 5, 1207-1220

Hair J, Black W, Babin B, Anderson R (2010). Multivariate data analysis. 7th ed. Prentice Hall New Jersey

Hernández Cerda ME, Valdez Madero G (2004) Sequía meteorológica In: Cambio climático: una visión desde México J Martínez and A Fernández Bremauntz (eds) Instituto Nacional de Ecología, Mexico City, Mexico, pp 315-325

INEGI (2009) Prontuario de información geográfica municipal de los Estados Unidos Mexicanos Clave 18014 Instituto Nacional de Estadística, Geografía e Informática https://www.inegi.org.mx/contenidos/app/mexicocifras/datos_geograficos/18/18014.pdf Accessed: 2020-06-30

INIFAP (2012) Programa de Acción ante el Cambio Climático de Nayarit Resumen Ejecutivo. Instituto Nacional de Investigaciones Forestales, Agrícolas y Pecuarias Tepic, Mexico. https://www.gob.mx/cms/uploads/attachment/file/164935/2012_nay_pacc.pdf

Jin Z, Cao J, Wu J, Wang S (2006) A Rb/Sr record of catchment weathering response to Holocene climate change in Inner Mongolia. Earth Surf Processes Landforms 31: 285-291

Krishnaswamy S, Lal D, Martin JM, Meybeck M (1971). Geochronology of lake sediments. Earth Planet Sci Lett 11: 407-414

Lefkowitz JN, Varekamp J C, Reynolds RW, Thomas E (2017) A tale of two lakes: the Newberry Volcano twin crater lakes, Oregon, USA. In: Geochemistry and Geophysics of Active Volcanic Lakes Ohba, T, Capaccioni, B Caudron, C (eds). Spec Publ 437: 253–288

Lozano-García S, Figueroa-Rangel B, Sosa-Nájera S, Caballero M, Noren AJ, Metcalfe SE, Tellez-Valdés O, Ortega-Guerrero B (2021) Climatic and anthropogenic influences on vegetation changes during the last 5000 years in a seasonal dry tropical forest at the northern limits of the Neotropics. The Holocene 31(5) 802–813

Martinez-Ruiz F, Kastner M, Gallego-Torres D, Rodrigo-Gámiz M, Nieto-Moreno V, Ortega-Huertas M (2015) Paleoclimate and paleoceanography over the past 20,000 yr in the Mediterranean Sea Basins as indicated by sediment elemental proxies. Quat Sci Rev 107: 25-46

McCorkle EP, Berhe AA, Hunsaker CT, Johnsone DW, McFarlane KJ, Fogel ML, Hart SC (2016) Tracing the source of soil organic matter eroded from temperate forest catchments using carbon and nitrogen isotopes. Chem Geol 445, 172–184

McGlue MM, Yeager KM, Soreghan MJ, Behm M, Kimirei IA, Cohen AS, Apse C, Limbu P, Smiley RA, Doering D, Lucas JS, Mbonde A, McInytre PB (2021). Spatial variability in nearshore sediment pollution in Lake Tanganyika (East Africa) and implications for fisheries conservation. Anthropocene 33, 100281

Mishra AK, Placzek C, Jones R (2019) Coupled influence of precipitation and vegetation on millennial-scale erosion rates derived from ^{10}Be. PLoS ONE 14: e0211325

Moges MA, Schmitter P, Tilahun SA, Ayana EK, Ketema AA, Nigussie TE, Steenhuis TS (2017). Water Quality Assessment by Measuring and Using Landsat 7 ETM+ Images for the Current and Previous Trend Perspective: Lake Tana Ethiopia. Journal of Water Resource and Protection 9,12, 1564-1585

Moreno-Moreno LR, Orozco Espinosa P, Barrón Arreola KS (2015) Turismo y medio ambiente Una aplicación del método de costo de viaje en la Laguna de Santa María del Oro, Nayarit In: Temas selectos de turismo y sustentabilidad, KS Barrón Arreola, MA Fonseca Morales (Eds) Universidad Autónoma de Nayarit, Tepic, pp 157-182 (in Spanish)

Neff JC, Ballantyne AP, Farmer GL, Mahowald NM, Conroy JL, Landry CC, Overpeck JT, Painter TH, Lawrence CR, Reynolds RL (2008) Increasing eolian dust deposition in the western United States linked to human activity. Nat Geosci 1: 189-195

Ngos III S, Sirocko F, Lehné R, Giresse P, Servant M (2008) The evolution of the Holocene palaeoenvironment of the Adawama of Cameroon: evidence from sediments from two crater lakes near Ngaoundéré In: Dynamics of forest ecosystems in central Africa during the Holocene: past-present-future. Palaeoecology of Africa J Runge (ed) CRC Press, Boca Raton, USA, pp 103-120

Pastor AV, Nunes JP, Ciampalini R, Koopmans M, Baartman J, Huard F, Calheiros T, Le-Bissonnais Y, Keizer JJ, Raclot D (2019) Projecting future impacts of global change including fires on soil erosion to anticipate better land management in the forests of NW Portugal. Water 11, 2617, 2-19

PO (2003) Acuerdo por el que se expide el programa de ordenamiento ecológico de la cuenca de Santa María del Oro, Nayarit Periódico Oficial, 12 February 2003, CLXXII, 19, Tepic, Mexico (in Spanish), 93 pp

Preiss N, Mélieres MA, Pourchet M (1996) A compilation of data on lead-210 concentration in surface air and fluxes at the air-surface and water-sediment interfaces J Geophys Res 101: 28847–28862

R Core Team (2021). R: A language and environment for statistical computing. R Foundation for Statistical Computing, Vienna, Austria. Available online at https://www.R-project.org/

Ranjan R (2019). A forestry-based PES mechanism for enhancing the sustainability of Chilika Lake through reduced siltation loading. Forest Policy Econ 106, 101944

Robbins JA (1978) Geochemical and geophysical applications of radioactive lead In: Nriagu, JO (Ed), Biogeochemistry of Lead in the Environment Elsevier Scientific, Amsterdam, pp 285-393

Rodríguez-Ramírez A, Caballero M, Roy P, Ortega B, Vázquez-Castro G, Lozano-García S (2015) Climatic variability and human impact during the last 2000 years in western Mesoamerica: evidences of late Classic and Little Ice Age drought events. Clim Past 11: 1239-1248

Rosenheim BE, Santoro JA, Gunter M, Domack EW (2013) Improving Antarctic sediment ^{14}C dating using ramped pyrolysis: an example from the Hugo Island Trough. Radiocarbon 55: 115-126

Ruiz-Fernández AC, Hillaire-Marcel C, Páez-Osuna F, Ghaleb B, Caballero M (2007) ^{210}Pb chronology and trace metal geochemistry at Los Tuxtlas, Mexico, as evidenced by a sedimentary record from the Lago Verde Crater Lake. Quat Research 67: 181-192

Ruiz-Fernández AC, Hillaire-Marcel C (2009) ^{210}Pb-derived ages for the reconstruction of terrestrial contaminant history into the Mexican Pacific coast: Potential and limitations. Mar Pollut Bull 59: 134-145

Ruiz-Fernández AC, Maanan M, Sanchez-Cabeza,JA, Pérez Bernal LH, López Mendoza P, Limoges A (2014) Cronología de la sedimentación reciente y caracterización geoquímica de

los sedimentos de la laguna de Alvarado, Veracruz (suroeste del golfo de México). Cienc Mar 40: 291-303

Ruiz-Fernández AC, Páez-Osuna F, Urrutia-Fucugauchi J, Preda M (2005) ^{210}Pb geochronology of sediment accumulation rates in Mexico City Metropolitan Zone as recorded at Espejo de los Lirios lake sediments. Catena 61: 31-48

Ryan SE, Dwire KA, Dixon MK (2011) Impacts of wildfire on runoff and sediment loads at Little Granite Creek, western Wyoming. Geomorphology 129: 113–130

Salminen R, Bautista M J, Bidovec M, Demetriades A, De Vivo B, De Vos W, Duris M, Gilucis A, Gregorauskiene V, Halamic J, Heitzmann P, Lima A, Jordan G, Klaver G, Klein P, Lis J, Locutura J, Marsina K, Mazreku A, O'Connor PJ, Olsson SA, Ottesen RT, Petersell V, Plant JA, Reeder S, Salpeteur I, Sandström H, Siewers U, Steenfelt A, Tarvainen T (2005) Geochemical Atlas of Europe Part 1: Background Information, Methodology and Maps. Geological Survey of Finland, Espoo

Sanchez-Cabeza JA, Druffel ER (2009) Environmental records of anthropogenic impacts on coastal ecosystems: an introduction. Mar Pollut Bull 59: 87-90

Sanchez-Cabeza JA, Ruiz-Fernández AC (2012) ^{210}Pb sediment radiochronology: an integrated formulation and classification of dating models. Geochim Cosmochim Acta 82: 183-200

Sanchez-Cabeza JA, Ruiz-Fernández AC, Ontiveros-Cuadras JF, Pérez-Bernal LH, Olid C (2014) Monte Carlo uncertainty calculation of ^{210}Pb chronologies and accumulation rates of sediments and peat bogs. Quat Geochronol 23: 80-93

Sankey JB, Kreitler J, Hawbaker TJ, McVay JL, Miller ME, Mueller ER, Vaillant NM, Lowe SE, Sankey TT (2017) Climate, wildfire, and erosion ensemble foretells more sediment in western USA watersheds. Geophysical Research Letters 44: 8884-8892

Saulnier-Talbot E, Pienitz R, Stafford TW Jr (2009) Establishing Holocene sediment core chronologies for northern Ungava lakes, Canada, using humic acids (AMS ^{14}C) and ^{210}Pb. Quat Geochronol 4, 278–287

Schuur EAG, Druffel ERM, Trumbore SE (2016) Radiocarbon and Climate Change Mechanisms, Applications and Laboratory Techniques. Springer, Switzerland

SEDATU (2013) Atlas de riesgos del municipio de Santa María del Oro, Nayarit. Secretaría de Desarrollo Agrario, Territorial y Urbano Santa María del Oro, Mexico

Serrano D, Filonov A, Tereshchenko I (2002) Dynamic response to valley breeze circulation in Santa Maria del Oro, a volcanic lake in Mexico. Geophys Res Lett 29:27-31

Sert I (2018) Applying of modified constant rate of supply model to lake sediments in ^{210}Pb dating and assessment of some heavy metals. J Nat Appl Sci 22: 598-607

Shen J, Wu X, Zhang Z, Gong W, He T, Xu X, Dong H (2013) Ti content in Huguangyan maar lake sediment as a proxy for monsoon- induced vegetation density in the Holocene. Geophys Res Lett 40: 5757-5763

SMN (2020) Normales Climatológicas por Estado/Nayarit Servicio Meteorológico Nacional, Comisión Nacional del Agua https://smnconaguagobmx/es/informacion-climatologica-por-estado?estado=nay Accessed: 2020-05-28

Smol JP (2008) Pollution of Lakes and Rivers A Paleoenvironmental Perspective. Blackwell Publishing, Oxford

Soeprobowati TR, Suedy SWA, Hadiyanto, Lubis AA, Gell P (2018) Diatom assemblage in the 24 cm upper sediment associated with human activities in Lake Warna Dieng Plateau Indonesia. Environ Technol Inno 10: 314–323

Sosa-Nájera, S, Lozano-García, S, Roy, P D, Caballero, M (2010) Registro de sequías históricas en el occidente de México con base en el análisis elemental de sedimentos lacustres: El caso del lago de Santa María del Oro. Bol Soc Geol Mex 62: 437-451

Steffen W, Sanderson A, Tyson PD, Jäger J, Matson PA, Moore B III, Oldfield F, Richardson K, Schellnhuber HJ, Turner II BL, Wasson RJ (2005) Global Change and the Earth System - A Planet Under Pressure Springer, New York

Till JL, Moskowitz B, Poulton S W (2021) Magnetic properties of plant ashes and their influence on magnetic signatures of fire in soils. Front Earth Sci 8, 1-16

Toy TJ, Foster, GR, Renard KG (2002) Soil Erosion: Processes, Prediction, Measurement, and Control. John Wiley & Sons, New York

UNSCEAR (2000) Sources and effects of ionizing radiation United Nations Scientific Committee on the Effects of Atomic Radiation UNSCEAR 2000 Report to the General Assembly, with Scientific Annexes. Volume I: sources United Nations, New York

Vázquez-Castro G, Ortega-Guerrero B, Rodríguez A, Caballero M Lozano-García S (2008) Mineralogía magnética como indicador de sequía en los sedimentos lacustres de los últimos ca 2,600 años de Santa María del Oro, occidente de México. Revista Mexicana de Ciencias Geológicas 25: 21-38

Wang J, Baskaran M, Niedermiller J (2017) Mobility of ^{137}Cs in freshwater lakes: A mass balance and diffusion study of Lake St Clair, Southeast Michigan, USA. Geochim Cosmochim Acta 218: 323-342

Wei G, Li XH, Liu Y, Shao L, Liang X (2006) Geochemical record of chemical weathering and monsoon climate change since the early Miocene in the South China Sea. Paleoceanogr Paleoclimatol 21: 1-11

Yim SA, Chae JS, Byun JI, Ko SH (2018) Characteristics of artificial radionuclides in sedimentary soil cores from a volcanic crater lake. J Environ Radioact 192:532–542

Xu M, Dong X, Yang X, Chen X, Zhang Q, Liu Q, Wang R, Yao M, Davidson TA, Jeppesen E (2017). Recent Sedimentation Rates of Shallow Lakes in the Middle and Lower Reaches of the Yangtze River: Patterns, Controlling Factors and Implications for Lake Management. Water 9, 617, 2-18.

Zamudio V, Méndez E (2011) The vulnerability of agricultural soils to erosion in the central-south region of the State of Nayarit, Mexico. Ambiente y Desarrollo XV 28: 11-40

Zárate-Del Valle PF, Gomez-Hermosillo CM; Venegas-Garcia DJ (2007) Crater-lake Santa Maria del Oro as a Pristine Reference for Persistent Organic Pollutants (POP's) and Heavy Metals Content in Environmental Investigations in Western Mexico (Project CONACYT-SEMARNAT 2002-C01-0463, in Progress). American Geophysical Union, Fall Meeting 2007. Eos Trans AGU 88:(52), Fall Meet Suppl, Abstract B33C-1427

Zhou K, Xu H, Lan J, Yan D, Sheng E, Yu K, Song Y, Zhang J, Fu P, Xu S (2020) Variable Late Holocene 14C Reservoir Ages in Lake Bosten, Northwestern China. Frontiers in Earth Science 7, 328, 1-11

FIGURE CAPTIONS

Fig. 1. Sampling information. A= Santa María del Oro Lake (SAMO) and Santa María del Oro City, NW Mexico; yellow dots indicate CB (Cerro Blanco meteorological station) and the soil sample location. B = the inset shows Mexico, Nayarit (grey) and the lake location (black circle); bathymetry and sampling locations of sediment trap and cores in SAMO (SAMO 14-1: 21.369° N, 104.565° W, 55 m depth; SAMO 14-2: 21.370° N, 104.572° W, 48.2 m; SAMO 14-3: 21.372° N, 104.572° W, 52 m; and shallow core: SAMO 18-4: 21.371° N, 104.577° W, 30 m (Agua Caliente Bay)). C = land use and vegetation in the catchment of SAMO.

Fig. 2. Dating Information for sediment cores from Santa Maria del Oro Lake, NW Mexico. A= activity depth profiles of $^{210}Pb_{tot}$ and ^{226}Ra; B= ^{210}Pb-derived age models and activities of ^{137}Cs and $^{239+240}Pu$ (orange and gray bars, respectively; logarithmic values); C= on the left, depth profiles of $F^{14}C$ values (empty circles) and ^{137}Cs activities (orange circles); on the right, conventional ^{14}C ages in sediment core SAMO 14-2.

Fig. 3. Temporal profiles of sediment variables in cores from Santa María del Oro Lake, NW Mexico. Units are: mass accumulation rate (MAR, g cm^{-2} yr^{-1}; logarithmic values); magnetic susceptibility (x 10^{-5} SI); clay, silt, sand, C_{org}, C_{inorg}, Al, Ti, Fe, K and Ca (%); Rb, Zr, Th, and Sr (µg g^{-1}).

Fig. 4. Factor analysis results for sediments from Santa María del Oro Lake, NW Mexico. A= loadings of variables for factors 1 and 2; B = score of observations (sediment core and soil samples).

Fig. 5. Temporal profiles of mass accumulation rates (MAR, g cm^{-2} yr^{-1}), meteorological data (Cerro Blanco Station), magnetic susceptibility (MS) and element ratios for sediment cores from Santa María del Oro Lake, Mexico. Filled dots indicate the maxima of MAR (orange) and corresponding minima or maxima (blue) of other variables.

Fig. 6. Cluster analysis for meteorological data (mean annual temperature, and accumulated precipitation and evaporation from Cerro Blanco Station (1963 - 2014) and variables (mass accumulation rate, MAR; magnetic susceptibility, MS; and the ratios Rb/Sr, Ti/Ca, and Ti/Al) from sediment cores collected at Santa María del Oro Lake, NW Mexico.

JOPL-D-20-00091 Historical reconstruction of sediment accumulation rates as an indicator of global change impacts in a tropical crater lake

The authors are grateful for the exhaustive review performed by the editors and reviewers. Efforts have been made to answer and solve all issues raised in the reports.

Editor in Chief Thomas J. Whitmore

Minor points Format for JOPL:

Q1. some citations show "et al," rather than "et al." ANSWER: none found; it seems that this was due to a font problem created with the production of the pdf file.

Q2. commas need to be removed between the names of authors and the dates in citation. ANSWER: done.

Q3. "and references therein" and "e.g." in citations: citations should only include authors and dates. ANSWER: corrected.

Q4. the font does not read well for some reson in the PDF. Could you please use Times New Roman 12? ANSWER: done.

Q5. fractional units need to be in exponential format. ANSWER: corrected

Q6. 2nd-level header "Sampling" in the Methods, please use a better header, because it's not clear if you are collecting cores or in the lab. ANSWER: the header "Sampling" was substituted by "Field work".

Q7. please update the "in press" paper with publication information. ANSWER: done.

Q8. The spacing on the DOF reference seems to be a problem (see this in the PDF version). ANSWER: corrected

Q9. please place a blank line between references so the references won't be combined accidentally during proof construction. ANSWER: done

Q10. Figure legends need to be listed separately from the figures, see Guidelines for Authors https://www.springer.com/journal/10933/submission-guidelines. ANSWER: corrected.

Q11. latitude and longitude are needed on the map in Figure 1. ANSWER: done.

Q12. some figures have S designations. Are you showing Electronic Supplementary Material? If so, this is not clear. If you are, Electronic Supplementary Material should be referred to in the text using sequential ESM numbers (e.g., ESM1, ESM2, etc.), preferably without reference to table or figure numbers, and those files need to be uploaded separately

ANSWER: yes, we referred with "S" to supplementary figures. Supplementary tables and figures are now in an integrated file, to be uploaded separately.

Q13. Table 2 lists submitted papers, but these can not be shown (or are "unpublished data"). Only published papers can be cited. Dates belong in parentheses. ANSWER: corrected.

Q14. Simbology misspelled, and should be "Symbols". ANSWER: corrected.

Associate Editor, Jaime Escobar

Both reviewers agree that the manuscript could be accepted for publication after major revisions. I concur with reviewers comments and suggestions. Both reviewers made detailed comments on issues that should be addressed before resubmission of the manuscript. Major comments include: (1) a clear documentation of the sedimentology of the cores, (2) a better discussion on results from the top part cms of the core, and (3) lack of data to test the hypothesis on anthropogenic development as the cause for changes in the sediment.

ANSWER: authors thank to the associated Editor for the handling of this MS. The main issues highlighted by the Editor have been addressed following the very useful comments received.

Reviewer #1

The submitted manuscript by Ruiz-Fernandez and co-authors deals with a detailed analysis of four short sediment cores from a crater lake in Mexico. They focused on high-resolution dating of sediment cores mainly with 210 Pb, complemented by independent methods like 137 Cs, plutonium isotopes and radiocarbon. With these high-resolution age models, the authors interpret predominantly elemental concentration data, magnetic susceptibility and mass accumulation rates in relation to anthropogenic impact and climate changes.

R1.1 Although the authors present a wealth of data and I'm convinced that the records potentially hold an interesting story about human impact over the recent decades, the manuscript in its current status lacks a clear focus. The manuscript has an overwhelming number of diagrams, which makes it hard to see the red line for the reader. The authors should ask themselves for which topic this manuscript should be citied. At the moment, the manuscript needs major revisions before it can be published in JOPL; in its current status the manuscript is maybe better suited for a regional or national journal, but that decision will be left to the editors.

ANSWER R1.1: the manuscript provides information on the sediment input trends over the past 100 years and explores the reasons for this sediment input variability, including the influence of anthropic activities and climate change, two main drivers of global change impacts. Efforts have been made to improve the presentation of our results to guide the readers more effectively. We expect that the manuscript will be of interest for a wide audience, including researchers interested in radiometric dating, in sediments as a contaminant, in the impacts of global change (anthropogenic and climate drivers), and in the conservation of lakes; but also, for researchers, public and private stakeholders specifically interested in Santa Maria del Oro Lake.

R1.2 Missing sedimentological aspects. What I miss most in this study is a clear documentation of the sedimentology of the cores. I'm aware that the authors sliced the cores after retrieval in 1-cm intervals, but the noisier upper part of the core is very likely the result of the occurrence of turbidites (this term does not appear in the manuscript!). That would explain the peaks in the sand fraction, in the detrital elements, the magnetic susceptibility (MS, see also my comment 3), and in MAR. If the authors would have a photograph (also from a core taken earlier), this aspect could be evaluated. If there are graded layers visible, then these could be turbidites triggered by heavy rain fall events or by earthquakes. Interestingly the sand fraction, as well as the detrital elements are higher also in the lower part. Could this pattern be explained with more frequent, but smaller turbidites?

ANSWER R1.2: As the reviewer indicates, the cores analyzed here were retrieved and directly sliced in the field, which hampered to perform their detailed lithological description. We made this decision because the cores contained liquified muds in their uppermost section and we feared that these might get mixed up during the road trip to the lab in Mazatlán, which would have ruined the ^{210}Pb dating. However, in 2014, we also retrieved three cores which were sealed and shipped to the Geo3BCN in Barcelona. These last cores were split longitudinally and a high-resolution image was taken using the CCD camera of an AVAATECH XRF core scanner (see below). We did not add this image in the first version of the manuscript because the core did not display the best preservation of the uppermost sediments (as we initially feared). However, on request of Reviewer 1, we have added it to the Supplementary Information (Fig. ESM1).

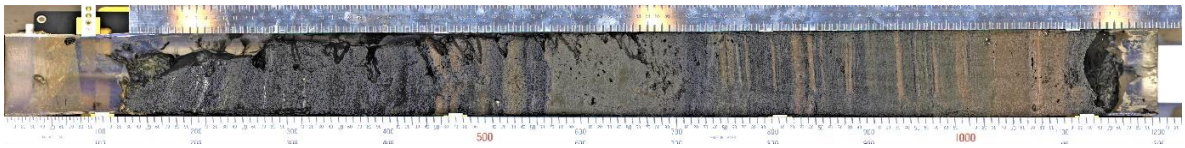

As the reviewer will appreciate, the sediments are mainly made up of clayey silts with no visible sandy layers. The uppermost 31 cm are composed of millimeter laminated dark greenish clay sediments with the intercalation of millimeter thick whitish lamina, most possibly formed by endogenic carbonates. The rest of the core is made up of a millimeter to centimeter thick alternation of dark and light clayey silts, except for the 44 - 58 cm core interval where homogeneous light greenish sediments are found. The basal contact of these laminae does not present erosive features nor coarser granulometry, ruling out the possible existence of turbidites suggested by the reviewer. Figure 3 shows that the mean content of sands in these sediments is ca. 2%, and only 1 sample showed percentages larger than 10%, which does not support the presence of turbidites.

On the other hand, the core was sliced into 1 cm samples, and giving the already described millimeter-thick lamination nature of these sediments, it is possible that sampling promoted mixing layers with different origins.

R1.3 Age model uncertainties. The authors present elaborated age models for the different cores using several independent methods. That is well done. The age models are robust for example in the 1960ies, where you have the 137Cs peak as independent marker horizon. I'm not so convinced that the age model has the precision in the top 10 cm to draw conclusions about the synchronicity of MAR events. The different records for core 14-1 and14-2 (in Fig. 3) are so similar that it is hard to believe that they are not synchronous. Here again would the sedimentology help to link the two cores. Another potential way would be to look at elements that are related to pollution (like Pb; but I do not know if that is the case in SAMO). But if this is the case then the two cores could be aligned against each other and evaluating the synchronicity of the MAR events. Furthermore, that could potentially question the link with the climate records (page 21, line 17).

ANSWER R1.3: we sympathize with the Reviewer´s doubts regarding the lack of synchronicity of the MAR maxima among cores, within a relatively small and deep lake, where it would be expectable to find more uniform sedimentary environments. However, our observation regarding the asynchronicity of the MAR is solely based on the radiometric results. Indeed, the $^{210}Pb_{xs}$ and MAR profiles in cores SAMO 14-1 and 14-2 have very similar shapes but, if we see both cores together, the $^{210}Pb_{xs}$ minima are not placed at the same depth and consequently, the MAR maxima are recorded several years apart (see below; uncertainty bars omitted on purpose for a cleaner view).

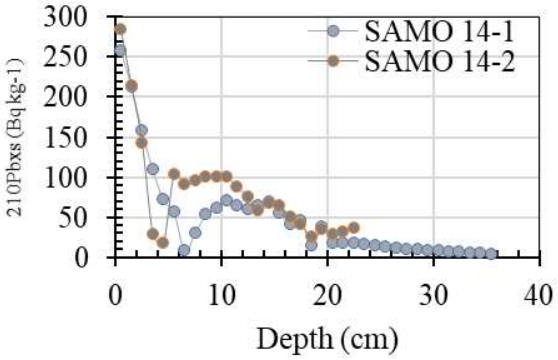

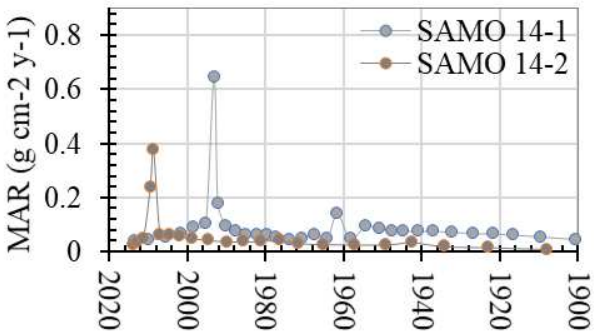

Visual inspection of the main lithological features of both cores may have been useful to link both cores, but unfortunately this information is not available. Chemostratigraphic profiles are also useful for correlation and stratigraphic interpretation. We do have measured trace elements (which are reported in another paper, in revision, related to trace element contamination trends in SAMO). Reviewer 1 has mentioned Pb, but this element was mostly below the detection limit (1 µg g^{-1}) in SAMO 14-2, thus, it is not useful for the proposed exercise; but let´s explore other elements. From the depth and temporal profiles of Cu, Zn, Al, and Ti presented below (SAMO 14-1 in black filled circles, and SAMO 14-2 in empty circles), it can be appreciated that the element profiles are very similar and that there is a very close alignment of the minima and maxima of the element concentrations, within the 10 cm segment (from the late 1980s onwards) for which the Reviewer expressed concern. Reviewer 1 may also take a look at the magnetic susceptibility profiles. In summary, the correlation (based on the ^{210}Pb-derived age models) of both cores is reasonably OK, and the MAR maxima are asynchronous.

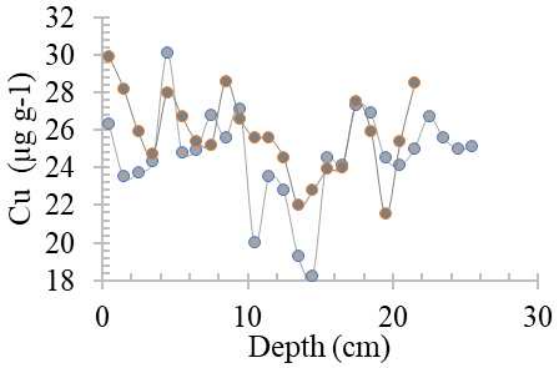

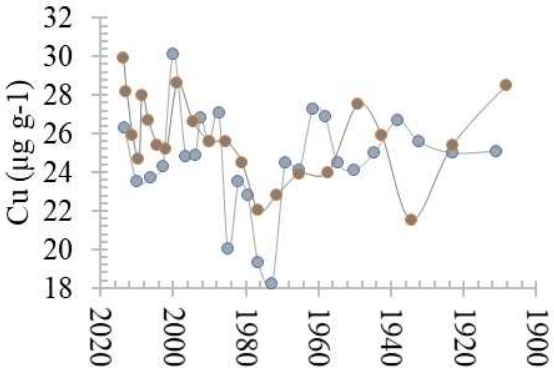

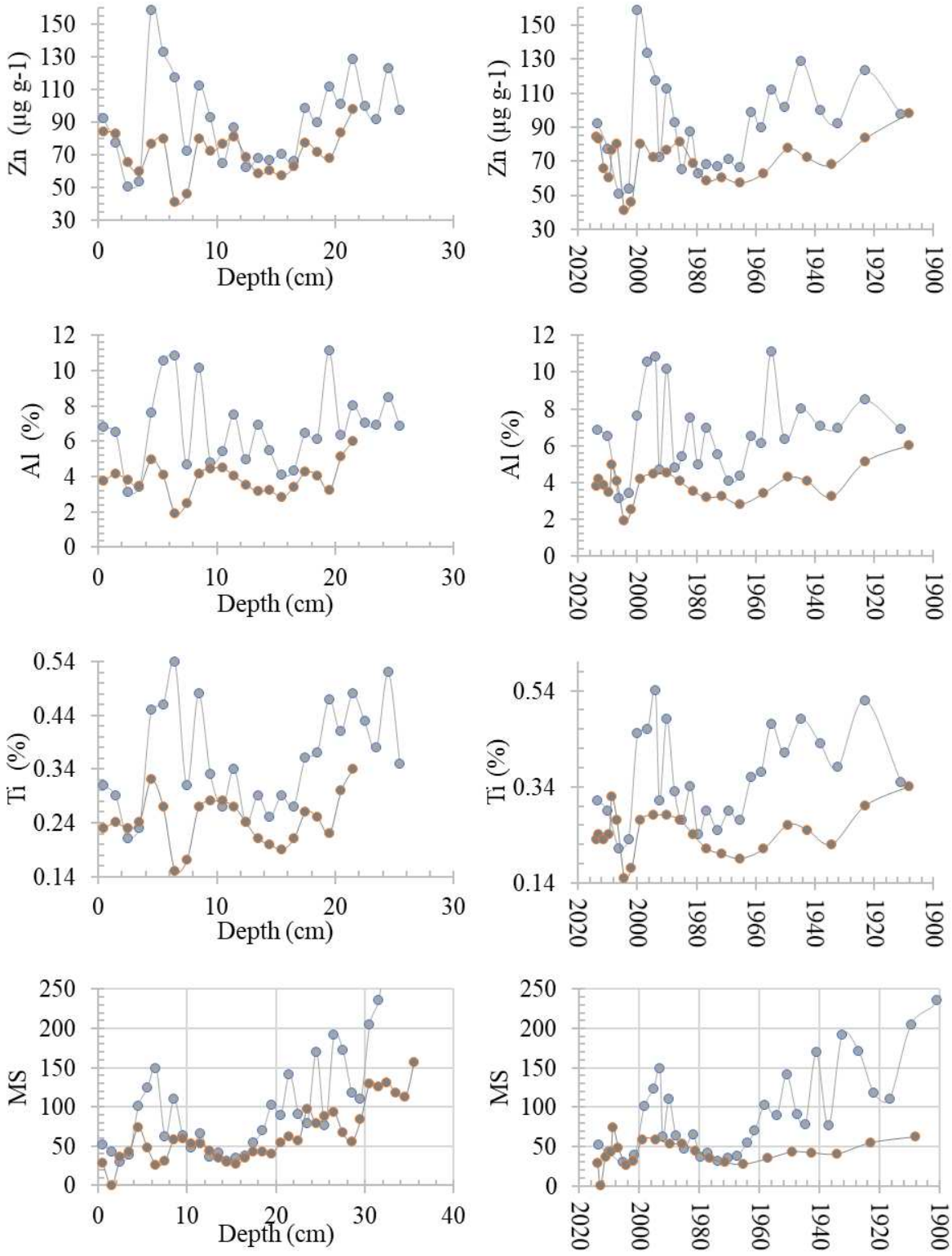

R1.4 Interpretation of the magnetic susceptibility record. The authors interpret the MS as a proxy for the formation of the secondary ferrimagnetic minerals (page 20, line 47). This cannot be

excluded but I think this is not the major driver for the MS variations. MS follows closely the different detrital elements (see Fig.3) and is therefore - my view - a nice proxy for detrital influx. In paleoflood reconstruction, MS is very often used to identify flood layers; a recent example is: Ekblom Johansson Fanny, Bakke Jostein, Støren Eivind Nagel, Paasche Øyvind, Engeland Kolbjørn, Arnaud Fabien, Lake Sediments Reveal Large Variations in Flood Frequency Over the Last 6,500 Years in South-Western Norway, Frontiers in Earth Science, 8, 2020, 239. URL=https://www.frontiersin.org/article/10.3389/feart.2020.00239
If the authors asses these three comments, the interpretation of the records would change.
ANSWER R1.4. The paragraph to which Reviewer 1 refers, explains the basis for the use of MS as a proxy to evaluate climate change, not the results of our study. As requested by Reviewer 1 (comment R1.10) this paragraph has been moved to the Introduction section, and maybe now the purpose of the paragraph is clearer. We agree that, in this study, MS might serve as a nice proxy for detrital influx, as indicated in the revised paragraph (section Discussion/ Influence of human activities on sedimentation):

> "The association of MS with terrigenous elements (Table ESM2, Fig. 4A) indicated that the strong changes of MS along the cores are related to changes in terrigenous supply to the lake, and that MS could serve as a proxy for detrital influx variations."

Minor comments:
R1.5 Introduction: The second paragraph discusses already the age model; this does not fit here. Use the introduction to frame the problem you are trying to address. I also miss recent references in the introduction that would show that the authors are addressing a current 'problem'.
ANSWER R1.5: the paragraph signaled by Reviewer 1 does not discuss the age model. This paragraph explains the radiometric methods used for sediment dating (following the closure of the previous paragraph); which is fundamental to evaluate sedimentation (addressed in the next paragraph). The problem that we are trying to address is the contamination of lakes by sediments, and the topic is addressed in the third paragraph of the introduction. We have introduced more recent references to show the topicality of the siltation problem.

R1.6 p. 4. line 45: Unclear if the 2600 year are the length of the record or if this number has something to do with the length the dry and wet periods.
ANSWER R1.6: it refers to both interpretations. The 2600 years is the period spanned in the sediment core, within which Rodríguez-Ramírez et al. (2015) observed the alternation of dry and wet periods. The sentence was rephrased to improve clarity:

> "the alternation of dry and wet periods within the past ca. 2600 years, …"

R1.7 p. 9, line 25: Where is the meteorological station? How far away from the lake. I think you mention this later in the text, but it is maybe already needed here. Add the location in Fig. 1.
ANSWER R1.7: the paragraph referred to by Reviewer 1 already included the exact location of the meteorological station. The updated paragraph now includes the distance from SAMO to Cerro Blanco station, and its location is also included in the revised version of Figure 1.

R1.8 p. 10, line 22: The authors use the term 'section' for their samples. For me, a section would be larger; I would use here: core 'samples'. (see also line 42)
ANSWER R1.8: yes, we use sections for core samples within a defined depth. The use of the term *section* is correct (definition in Oxford dictionary: any of the parts into which something is

divided); and its use has been also established for ^{210}Pb-dating methodology in Sanchez-Cabeza & Ruiz-Fernández et al., 2012.

R1.9 p. 13, line 22: The authors mention here C_{inorg} and they also introduce the LOI methods earlier, but they never show any data in the manuscript. A further indication that a clear focus of the manuscript is missing.
ANSWER R1.9: Reviewer 1 is almost right. C_{org} and C_{inorg} were measured in all cores and C_{org} was shown in Fig. 2S (in the supplementary material). The figures in the main body of the manuscript showed only those relevant variables for the factor analysis, which was used to identify the main processes that control the element temporal variations in the cores, to understand the MAR variability. In the original version of the manuscript, both C_{org} and C_{inorg} were eliminated from the factor analysis due to their low communalities (< 0.1) in the first exploratory FA, since significant variables within a factor should have *at least* a factor loading > |0.3| and a communality > 0.20 (Child (2006). In the revised version of the manuscript, the FA analysis includes soil samples (as requested by Reviewer 2, ANSWER R2.27), and now C_{org} and C_{inorg} have acceptable communalities (thus, included in the final FA; Fig. 4, Table ESM2).
Reference cited: Child D (2006) The essentials of factor analysis, 3rd edn. Continuum International Publishing Group, Bodmin, p 180.

R1.10 p. 14, line 27: Here, a detailed interpretation of the 3 ratios needs to be added. I know that the authors explain it a little bit later in the text, but the reader needs to know it already here.
ANSWER R1.10: the paragraph describing the basis on the use of the 3 ratios was moved up in the Introduction section, according to the reviewer´s recommendation.

R1.11 p. 14, line 32: I'm asking myself how fast would the weathering intensity would change. I guess it would be on the time scales of decades to centauries…so do you have a chance to see this in the historical records?
ANSWER R1.11: from the data in our core profiles and the general decreasing trends (between the 1900s and 1950s) in most terrigenous elements and MS, we may speculate that weathering intensity was highest in the past.

R1.12 page 20, lines 1-8: Here the authors discuss the difference between an upland and a lowland lake. According to the authors, is SAMO now an upland or lowland lake?
ANSWER R1.12: this paragraph was eliminated in the revised version.

R1.13 Fig. 1: 'Bathymetry' instead of 'Bathygraphy'
ANSWER R1.13: corrected.

R1.14 Fig. 1: Add the location of the meteorological station and of the soil sampling site.
ANSWER R1.14: done.

R1.15 Fig. 3: The captions says only something about the units for certain measurements, not all!
ANSWER R1.15: corrected.

R1.16 Fig. 3S: Add here that these are 'annual' precipitation and evaporation values. Check also in the text. My view it would be more interesting to look at the occurrence of extreme precipitation events that potentially triggered turbidites.

ANSWER R1.16: the caption of this figure (now 4ESM) was updated as indicated. We do not have evidence of turbidites, but Figure 5 already shows that MAR maxima correspond to precipitation minima (filled blue dots). The figure 5 caption has been revised to indicate this feature.

Reviewer #2 Reviewer 2 uploaded comments as a PDF file.

The present study builds up on a large dataset. These data clearly have the potential to be published. However, the current presentation of the data, and the analyses (particularly the meteorological data, e.g., extreme precipitation events in an ENSO sensitive region…) would highly benefit from a major revision. Therefore, the authors are encouraged to address the Major comments in the attached report.

The present manuscript describes the paleolimnological study conducted in the sediments of Lake Santa María del Oro, an endorheic crater lake in Pacific Western Mexico. Based on 4 sediment cores (one near shore, three close to the depocenter), a sediment trap, and one soil sample from the watershed, the authors reconstructed mass accumulation rates (MAR)- as well as other geochemical proxy-trends over the last ~100 years. The authors further analyzed meteorological data (time series ~55 years) from a nearby weather station to assess the influence of environmental and anthropogenic influences on the sedimentation processes. The approach relies on well constrained sediment chronologies to i) compare the processes within the different sediment cores (here ANOVA and for temporal evolution: factor analysis), ii) between the meteorological data and the sediments (here hierarchical cluster analysis), and iii) between local developments (land use, population growth) and the sediment- accumulation (no analysis presented). Therefore, the authors established independent ^{210}Pb- sediment chronologies (based on the CF-model) per sediment core and compared them with independent chrono-markers (^{137}Cs, $^{239+240}$Pu, and post-bomb ^{14}C). Radiocarbon analyses for further downcore reconstructions were hindered by a substantial reservoir effect.

The authors find that the MARs varied over the past ~100 years, and that the post-1950 levels are slightly higher than the pre-1950 levels (except for the sediments in the vicinity to the shore, where the values were significantly higher), and that the most recent MAR-values correspond to the pre-1950 levels. The comparison with the meteorological data revealed that the MAR peaked usually during years with minimum precipitation. Explained by: i) higher soil erodibility due to decreased soil moisture, ii) increased bush fires (destroyed vegetation cover), iii) slightly increased aeolian input, iv) increased autochthonous productivity, and v) land-use signal. Inter-core comparison reveals that the MAR differs per coring location (e.g. peak values), which can indicate that a regional signal (e.g., microclimate, weather) is less likely to control MAR. Interestingly, the MARs generally decreased over the last decade, however, reasons were not emphasized.

General comments

The present study builds up on a large dataset. These data clearly have the potential to be published. However, the current presentation of the data, and the analyses (particularly the meteorological data, e.g., extreme precipitation events in an ENSO sensitive region…) would highly benefit from a major revision. Therefore, the authors are encouraged to address the Major comments in the following report.

R2.1 Title. The title promises more than the study addresses. The authors are encouraged to reflect more on the title and infer it rather from the presented study, make it more precise/concise.

ANSWER R2.1: we believe that the title reflects what we explain in the manuscript. For your perusal, we divided the title into parts (in italics) and explained how each part corresponds to

what is treated in our manuscript (in parenthesis). Our manuscript addresses the *historical reconstruction of sediment accumulation rates* (based on MAR temporal variations, derived from ^{210}Pb dating), and this has been used *as an indicator of global change impacts* (which includes both land-use changes and global warming) *in a tropical crater lake* (characteristics of SAMO). Perhaps the problem is the concept of "global change", but this is already explained in the first paragraph of the introduction. Please note that global change refers to the changes that occur on a local scale but are so ubiquitous around the planet that when aggregated have a global-scale effect (Steffen et al., 2005).

Reference cited: Steffen W, Sanderson A, Tyson P D, Jäger J, Matson P A, Moore B III, Oldfield F, Richardson K, Schellnhuber H J, Turner II B L, Wasson R J (2005) Global Change and the Earth System - A Planet Under Pressure Springer, New York

R2.2 Introduction. The introduction might benefit from a more concise framing towards the hypothesis of the present study. Furthermore, it provides the opportunity to put more emphasis on the strengths of the chosen approach to test the hypothesis (e.g., showing that high-resolution ^{210}Pb-chronologies have not yet implemented in this lake, presenting element ratio-descriptions that the ratios can be used to investigate the factors controlling sedimentation, etc.).

ANSWER R2.2: done.

R2.3. Hypothesis. The authors address the hypothesis that changes in the sediment input to SAMO are mostly due to anthropogenic development in the catchment and secondarily influenced by climate variability. Unfortunately, no data/time series (population growth, land-use intensity/change, tourism development) were presented to test for the first part of this hypothesis.

ANSWER R.2.3: Reviewer 2 is right. We did mention in the Discussion section that no significant correlations were observed between MAR with population growth or cultivated area in Santa María del Oro municipality, but we did not show the data. The data is now included in the ESM file of the revised version, as figures 5ESM and 6ESM.

The population growth plot includes data since 1890, but the cultivated area data is only available since the late 1970s. In any case, neither population growth nor cultivated area temporal variations explain the MAR fluctuations observed in the sediment records.

R2.4 **Methods and Data.** The methodological concept is plausible and suitable to test the hypothesis. MARs and SARs are derived from the chronologies, and therefore the core/heart of the present study. However, more emphasis has to be put on the uncertainties, model selection, drawbacks of the model choices. The discussion barely addressed these things, but rather focused on radiocarbon dating data that was not included in the hypothesis test (and hence is stealing space, resp. is not concise). The meteorological data description needs to be improved (gap years, etc.). The structure and order of the sub-chapters need to be reassessed.

ANSWER R2.4: new text and text improvements regarding ^{210}Pb dating (Introduction, Materials & methods/Sediment dating, Discussion/Reliability of the ^{210}Pb-derived age models) and the meteorological data (Methods/Meteorological data & Statistical analyses) are included in the revised version of the text, to address the details requested by Reviewer 2. Regarding the gaps in the meteorological data, we included:

> "Missing records accounted ~2% of the total expected data for precipitation (14 monthly observations in eight different years), 12% for evaporation (65 observations in 13 different years, including the whole period 2009-2012) and 6% for temperature (36 values in 8 years,

including almost the whole period 1963-1964)."

Efforts were also made to improve the structure and order of the sub-chapters upon the comments from all reviewers.

R2.5 Results. The results are well described, but the visual representation needs to be revised/improved (in terms of layout ❼ JOPL guidelines, but also in terms of how to present the data without losing the focus to the story).
ANSWER R2.5: efforts have been made to improve the visual representation of the data. We have also corrected the details related to the JOPL guidelines, according to the remarks made by the Editor-in-chief.

R2.6 Discussion. The authors would have the potential to emphasize strengths and discuss uncertainties of their chronologies and approach in this chapter. However, the discussion is rather broad and speculative, and a substantial part of it is taken by discussing the radiocarbon dating that was not included to test the hypothesis. Although, one can include this, one should at least discuss why previous studies in this lake have not had this issue and were able to establish ^{14}C-chronologies. And the weight has to be drastically reduced (it is a side arm and not the major story line…).
ANSWER R2.6: we apologize for not delving further into the uncertainties and approach followed in this study. ^{210}Pb dating is a very well-established method and our approaches are well described in the two cited papers (Sanchez-Cabeza and Ruiz-Fernández, 2012; and Sanchez-Cabeza et al., 2014). We are trying to keep the text concise as requested in the guidelines of JOPL and to comply with the established limit of words. We consider that it is important to present the ^{14}C dating data, and we have added some possible reasons why previous studies in this lake have not had issues establishing ^{14}C-chronologies (Discussion/^{14}C ages):

"No previous study at SAMO reported problems related to ^{14}C dating. This may be due to the use of matrices other than bulk sediments (peat and wood; Vázquez-Castro et al. 2008, Rodríguez-Ramírez et al. 2015) and, when bulk sediments were used, age inconsistencies were not discussed (Sosa-Nájera et al. 2010; Lozano-García et al. 2021). None of those studies reported ^{210}Pb dating which, in this case, confirmed that the surface sediments in the SAMO cores are modern, thus, the ^{14}C values reflect a strong reservoir effect".

R2.7 Conclusions. Despite the consistent observation that MARs decreased in the last decade (reasons were not clearly discussed, but according to the introduction this is a positive development), the authors conclude that measures have to be implemented to protect the lake of high sediment input. Totally agreed we have to protect these resources. The data, however, only vaguely and insignificantly support this conclusion.
ANSWER R2.7: the lake has overcome periods of high sedimentation, associated with the development of anthropic activities and climate forcings, which highlight the lake´s susceptibility to siltation problems. Despite MARs decreased in the last decade, high sedimentation pulses may happen again. Considering that dry conditions, wildfires, and soil erosion may increase due to climate change (promoting higher sedimentation in downstream continental aquatic environments), unregulated human activities can only worsen this problem. Thus, we consider that proper management strategies should be implemented to control erosion in the catchment and avoid that the lake is affected. We updated the conclusion according to the previous explanation.

Please find below more detailed comments: 'Major comments' (p. 2) refer to conceptual questions/suggestions, 'Minor comments' (p. 5) provide line by line – questions/suggestions, 'Figures and captions' (p. 7) provide suggestions for the figures and 'Supplementary material' (p. 9) contains comments about the SI.

Major comments

R2.8 References There is at least one instance of a sentence that was copy&pasted from a previous study (word by word). It is crucial to indicate it as such e.g., using "" (make sure to comply with JOPL guidelines and plagiarism guidelines!). Also, there is at least one reference to an AGU-abstract, and when reading it, the actual information was not present. Then the authors have cited in the text Croudace and Rothwell (2015) (the editors of the book), but - speculatively- wanted to refer to Davies et al. (2015) (a paper in Croudace and Rothwell 2015, presenting different elemental ratios in a table). Furthermore, some references lead to Spanish articles (please refer to JOPLs author guidelines, and make sure that this is appropriate). More details have been indicated in the minor comments section.

ANSWER R2.8: The text has been revised to improve citations. References in Spanish are kept, as nothing is indicated on this subject in the JOPLs author guidelines, and nowadays automatic translations can be a reasonable solution for interested readers.

R2.9 The authors are encouraged to support key statements throughout the manuscript by citations!

ANSWER R2.9: we consider that the key statements are supported by citations. There must be some other that Reviewer 2 consider also relevant, but unfortunately, these were not indicated. Bear in mind that, according to JOPL guidelines, the References section is limited to 60 citations.

R2.10 In the Methods section, please do refer to the statistical software that was used for the data treatment (R, SPSS, MATLAB, etc.) including the relevant package references. The reader should be able to reproduce the calculated results.

ANSWER R2.10: done.

Artwork

Details to the artwork can be found in the figures section of this document.

R2.11 Please make sure that the fonts size, line width and transparency (e.g., Fig. 5) and dot sizes are in accordance with the JOPL-guidelines and that color code is color vision deficiency friendly (one could also take advantage of dashed, and dotted lines…).

ANSWER R2.11: efforts have been made to improve the figures according to the Reviewer´s recommendations. Please note that there are no specific rules for figures in the JOPL-guidelines.

R2.12 Figures 3 and 5 are too small and a bit messy (overlapping axis-numbering, not consistent axes-ranges for the same variables in the same sediment core, etc., more details below).

Taking advantage of presenting the data (general trends in elements,…) using correlation-matrices could be beneficial (this would probably even allow to combine Fig. 3 and 5; Fig. 3 and 5 could then be moved to the Supplementary material). Correlation-plots could be made per sediment core for example. This would greatly ease the density of plots and help identifying similar trends relatively easy and enable the identification of significant correlations ($p<0.05$).

ANSWER R2.12: the correlation analysis was eliminated from the updated version of the text. Figures 3 and 5 show different things, and we consider that substituting them with a correlation

matrix would not help to convey our message.

R2.13 Breaks in plot-axes where single outliers compress the overall trends (e.g. MAR in Fig. 3) would greatly increasethe readability, and ergo one could better follow the discussion.
ANSWER R2.13: efforts were made to improve the figures. We were unable to add the breaks by using R or MSExcel (the tools that we used to create the figures); instead, we have plotted the MAR as logarithmic values to improve readability.

R.2.14 It is important to make sure that the figure captions contain all the necessary information to understand the details of the figures (e.g., what do horizontal lines represent in Fig. 3, or filled/empty dots in Fig. 5, etc.).
ANSWER R2.14: done.

Chronological control and age-depth models

R2.15 The chronological control is the core/heart of the study. It directly impacts the SAR and MAR, both crucial for testing the presented hypothesis. Furthermore, the chronology directly impacts the comparison of the sediment proxies with the meteorological data from the weather station. Therefore, the chronologies need to be robust.
ANSWER R2.15: we consider that the ^{210}Pb-derived chronologies are robust and well corroborated by relevant and independent stratigraphic markers. Please see answer 2.17.

Radiocarbon dating

R2.16 Unfortunately, the radiocarbon dates were affected by a substantial reservoir effect and therefore, could not be used to constrain the age-depth model. Here, one may wonder how the previous studies have been able to successfully implement ^{14}C-chronologies in the very same sediments. Is it because the sequences of the present study are too short to extend beyond ~500 cal yr BP into the "safer" ^{14}C-ranges, or is it because the previous studies tried to date terrestrial microfossils rather than bulk sediments as it was the case in the present study? Have the authors tried to pick terrestrial microfossils (identification by microscope, binocular) and to date them? One should mention in the discussion section that previous studies (further back in time) were able to establish radiocarbon chronologies (1-2 sentences).
Overall, what is the gain of information when including the downcore radiocarbon samples in the paper? Except for the post-bomb dates used as additional chrono markers (to constrain/validate the ^{210}Pb-chronologies), it is notclear how the other downcore radiocarbon samples do contribute to achieving the goal of the study (which explicitly mentions ^{210}Pb-chronologies).
Comparison of the ^{210}Pb-chronologies with ^{14}C-samples
Why were the uncalibrated ^{14}C-ages compared to the calendar ages (derived from ^{210}Pb-chronologies) to assess the reservoir effect? And why not the calibrated (IntCal20) years cal. BP ages (resp. transformed into CE/AD)?
Therefore, a direct/radical question: Could it be beneficial for the manuscript to eliminate the entire radiocarbon- dating sections (methods, results, discussion) to make the story more concise?
ANSWER R2.16: none of the previous studies in SAMO, where ^{14}C has been used, reported problems with ^{14}C dating. ^{14}C analysis were performed on peat and wood (woody-peat layers) for a single core (collected at 12 m of water depth) used in Vázquez-Castro et al. (2008) and Rodríguez-Ramírez et al. (2015); and on bulk sediments for cores in Sosa-Nájera et al., 2010 (60 m) and Lozano-García et al., 2021 (57 m). The ^{14}C profiles derived from bulk sediments showed age reversals and very old layers, but these were not highlighted nor discussed in the papers.

It is possible that the problems we faced with ^{14}C dating might be related to the use of the bulk sediments, but maybe also with the sampling location (note from the previously mentioned studies that the 2 cores showing age inconsistencies were deeper than the other one). Previous studies elsewhere (e.g. Zhou et al., 2020, https://doi.org/10.3389/feart.2019.00328) have stressed that the reservoir effect can be temporally and spatially variable in the same lake due to varying degrees of CO_2 air-water exchange and mixing, or to variations in old carbon input from the catchment. We did not try to pick terrestrial microfossils. The Introduction section of the original paper mentioned the previous studies performed in SAMO which used ^{14}C dating. A new paragraph was added in the Discussion section to synthesize this information (please refer to answer R2.6).

The comparison between conventional ^{14}C ages and ^{210}Pb dates is an alternative strategy to estimate reservoir ages (Saulnier-Talbot et al., 2009; Hou et al., 2012; Treinen-Crespo et al., 2021) through paired ^{14}C-alternative dating methods. The conventional (instead of calibrated) ^{14}C ages are used because calibration requires the knowledge of the reservoir effect (usually constant regional offsets from the atmosphere) but this should be improved by using age offset (e.g. the local reservoir age) when this is known (Blaauw et al., 2011; DOI:10.1016/j.quascirev.2011.07.014). The purpose of the comparison between conventional ^{14}C and ^{210}Pb dates is precisely to estimate this age offset.

We want to keep the information on ^{14}C. It is true that we did not succeed to provide a reliable ^{14}C-based age model, we were unable to extend our evaluation on MAR for a longer period (when we anticipated that human impact on the environment was minor), and the ^{14}C ages do not contribute to the explanation of the recent MAR variability in the lake. Still, we consider that the ^{14}C data is valuable. We have gained knowledge about the reservoir effect in SAMO and we consider that it is important to share our findings with the scientific community. We believe that, albeit modestly, these findings would help the scientific community to realize that the reservoir effect is a common problem in many lakes, ^{14}C dating is not straightforward, the reservoir effect needs to be evaluated, and that the combination of ^{210}Pb and ^{14}C is useful for this purpose.

^{210}Pb dating

R2.17 The authors established for each sediment core individual ^{210}Pb chronologies. This gives the unique opportunity to understand lake-internal depositional processes. To corroborate the reconstructed chronologies, they were compared with independent chrono markers (^{137}Cs, $^{239+240}Pu$, ^{14}C post-bomb). Such a profound dataset is rare and has a huge potential. The authors decided to use the CF-model, but they have not explained why, nor have they elaborated on its strengths/drawbacks. Furthermore, the age-uncertainties (MC-simulations) were not presented (except for SAR/MAR in Fig. S1). Furthermore, did the authors consider running other widely used "standard" models (CF:CS, CIC, SIT, CRS), or to implement a missing inventory correction, similar to Tylmann et al. (2014, https://doi.org/10.1016/j.quageo.2013.04.003)? Presenting a range of models and then using the independent chrono markers to identify the "best-performing" model (e.g., von Gunten et al., 2009, https://doi.org/10.1007/s10933-008-9284-5) could help taking more advantage of the unique dataset and also make a stronger argument for the comparison to the meteorological dataset.

ANSWER R2.17: The CF model was used because it is robust and widely applicable in a variety of environments. It considers that ^{210}Pb activities are inversely related with the sediment input (Krishnaswami et al., 1971; https://doi.org/10.1016/0012-821X(71)90202-0) and its only hypothesis is that ^{210}Pb flux to the sediments is constant, which allows estimation of variable sedimentation rates with time. From our ^{210}Pb profiles (Fig. 2A, upper row) we can observe some

^{210}Pb activity minima or maxima along the cores, that indicate variable sedimentation inputs, thus, this model was our best option. We justified our choice of the dating model in the revised version of the Data treatment/Sediment dating section.

It does not make sense to try all kinds of ^{210}Pb dating models just because they are available. The selection of the ^{210}Pb dating models should be based on a careful consideration of the hypothesis behind them. From the list that you have suggested: CFCS or CIC models were not even considered because these are limited by the assumption of constant sedimentation rates (Sanchez-Cabeza and Ruiz-Fernández, 2012; https://doi.org/10.1016/j.gca.2010.12.024) which, as mentioned before, is not the case in SAMO cores (please note, from JOPL guidelines: "assumptions of constant sedimentation rate, especially over extended periods when there have been human or climate influences, are not justified"). The CRS model is another way to call the CF model (Sanchez-Cabeza and Ruiz-Fernández, 2012 includes a review on the names of the ^{210}Pb dating model). We do not use the SIT or THERESA models because of their complexity and their "black box" function (we assume that this is the reason why these models are not widely used by the scientific community).

We did not use "missing inventory-corrections" because these were not needed, which can be easily appreciated from the profiles themselves (the profiles clearly show when excess ^{210}Pb vanished). In addition, one way to test if a sediment core has incomplete inventory issues is to convert the inventories into ^{210}Pb fluxes and verify if these values are compatible with the expected ^{210}Pb fluxes in the region (these values were already presented and discussed in the previous version of the manuscript).

Finally, we have confirmed the dating of the SAMO cores by using a new and powerful dating method based on a Bayesian approach (Plum) (Aquino-López et al., 2018; https://doi.org/10.1007/s13253-018-0328-7). This model is based on the same main hypothesis assumptions of the CF model, but has two important advantages: little interaction of the user is needed to determine the equilibrium depth (which eliminates the need to determine the excess ^{210}Pb inventory); the age calculation eliminates the problem of "tailing" towards older ages, common when CF model is used; and it provides uncertainties based on a Bayesian statistics. You can see the comparison of the ^{210}Pb chronology results obtained for SAMO 14-2 in Aquino-López et al., 2020 (https://doi.org/10.1016/j.quageo.2020.101106) and this information is briefly mentioned in the Discussion. We do not present nor discuss the results of the comparison of the age model for both dating models in this paper because of the length limitations established by JOPL (9,000 words). You may wonder why we did not substitute the CF age model by the Plum age model; we did not because this software allows us to represent and extract the chronologies but, so far, we cannot extract the values and uncertainties of MAR to be used for further calculations (which we need for further applications).

We have no doubts or drawbacks to discuss the ^{210}Pb dating of the cores; perhaps only that it is not possible to corroborate pre-nuclear test ages, but this is a well-known problem of the for recent age corroboration (already addressed in the references we provided concerning the ^{210}Pb methodology). This problem could be solved if other stratigraphic features (of known dates) could be identified, which is not the case in this study.

R2.18 The current visual presentation (Fig. 2) of this nice dataset understates its potential. Adding the background (^{226}Ra) and total measured ^{210}Pb-activities per sample to the first panels of Fig. 2 per sediment core would be beneficial.

Secondly, it is necessary to show the actual age-depth model(s) (age vs depth) per sediment core, including the calculated uncertainties (they were mentioned in the methods, but never discussed,

nor presented in any figures, except for the Supplementary SAR/MAR plots). The age-depth models including uncertainties could be plotted in the second panel-row and the additional chrono-markers (1963-peaks, etc.) might be indicated with dots. This would enable a visual assessment of the model-performance for the reader.

ANSWER R2.18: the ^{210}Pb dating method uses the excess ^{210}Pb activities and these are the relevant values to be shown; the ^{226}Ra values obtained were already reported in Table 1 of the original version of the MS. However, to suit the Reviewers 2 request, the revised version of Figure 2 now includes the ^{226}Ra data (upper row); as well as the age models (middle row).

Independent chrono markers

R2.19 Fig. 2 shows that the "bomb"-peaks are quite clear, which is very important for a clear identification. However, the onset of the artificially emitted radionuclides drastically varies between the sediment cores. According to UNCEAR (please see figure at the end of this document), the onset peaks would be expected at around 1952-1954. In the present plots it seems that SAMO18-4 starts already in 1924 and SAMO14-2 in 1930. There are probably two main explanations: 1) post-depositional mobility of ^{137}Cs through the sediments, 2) a tailing towards old ages of the age-depth model. To exclude the latter, plotting the age-models and then seeing how the ^{137}Cs-onset lines up would be encouraged. Additionally, one might wonder why the ^{137}Cs would behave differently in the three "closer" cores from the deepest region of the lake. To convince the reader further, the authors are encouraged to discuss the reasons for these different ^{137}Cs-onsets in the chronology-discussion section.

ANSWER R2.19: Yes, the onset of ^{137}Cs is different among cores, as well as the shape of the ^{137}Cs, ^{210}Pb, and some element profiles. All these features account for uneven sedimentary/geochemical processes across the lake. The ^{137}Cs mobility and the different onset dates for ^{137}Cs is a common feature, reported in studies elsewhere (e.g. Klaminder et al., 2012, 10.1111/j.1365-3091.2012.01343.x; Corcoran et al 2018; 10.1016/j.jglr.2018.05.013).

We must take into account that SAMO is a oligomictic lake, that does not completely mix each year, and the deep part of the lake is anoxic, which promotes reduced conditions that influence redox-sensitive elements (such as ^{137}Cs) that would contribute to the post-depositional mobility of ^{137}Cs through the sediments. Is it reasonable to believe that diffusion and depth penetration of ^{137}Cs should be uniform in the whole sediment floor? We would say no. Cs mobility depends on the concentration of other cations (e.g. Na^+, K^+, Ca^{2+}, NH^{4+}, Rb^+; Steefel et al., 2003 (10.1016/S0169-7722(03)00033-0) which compete with Cs for exchange sites in the sediments; therefore, the variability of these cation concentrations in porewater would also influence how much ^{137}Cs is displaced downward the sediment. Hence, unless ^{137}Cs downward diffusion is proven negligible, the onset of ^{137}Cs should not be used as a stratigraphic marker to corroborate ^{210}Pb. This has been already clearly established many years ago by Smith et al. (1998): "…dating sediments by "first appearance" of ^{137}Cs is not reliable".

Cited reference:

Smith et al., 1998. The mobility of radiocaesium in lake sediment and implications for dating studies. In: Seminar on Dating of sediments and determination of sedimentation rate. Illus, E. (ed.), STUK-A145. Radiation and Nuclear Safety Authority, Helsinki (Finland), 76-93.

Climate data

R2.20 Precipitation, Temperature and Evaporation data were retrieved from a nearby weather station. The authors statedthat more thorough analyses were hindered due to gaps in the record, or the short extend of the time series. Please add to the data/methods section which and how many

years were missing. Idea: Have the authors compared the weather station retrieved meteorological data with a CRU-dataset, or a reanalysis data set for the given grid cell and using (when high correlation) these complete timeseries instead (and probably also covering the period 1900-2014)?
ANSWER R2.20: regarding the missing data, please refer to answer R2.4.

As suggested by Reviewer 2, we have retrieved the temperature and rain data from the CRU dataset and contrasted the trends against the meteorological station data set used here (you can see the plots on the right). Maybe the general trends are similar but, as expected, the minimum values of rainfall (in which we are especially interested) are not well captured by the CRU data. Thus, we did not continue with this data analysis.

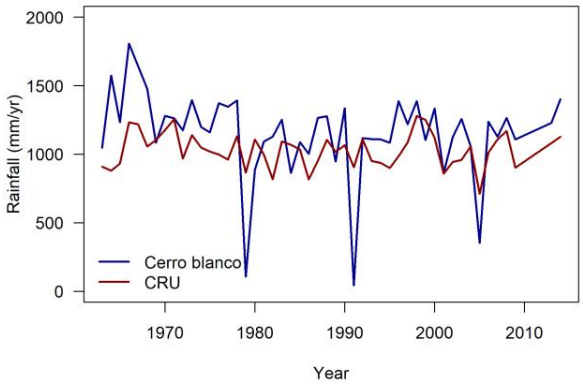

R2.21 Fig. S3 represents the meteorological data. However, no gaps are visible due to the linear connection-lines between the annual sums. Also, the moving average (5-year filter) does not start/ end at the same year for Precipitation compared to Evaporation. Temperature was included as a parameter in the cluster analysis, but is not presented in Fig. S3. Please add the temperature timeseries and address the other things.
ANSWER R.2.21: we have eliminated the connection lines to make visible the gaps. Yes, in our database, the precipitation and evaporation data do not have the same starting/ending point (see answer R2.4). The temperature time series is now added in Fig. ESM4.

R2.22. According to the methods section, the meteorological data were pooled (regularized) to the proxy-data resolution. Supposedly that this has been done for each sediment core individually (for the cluster analyses)? From Fig. 5, however, each SAMO-core was compared to the same climate-time series (the four evapo/precip curves look the same). Is this because the proxy-data were pooled to the meteorological data rather than the meteorological data to the proxy-data? Or because each proxy-time series appeared to have the exact same time-resolution (which according to Fig. 2 seems to be unlikely the case).
ANSWER R.2.22: the annual accumulated precipitation and evaporation data were pooled to match the period recorded at each dated sediment section (not the other way around). This information was used *only* for cluster analysis (Figure 6). Figure 5 contains the precipitation and evaporation data as it was retrieved.

R2.23. Additionally, how have the gap-years in the meteorological time series been treated during the "pooling". Please elaborate in the methods section the data handling more thoroughly and address the above points.
ANSWER R2.23: please, see answer R2.4.

R2.24Surface runoff can sometimes also be influenced by heavy rainfall events (a lot of mm in a few hours/days) causing floods and ergo increased soil erosion and leading to instantaneously deposited layers (flood layers). Have the authors considered the possibility of extreme precipitation events, that might occur during an average/extreme dry year? Could it be that this

would lead to a bias in the interpretation of e.g., the MAR-meteorological data comparison?
ANSWER R2.24: as you can observe in Fig. 5, all MAR maxima (except for the most recent MAR maximum in SAMO 18-4) corresponds to precipitation minima.

R2.25. According to climate diagrams (e.g. presented in Vasquez-Castro et al, 2008, Fig. 1d) Summer/Fall months are the wettest months per year measured by this weather station. Have the authors investigated the "seasonal bias" and whether this could influence the interpretation (e.g., comparison of proxies with monthly, or seasonal-sum/- average time series instead of annual mean time series)?
ANSWER R2.25: it is not feasible to explore this possibility because the dating resolution is not small enough (each section comprises at least 1.5 to 2 years).

R2.26Sampling, samples and statistical analyses
The sediment cores were subsampled in the field at 1cm- resolution, non-stratigraphically (according to the methods section). Yet, according to a photo of a sediment core from SAMO in Vazquez-Castro et al. (2008), the sediments (at least in the therein presented section) are layered and in the top sequence they are described as "Láminas y capas delgadas de limos". Could it be that the sampling-strategy (1cm contiguous sub sampling) affects the interpretation, particularly when considering the proxy-meteo comparison (for example that a "flood layer" was split and, hence, divided on two samples)? And if so, could this cause a distortion of the interpretation - should this be addressed in the discussion?
ANSWER R2.26: please see the picture in answer R1.2. Yes, the core is laminated. We cannot rule out the possibility that the sampling strategy homogenized some lithological features recorded in the sediment profiles; flood layers, *if existing*, are not identifiable neither by sight nor through the grain size analysis. However, our data show that the MAR and MS maxima belong to rainfall minima (Fig. 5), thus, these hypothetical flood layers are not relevant for our explanation. The limitations of the sampling strategy are mentioned in section Discussion/Influence of climate variability on sedimentation:

> "These results may be conditioned by some limitations. The meteorological data come from a station 5 km apart and 200 m above the SAMO altitude, so they may not accurately reflect the specific conditions at the study site, and these time series are relatively short and have several gaps (mainly evaporation data). Moreover, the cores were cut into 1 cm thick sections and, given the millimeter-laminated nature of these sediments, it is possible that sediments with different origins may have been mixed. In addition, within the period for which meteorological data are available (1964-2014), the geochemical records of the sediment cores are noisier (Fig. 3)."

R2.27 Was the soil sample also analyzed with the XRF-system? And if so, could this information be used to strengthen the argument of the sediment provenance?
ANSWER R2.27: we collected 10 soil samples around SAMO that were analyzed by XRF. We have redone the factor analysis, including the information from these soil and the sediment core samples. In the updated figure 4 (A) the distribution of the elements is the same as in the previous version (Ca and Sr on the left side, terrigenous indicators on the right side of the biplot), and figure 4 (B) shows all the soil samples grouped on the positive side of factor 1 (characterized by the association of terrigenous element indicators) where most of the SAMO 18-4 samples are also found. The soil sampling locations are now shown in the updated version of Figure 1.

R2.28 The authors are encouraged to elaborate the data handling prior the statistical analyses more. Were the data normalized, scaled, tested for normality, etc., prior the ANOVA, FA, and cluster analysis?

ANSWER R2.28: thinking on conciseness, this section includes only what we have done. We did not test for normality, based on the Central Limit Theorem, which indicates that the means from a nonnormal population approaches a normal distribution if the sample size is large enough (n>30) (Norman & Streiner, 2008). Neither factor analysis nor cluster analysis requires that the data is normally distributed (Hair et al., 2010).

Reference cited:

Hair JF, Black WC, Babin BJ, Anderson RE (2010). Multivariate Data Analysis. Prentice Hall, 785 pp.

Norman GR, Streiner D L (2008). Biostatistics: The Bare Essentials. PMPH USA (BC Decker), 393 pp.

Minor comments (by lines)

R2.29. The pdf did not provide continuous line numbering. Therefore, lines were counted visually as in the pdf per page. CODE: PxyzLxyz: Pxyz refers to Page xyz, Lxyz refers to Line xyz on page. ❼ P4L10: refers to page 4 line 10 (counted in the pdf from top line downwards, P-numbering as in the received pdf). Continuous line numbers would be appreciated in the future.

ANSWER R2.29: we are sorry for the inconvenience. When we uploaded the manuscript for the first time it had a line number, but we noticed that the platform assigned line numbers too, thus we have eliminated the line numbering from the MSWord document. We will introduce the line numbers again in the revised version of the text.

Abstract

R2.30 P2L3: "…(SAMO, NW…" ❼ "…(SAMO, Pacific W…"? As I understand the map, the location is rather in the pacific western part of Mexico and not in the NW part? And previous studies also referred to it as W Mexico. Please change this throughout the manuscript and adapt the figure accordingly.

ANSWER R2.30: I guess that diverse criteria may be applied, depending on the purpose of the regionalization. Diverse authors place the State of Nayarit as part of NW Mexico (which comprises the states of Baja California, Baja California Sur, Sonora, Sinaloa, and Nayarit) when studying regional aspects on geological history (Brusca, 2019), climate patterns (Brito-Castillo et al., 2010), biological connectivity (Palacios & Alfaro, 2005; Ruiz-Luna et al., 2010) or socio-economic development (OECD 2006; de Haro-Mota et al., 2015; SIAP, 2020). We prefer to keep SAMO, in the Nayarit State, as NW Mexico.

References cited:

Brusca, 2019. A brief geologic history of northwestern Mexico. http://rickbrusca.com/http___www.rickbrusca.com_index.html/Sea_of_Cortez_files/Geology%20of%20NW%20Mexico.pdf

Brito-Castillo L, Vivoni ER, Gochis DJ, Filonov A, Tereshchenko I, Monzon C, 2010. An anomaly in the occurrence of the month of maximum precipitation distribution in northwest Mexico. J Arid Environments 74, 5, 531-539.

De Haro Mota R, Marceleño Flores S, Bojórquez Serrano JI, 2015. Potential of socioeconomic development in the regions of Nayarit, Mexico. Revista Bio Ciencias 3(3): 195-207

Ruiz-Luna A, Cervantes Escobar A, Berlanga-Robles C, 2010. Assessing Distribution Patterns, Extent, and Current Condition of Northwest Mexico Mangroves. Wetlands, 30:717–723.

Seabird Research and Monitoring Needs in Northwestern México. Palacios E & Alfaro L, 2005. USDA Forest Service Gen. Tech. Rep. PSW-GTR-191.

OECD 2006. Agricultural and Fisheries Policies in Mexico. Recent achievements, continuing the reform agenda. Organisation for Economic Co-Operation and Development, Paris, 338 pp.

https://www.oecd.org/fr/mexique/agriculturalandfisheriespoliciesinmexico--recentachievementscontinuingthereformagenda.htm

SIAP, 2020. Frontera Agrícola región Noroeste. Servicio de Información Agroalimentaria y Pesquera. Gobierno de México. http://infosiap.siap.gob.mx/gobmx/datosAbiertos.php

R2.31 P2L10: "^{14}C-dating of SAMO…" ➹ "Radiocarbon (^{14}C) dating…" (beginning of sentence…)P2L18: "…0.05±0.04 g cm^{-2} yr^{-1})" ➹ remove comma before closing brackets
ANSWER R2.31: done.

1. Introduction

R2.32. P3L3: I would expect to see the publication of Jenny et al. (2019):
ANSWER R2.32: the publication of Jenny et al. (2019) does not fit in the sentence referred by Reviewer 2 since it refers to 2nd half of the twentieth century, but the suggested publication addresses the impact of humans well before the great acceleration, out of the time frame that we are investigating. The introduction of this citation would require a new paragraph, but we mind the text and reference limits established by JOPL.

R2.33. P3L6: "…the impacts of CG…" ➹ change "CG" to "GC" to be consistent with your Code
ANSWER R2.33: done.

R2.34. P3L10-11: please elaborate or refer to publication: why are the last ~100 years "the period of interest for most GC studies"; also: please add references to key papers regarding the ^{210}Pb chronologies (Appleby, etc.).
ANSWER R2.34: done.

R2.35 P3L13: what about the onset of ^{137}Cs (between 1952-1954, see Fig. 1 at the end of this document)? ➹ could this serve as an additional chrono marker too in the present study lake? I realize from Figure 2 that the "onset"-date of ^{137}Cs varies drastically between the cores and goes sometimes back to 1930 (before the first nuclear weapon)
ANSWER R2.35: the onset of ^{137}Cs was not useful as an additional chrono marker in our study as Reviewer 2 has already noted; the issue of ^{137}Cs post-depositional mobility is addressed in the first paragraph of the section "Reliability of the ^{210}Pb-derived age models" (Corroboration of the ^{210}Pb-derived age models" in the previous version of the paper). As the onset of ^{137}Cs was not used in our paper, we do not elaborate further on this regard.

R2.36. P4L10: Santa M. del Oro Lake ➹ change to "Lake Santa…" (consistency throughout the manuscript!)
ANSWER R.2.36: all text refers now to Santa María del Oro Lake

R2.37 P4L10: is it really NW Mexico, and not rather Pacific SW Mexico? Please check this in detail and also adjust the figures (legends) accordingly
ANSWER R2.37: please refer to ANSWER 2.30.

R2.38. P4L13: "western Mexico" ➹ consistency: is it Pacific-SW, or W, make sure it is consistent throughout the manuscript!

ANSWER R2.38: to avoid this conflict of interpretation, we have updated the paragraph to eliminate the geographical location.

R2.39 P4L13: Zárate del Valle et al., 2009: refers to an AGU abstract, is this correct? I could not find the paper. Pleasechange.
ANSWER R2.39: the citation was revised; the reference in the list of references was correct and the abstract can easily be found in the AGU Abstract Browser following the data in the reference. For your information: https://abstractsearch.agu.org/meetings/2007/FM/B33C-1427.html.

R2.40. P5L8: "…this study was…" ❼ probably change "was" to "is"?
ANSWER R2.40: the paragraph was updated:

"Our objective was to evaluate the temporal variations in sediment input to SAMO, using a combination of ^{14}C and ^{210}Pb dating. This is the first study on the recent evolution of accumulation rates in the lake, and we hypothesized that these changes are mainly due to anthropic induced catchment erosion, caused by population growth and agricultural activities.".

R2.41. P5L11: population growth and economic activities: I think that it would be necessary to provide some data (timeseries of pop. growth, agriculture trends, tourism, etc.) to underline your argument ❼ e.g. add æsentence/figure in study site description or add a figure in the SI (if data available and allowed to be published).
ANSWER R2.41: population growth of the Municipality of Santa María del Oro is available; it was not included because it did not show any correlation with the changes in MAR and we considered that we already have too many figures. However, upon the request of Reviewer 2, this figure is now included as part of the supplementary information (Fig. ESM5). The time series of economic activities are very short and thus, not useful for our evaluation (agriculture: 2003-2018) but, it is also shown in Fig. ESM6.

2. Study Area
R2.42. P5L17: "…at ~4km from the…"❼ add NE: "…at ~4km NE from the…"
ANSWER R2.42: done.

R2.43. P5L20: add info about watershed size, and calculate the catchment/lake area ratio (for erosion pattern)
ANSWER R2.43: the information on the watershed size is not available.

R2.44. P5L22: the entire sentence is a word-by-word copy&paste citation !!! indicate the entire sentence with "", checkout journal guidelines
ANSWER R2.44: the sentence has been updated as follows:
"SAMO is fed by rainfall, surface runoff, and groundwater, whereas water outflows mainly through evaporation and seepage (Rodríguez-Ramírez et al. 2015) but also local by water consumption".

R2.45. P6L9: add pH value, e.g., cite it from previous studies
ANSWER R2.45: done.

R2.46. P6L10: "Weather is…" ➏ reformulate "the present-day weather is…" and one could refer to the paper of Vazques-Castro et al. (2008) for the climate diagram
ANSWER R2.46: the sentence has been updated as follows:
"The climate in the region is classified as semi-warm sub-humid with summer rains (INEGI 2009)."

R2.47. P7L6: Question: why was the sediment trap put at 30m depth? Probably elaborate a little here (why not setting it one meter above the sediment surface?)
ANSWER R2.47: our two traps were placed to study processes related to the thermocline (at 8 m and 30 m, above and below the thermocline (Cardoso-Mohedano et al., 2019).

R2.48. P7L9: "bulk dry density" ➏ change to "dry bulk density"
ANSWER R2.48: done.
R2.49. P7L22: "^{14}C analyses": at the beginning of the sentence: change to "Radiocarbon (^{14}C) analyses"
ANSWER R2.49: done.

R2.50. P10L8: "variables: MS" ➏ remove spacing
ANSWER R2.50: done.

3. Results

R2.51. P12L15: "… the core mean SAR…" ➏ what is a core mean SAR? Probably "…the mean SAR values per core…"?Ditto for MAR
ANSWER R2.51: revised.

R2.52. P13L3: "deep cores" ➏ is confusing rather "cores from the deepest coring locations"?
ANSWER R2.52: revised.

R2.53. P13L17: The asynchronous MAR were also characterized by a peak in sand ➏ flood layer?
ANSWER R2.53: no. There is no evidence of flood layers. The highest value of sand, found in a single dated section of the core is ~12% (not coincident with a MAR maximum). See Fig. 3.

R2.54 P14L5: why were LOI derived proxies not included in the FA?
ANSWER R2.54: these were included at the first exploratory analysis of the previous version of the MS, but the communalities were too low to be kept in the final one. In the revised version of the FA that included the soil samples (see answer R2.27) both C_{inorg} and C_{org} (derived from LOI) have now acceptable communalities and were kept in the final analysis (Table 2ESM and Figure 4).

R2.55. P15L6: temperature not mentioned. In SAMO14-1 and-3 it is with precip and evapo, in SAMO14-2 and 18-4 not. Why is this? Please add a sentence about temp and add a sentence in the discussion too.
ANSWER R2.55: temperature is now mentioned in this paragraph. The purpose of the cluster analysis was to assess the potential of elemental ratios to be used as climate proxies; results showed that only Ti/Al ratios were consistently related with rainfall and evaporation, thus temperature was not discussed further.

4. Discussion

R2.56. P16L7: Here I would also expect to read 1-2 sentences about the different onset years of the ^{137}Cs.
ANSWER R2.56: since we did not use it, we consider that there is no reason to discuss it. Please refer to answer R2.19.

R2.57. P16L10: "This is caused…." ❼ sentence is confusing, probably rather "This is caused by the different transfer-processes…?" and delete "transfer" in the second part?
ANSWER R2.57: this sentence was deleted.

R2.58. P17L1: Why comparing uncalibrated ^{14}C ages to calendar ages?
ANSWER R2.58: please refer to answer R2.16.

R2.59. P17L13: "…implying that the core sediment dates…" ❼ probably change to "sediment-core dates"?
ANSWER 2.59: this sentence was deleted.

R2.60. P17L16: "depth-to-surface ratio" ❼ does this refer to "relative depth" (Wetzel and Likens, 1991)?
ANSWER R2.60: this sentence was eliminated, attending comment R2.6, suggesting "the weight (of ^{14}C discussion) has to be drastically reduced".

R2.61. P17L23: "…making very difficult…" ❼ "…making it very difficult…"
ANSWER R2.61: this sentence was eliminated, attending comment R2.6, which requests reducing the discussion on ^{14}C ages.

R2.62. P19L9: I would like to encourage the authors to add a correlation matrix to the SI
ANSWER R2.62: please refer to answer R2.12.

R2.63. P19L13: "…source of sediments accumulating in SAMO cores…" ❼ rather "…source of sediment accumulation observed in the SAMO cores…"? Because I don't think that the erosion influences the SAMO-cores (they are in the core fridge, or the lab, resp. subsampled…)
ANSWER R2.63: done.

R2.64. P20L1: This paragraph is correct, but SAMO is not an "upland lake", correct? Therefore, I do not understand whyto discuss this here, or at least I was not following the framing.
ANSWER R2.64: the paragraph was eliminated.

R2.65. P20L9: "… since 1964 confirmed […] is drier": what was confirmed, and drier than what? I do not understand thekey message here. Probably the entire paragraph could be summarized in a sentence?
ANSWER R2.65: the sentence was eliminated.

R2.66. P20L22: Citation: Croudace & Rothwell 2015: probably rather Davies et al. (2015)? If it refers to the paper of Davies et al. (2015, the table with all ratios) in the book of Croudace and Rothwell 2015. Or one could even referto the original literature (Litt et al., 2009).

ANSWER R2.66: done.
R2.67. P21L6: "eolian input" ➔ change to "aeolian input" consistency throughout manuscript!
ANSWER R2.67: done

5. Conclusion
R2.68. P23L2: "…shallow lake area lake…" ➔ change to "…shallow lake area…"
ANSWER R2.68: the sentence was eliminated.

Figures and captions
R2.69 Fig. 1
ANSWER R2.69: Reviewer 2 provided several options to improve Fig. 1. We indicate below what we have done according to these suggestions.

- Map in the left panel:
  - Please visually indicate the weather station NW of the lake. Done.
  - Please add the coordinate-system (Lon/Lat). Done.
  - Please add the urban areas. Barely visible, but they are there.
  - Please add the watershed boundaries to the map. This would help understanding theprocesses/sources that directly influence the sedimentation better. Not available.
  - One could also present the "unclassified" basemap of Fig. 4S. We improved the Google Earth map as suggested below.
  - Otherwise, one could also replace the left panel entirely with the nice map from Fig. 4S. We introduced the nice map to Fig. 1.
  - Is it possible to replace the "Google Earth" part? E.g. cut it off and refer to Google Earth in the figure caption? And add the N-arrow, and Distance-measure bar in the similar style to the rightpanel? Done.
- Bathymetric map:
  - Add the coordinate system. It is already provided in Figure 1.
- Caption:
  - "NW Mexico" ➔ rather "Pacific SW Mexico"? Please refer to answer R2.30
  - For consistency: please add the coordinates of the sediment trap too. We would prefer not to, as we fear vandalism problems on site.

R2. 70. Fig. 2
ANSWER R2.70: Reviewer 2 provided several options to improve Fig. 2. We indicate below what we have done according to these suggestions.

- Overall:
  - This figure is a "core-figure" for the manuscript (MAR/SAR). This is an exciting dataset! Thanks, we agree.
  - The manuscript would substantially benefit if the authors would plot the age-depth models. The age-depth models are now included.
  - One could test different "standard" age-depth models and add panels representing them: e.g., CIC, CF:CS, CRS (also with Missing inventory corrections). Please refer to answer R2.17.
    - i) age-uncertainties would be visually represented, and can be included for the comparison with weather station data. The weather station data is not included in this figure.
    - ii) "match" between ^{210}Pb- derived models and ^{137}Cs-derived chrono-markers would bevisible. Done.

- One could present the ^{137}Cs-ativity panels in the supplementary material and instead present the age-depth models in this row (and indicate the onset, and bomb peak depths as observed from the ^{137}Cs-profiles with dots in the age-depth models). No onset dots included; please refer to answer R2.17. The ^{137}Cs and $^{239+240}$Pu activities are plotted together with the age models.

- For the ^{210}Pb-activity panels ("upper row"):
  - Please add the unsupported activities (background, ^{226}Ra) and the total activity. This would reveal possible fluctuations in the background activity. Resp. it would highlight whether the supported or the unsupported activity fluctuated (particularly in the low-activity bottom-core sections, and could probably also reveal causes for the quick drop observed in the top 10 cm and the thereafter slow downcore-increase). ^{226}Ra data has been added, when it was available.
  - Add labels to the second y-axes "Year CE" (or similar, refer to JOPL's date-style) Done.

- ^{137}Cs-profiles ("middle row"):
  - **SAMO14-2:** onsets of Cs and Pu are in 1929 ❼ too early according to literature (1952-1954). Why only plotting 10 Cs-samples and not ~19 as has been done in the panel below (vs. F^{14}C)? Where did these samples disappear? Regarding ^{137}Cs, please refer to answer R2.17. As per ^{239}Pu, this is also a natural radionuclide and background values can be sometimes be detected in sediments (Hancock et al., 2014). In this study, ^{137}Cs and plutonium isotopes should be considered as stratigraphic markers for the period of maximum fallout. As per the differences in the number of ^{137}Cs data, it was a plotting mistake, since Fig. 2 ^{137}Cs vs F^{14}C included ^{137}Cs data that was reported as detected, but below the minimum detectable activity (and should not have been plotted).
  - **SAMO18-4**: what is the reason for the high Cs-activity at the bottom of the sequence (here datedto 1924)? Please refer to answer R2.17.
  - In SAMO14-2 and SAMO-18-4 age discrepancies by the onset of Cs-activities can be observed. The literature indicates an onset-horizon between 1952 and 1954 (see Fig. at the bottom). Yet, here we observe above-0 activities already substantially earlier. This could be due to: i) pore- mobility of ^{137}Cs, or an artifact of the age-model selection. Testing different ^{210}Pb-age-depth models could resolve this discrepancy. Please refer to answer R2.17.
- ^{14}C-profiles ("lower row"):

  - Left panel: more ^{137}Cs samples plotted than in above figure, reason? A plotting mistake.
  - Right panel: would it make more sense to plot the calibrated years (cal. BP) rather than the ^{14}C- ages here to ease comparison with the ^{210}Pb-profile of SAMO14-2? No. This information has the purpose to evaluate the reservoir effect, which should be used for calibration.

R2.71. Fig. 3

ANSWER R2.71: Reviewer 2 provided several options to improve Fig. 3. We indicate below what we have done according to these suggestions.

- Overall:
  - A nice overview of the entire dataset. Presenting here only the elements and proxies

that are thoroughly addressed in the manuscript and dislocating the other panels in the supplementary material could ease the Figure. This would give more space for the "key proxies" and greatly increase the readability. We have revised Figure 3 and kept only the relevant variables according to the factor analysis.

- Numbers of x-axes tend to overlap with one another and sometimes they are missing, please change that. Efforts were made to improve these axis problems.
- Please add more tick-marks to the x-axes (e.g., at least one in the middle) ➹ increases readability. Done.
- Some values tend to be plotted "outside" of the scale bar (on the left side of the plots). Please setthe x-axes in a way that includes the range of the values. Done.
- What do the vertical/horizontal lines represent? If not relevant, please remove them, or otherwise please explain them in the caption. Removed.
- The fonts-size is rather on the small side, please comply with JOPLs-guidelines. The font size was increased.
- For the MAR curves: in SAMO14-1 and -2 the trend is "hidden" by the outliers, which force theentire scale bar. One could "cut" the scale bar ➹ this would "stretch" the range and make the MAR trend more visible. This would help understand the "composition" of the MAR. We have used logarithmic values of MAR.

- Question:
  - How do the trends of MS, Ca, and Ti compare to those reported in Sosa-Najera (2010)? Trends are similar. Could probably be addressed in discussion. Please mind the length of the text. We think that this comparison would not add value to the purpose of the manuscript.
- Caption:
  - Add the Units of MAR, Done.
  - add "MS": Magnetic Susceptibility (**MS**, x10….) Done.

R2.72 Fig. 4

ANSWER 2.72:

- Biplots
  - Please add the explained variances to the axes: Factor 1 (60%); Factor 2 (11%). Done.
- Left panel: is it possible to add the samples per core (similar to the right panel) in the backgroundto see how the locations compare? The software that we used (Minitab) has only the options that we presented in the manuscript. We have tried to make a composite figure by using MSExcel, but there is a problem with scales since the coordinates of the variables are too different from those of the samples (see the values of the coordinates on both panels) and the variable appear balled up in the center of the chart, hidden behind the samples.
- Caption
  - Refine the caption: What does the left biplot show, what does the right biplot show? Done
  - Is it really NW Mexico? All other studies indicate W, or Pacific W Mexico. Please change andbe consistent throughout Manuscript. Please refer to answer R2.30.

R2.73 Fig. 5

ANSWER 2.73:

- Overall:
  - The readability is not easy: enlarge the plot-boxes ➹ e.g., remove the y-axes labels from columns 2-4, leave it as "example" in column 1, and color the y-axis according to the color of the data (Left blue, right brown). Done.

- Make the color denser, and be sure to use a color-blind friendly palette, otherwise one could alsouse a dashed curve for the MAR. We have checked several color-blind-friendly options and it seems that the combination orange-blue is fine (https://jfly.uni-koeln.de/color/).
- X-axes:
  - Change x-axis of Ti/Ca plot from SAMO14-2, it starts at 1895, all others do start in 1900 Done.
  - The extend of the x-axes in the first 2 plot rows are different (2010 is not at the same position in relation to right-hand x-axis) -> adjust this Yes, the first 2 plot rows include meteorological data (only available since the 1960s) and the rest of the plots include data from the cores (since 1900s). The year 2010 is now in the same position in all x-axes.
  - Y-axes:
  - Make sure that the MAR-extends on the right-hand axes are always the same per Lake for rows 1 and 2; and for rows 3 to 6. Done.
  - Example: SAMO18-4: sometimes MAR goes to 3, sometimes to 4, even though it isthe exact same data! Please change this. Done.
  - Please increase the visibility of the tick marks on right hand axes Done
- Caption:
  - Explain the meaning of the filled sample dots and the meaning of the hollow sample dots Done.
  - Add a bracket after "meteorological data" and write the name of the weather station, otherwiseone can assume that the meteorological data are from the lake Done.

R2.74 Fig. 6

ANSWER 2.74:

- Dendrograms:
  - Adjust the fonts size and position of "SAMO 18-4" according to the other panels Done.

R2.75 Table 2

ANSWER 2.75:

- Is there any information about watershed/lake area ratio available per study? This could be a factor influencing MARs. Unfortunately, the watershed area is not available.
- Adding each analyzed SAMO sediment core individually to this table could be beneficial. The individual values per core are already presented in Table 1.

Supplementary material

R2.76 Fig. S1. Is it possible to separate the plots per sediment core? (plot them on individual x-axes)? This would greatly improve the readability and allow the reader to visually detect trend turns in SAR/MAR trends (e.g., pre-1950, post-1950, post-1980, post-2010) better.

ANSWER 2.76: done.

R2.77 Fig. S2

- To save space, respectively to enlarge the panels and make them better readable, one could label only the x-axes of the panel row 4 with (SAMO14-1, SAMO14-2…). This would allow to enlarge the plots vertically which in turn would increase the chance to see the differences in e.g., the Mn-boxplots.

ANSWER 2.77: done.

R2.78 Fig. S3

- Please make sure that the time series gaps are indicated in the plot (e.g. line breaks!)

- Please adjust start/end year of the moving averages per variable (that they are 1:1 comparable…)
- Please add a temperature plot since it was used in the cluster analysis.

ANSWER 2.78: sorry, it is not possible to introduce the line breaks, because the missing values are not the same for all variables. The time series gaps are explained in the text (see answer R2.4). We have added background lines (per year) and, following these lines, the years with missing values are more visible (we hope this helps). The data for each variable start in different years, so it is not possible to adjust the start/end of the moving averages. The temperature plot was included.

R2.79 Fig. S4

ANSWER 2.79:

- Please add the watershed boundaries to the map. This would help understanding the processes/sources that directly influence the sedimentation better. Watershed information is not available.
- Please replace "Simbology" with "Legend". It was replaced by "Symbols" as per Q14.
- Isolines are not visible on the map, please change width/color of the lines, or remove from legend. Removed.
- The resolution of the figure seems to be blurry, can this be changed? We have produced the figure at a resolution of 600 dpi.
- Please indicate settlements that are relevant for the pollution. E.g., tourism bungalows, etc. This is very difficult with the image size. Making the hotels and restaurants visible would imply making the zoom of at least three different areas of the lake and there is no space for this. But we would consider that anyone interested in seeing that, can easily locate SAMO in Google Earth.

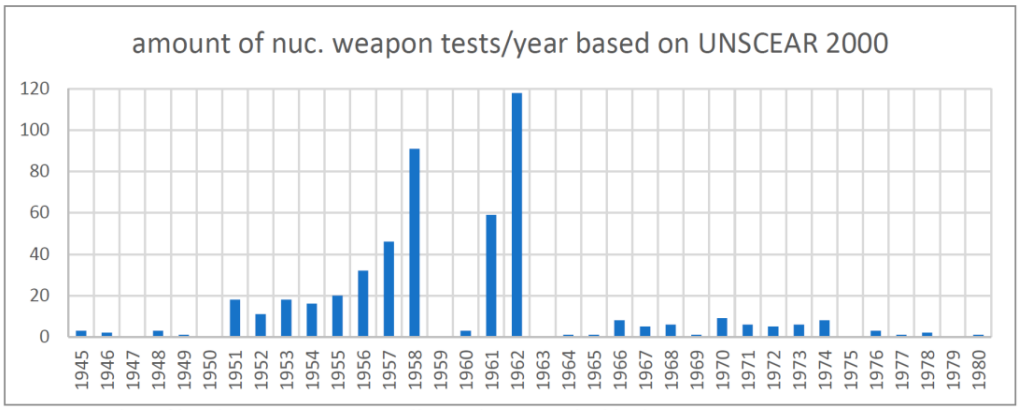

Fig. 1 Number of bomb tests per year according to the report cited in the present paper (UNSCEAR, 2000).